LIFETIME OF POSITIVE ELECTRONS IN METALS

by

GARTH JONES

B.A., University of British Columbia, 1953
M.Sc., University of British Columbia, 1955

A THESIS SUBMITTED IN PARTIAL FULFILMENT OF THE REQUIREMENTS FOR THE DEGREE OF

DOCTOR OF PHILOSOPHY

in the Department

of

PHYSICS

We accept this thesis as conforming to the required standard

THE UNIVERSITY OF BRITISH COLUMBIA

October, 1959.

In presenting this thesis in partial fulfilment of the requirements for an advanced degree at the University of British Columbia, I agree that the Library shall make it freely available for reference and study. I further agree that permission for extensive copying of this thesis for scholarly purposes may be granted by the Head of my Department or by his representatives. It is understood that copying or publication of this thesis for financial gain shall not be allowed without my written permission.

Department of Physics

The University of British Columbia,
Vancouver 8, Canada.

Date November 2nd, 1959.

GRADUATE STUDIES

Field of Study: Nuclear Physics

Cosmic Rays and High Energy Physics ..... J. R. Prescott

Group Theory Methods in Quantum Mechanics ..... W. Opechowski

Physics of Nuclear Reactions ..... J. B. Warren

Quantum Theory of Radiation ..... F. A. Kaempffer

Other Studies:

Advanced Electronics ..... R. E. Burgess

Physics of the Solid State ..... J. B. Gunn

Numerical Analysis ..... F. M. C. Goodspeed

Linear Analysis and Group Representations ..... H. Davis

Analogue Computers ..... E. V. Bohn

The University of British Columbia

Faculty of Graduate Studies

PROGRAMME OF THE

FINAL ORAL EXAMINATION

FOR THE DEGREE OF

DOCTOR OF PHILOSOPHY

of

GARTH JONES

B.A., University of British Columbia
M.Sc., University of British Columbia

IN ROOM 301, PHYSICS BUILDING

THURSDAY, NOVEMBER 5th, 1959 at 2:30 p. m.

COMMITTEE IN CHARGE

DEAN G. M. SHRUM: Chairman

J. B. WARREN	W. C. BINNING
G. M. GRIFFITHS	C. FROESE
F. A. KAEMPFFER	F. K. BOWERS
W. OPECHOWSKI	W. M. ARMSTRONG

External Examiner: Dr. A. T. STEWART

Dalhousie University, Halifax

ABSTRACT

Positron lifetimes in a variety of metals have been measured using a high-stability time sorter developed in this laboratory. This instrument consists of a time-to-pulse-height converter containing high-frequency microwave diodes as the discriminating elements, and limiter circuits specially designed for high stability and count-rate insensitivity. The intrinsic electronic resolution time of the time-sorter is .05 nanoseconds, with an electronic stability of $\pm$ x 10^{-11} seconds over the course of a day. A resolution time for the prompt gamma rays of Co^{60} of 0.8 nanoseconds was readily obtained. In addition, the time sorter was characterised by a linear time calibration over the range involved in the lifetime measurements of one to ten nanoseconds.

The absolute lifetime of positrons in aluminum was measured by two methods which differed primarily in the means employed for obtaining the prompt resolution curve for the instrument.

The first method involved the use of Co^{60} as a prompt source of coincident gamma rays. Positron lifetimes were measured by analyzing the delayed coincidence resolution curve resulting from the use of a Na^{22} source of positrons embedded in an aluminum absorber. The delayed coincidence resolution curve was determined by measuring the time interval between detection of the 1.28 Mev gamma ray in one channel (indicating the instant of emission of the positron) and detection of the 0.51 Mev radiation in the other channel (indicating the instant of annihilation of the positron). An analysis of the first two moments of the resulting resolution curves enabled a determination of the first two moments of the probability distribution characterizing the annihilation of the positrons. The mean lifetime of this distribution was found to be $(2.45 \pm 0.15) \times 10^{-10}$ seconds and the square root of the second moment about the mean was $(2.50 \pm 0.15) \times 10^{-10}$ seconds. The equality of these two values suggests an exponential probability distribution for positron annihilation in aluminum, since most other probability distributions would yield significantly different values for these two characteristics of the distributions.

The second method was distinguished by the use of annihilation gamma rays as the prompt source. Although it was impossible to obtain a measure of the mean lifetime of the annihilation probability distribution, because of the symmetric nature of the resulting resolution curves, analysis of the second moments (which correspond to a measure of the width of the curves) yielded a value for the square root of the second moment about the mean of $(2.65 \pm 0.25) \times 10^{-10}$ seconds, in agreement with the corresponding value obtained by the first method.

In addition, comparisons of the mean lifetime of positrons in a variety of metals (twenty-two in number) to that in aluminum were obtained. The results of these measurements indicated a range of lifetimes from 2.0 to 2.7 (x 10^{-10} seconds) but failed to indicate any dependance of the lifetime on the conduction electron density as would be expected for a pure collisional annihilation process. Instead, the positron lifetimes were found to be shortest in those metals characterised by dense crystal structures. An interpretation of these results in terms of annihilation of the positron from a bound negative positronium ion state is presented, the annihilation being characterised by an intrinsic mean lifetime of about 3.2×10^{-10} seconds. In metals with crystal lattices of small dimensions, the resulting shortened lifetime is attributed to an enhanced positron annihilation rate due to "pick-off" annihilations between the positron in the positronium ion and core electrons of the surrounding metal ions. Finally, this interpretation is shown to be in qualitative agreement with the results of the annihilation radiation angular correlation measurements with the high-momentum component of these measurements being attributed to the "pick-off" annihilations with the metal ion core electrons.

ABSTRACT

Positron lifetimes in a variety of metals have been measured using a high-stability time sorter developed in this laboratory. This instrument consists of a time-to-pulse-height converter containing high-frequency microwave diodes as the discriminating elements, and limiter circuits specially designed for high stability and count-rate insensitivity. The intrinsic electronic resolution time of the time sorter is .05 nanoseconds, with an electronic stability of $\pm$ 1 x 10^{-11} seconds over the course of a day. A resolution time for the prompt gamma rays of Co^{60} of 0.8 nanoseconds was readily obtained. In addition, the time sorter was characterised by a linear time calibration over the range involved in the lifetime measurements of one to ten nanoseconds.

The absolute lifetime of positrons in aluminum was measured by two methods which differed primarily in the means employed for obtaining the prompt resolution curve for the instrument.

The first method involved the use of Co^{60} as a prompt source of coincident gamma rays. Positron lifetimes were measured by analysing the delayed coincidence resolution curve resulting from the use of a Na^{22} source of positrons embedded in an aluminum absorber. The delayed coincidence resolution curve was determined by measuring the time interval between detection of the 1.28 Mev gamma ray in one channel (indicating the instant of emission of the positron) and detection of the

0.51 Mev radiation in the other channel (indicating the instant of annihilation of the positron). An analysis of the first two moments of the resulting resolution curves enabled a determination of the first two moments of the probability distribution characterizing the annihilation of the positrons. The mean lifetime of this distribution was found to be $(2.45 \pm 0.15) \times 10^{-10}$ seconds and the square root of the second moment about the mean was $(2.50 \pm 0.15) \times 10^{-10}$ seconds. The equality of these two values suggests an exponential probability distribution for positron annihilation in aluminum, since most other probability distributions would yield significantly different values for these two characteristics of the distributions.

The second method was distinguished by the use of annihilation gamma rays as the prompt source. Although it was impossible to obtain a measure of the mean lifetime of the annihilation probability distribution, because of the symmetric nature of the resulting resolution curves, analysis of the second moments (which correspond to a measure of the width of the curves) yielded a value of the square root of the second moment about the mean of $(2.65 \pm 0.25) \times 10^{-10}$ seconds, in agreement with the corresponding value obtained by the first method.

In addition, comparisons of the mean lifetime of positrons in a variety of metals (twenty two in number) to that in aluminum were obtained. The results of these measurements indicated a range of lifetimes from 2.0 to 2.7 ($\times 10^{-10}$ seconds)

but failed to indicate any dependence of the lifetime on the conduction electron density as would be expected for a pure collisional annihilation process. Instead, the positron lifetimes were found to be shortest in those metals characterised by dense crystal structures. An interpretation of these results in terms of annihilation of the positron from a bound negative positronium ion state is presented, the annihilation being characterised by an intrinsic mean lifetime of about 3.2×10^{-10} seconds. In metals with crystal lattices of small dimensions, the resulting shortened lifetime is attributed to an enhanced positron annihilation rate due to "pick-off" annihilations between the positron in the positronium ion and core electrons of the surrounding metal ions. Finally, this interpretation is shown to be in qualitative agreement with the results of the annihilation radiation angular correlation measurements with the high-momentum component of these measurements being attributed to the "pick-off" annihilations with the metal ion core electrons.

ACKNOWLEDGEMENTS

To my supervisor, Professor J.B. Warren, I wish to express my gratitude for the many enlightening suggestions and advice so readily offered throughout the course of this work.

I am also grateful to Professor G.M. Griffiths and Dr. B.L. White for many stimulating discussions and useful suggestions. The frequent assistance offered by the other members of the Van de Graaff group, and especially the Physics workshop staff, are also acknowledged. Thanks are also due Mr. R.G. MacNaughton for assistance in the recording of data, and Mr. E.D. Earle for assistance in the preparation of drawings.

I am especially indebted to my mother for her untiring efforts in the preparation and typing of this thesis.

Finally, I wish to express my gratitude to the National Research Council for their financial support in the form of NRC Studentships during the course of this work.

TABLE OF CONTENTS

TABLE OF CONTENTS (Contd.)

TABLE OF CONTENTS (Contd.)

TABLE OF CONTENTS (Contd.)

LIST OF ILLUSTRATIONS

LIST OF ILLUSTRATIONS (Contd.)

CHAPTER I

INTRODUCTION

Gell-Mann (1959) recently described the electron and muon as ....

" ... pure Dirac particles with electrodynamic coupling of the conventional form. It now seems clear also that the weak couplings of electron and muon are identical in form and strength, both involving the neutrino (presumably the same neutrino, although we have no way of proving that at the moment). Both electron and muon lack, so far as is known, any other interaction whatever, except the gravitational. ...
It is evidently important to refine existing measurements of the muon and electron still further, ... in order to see whether the equivalence of the two particles really persists down to small distances."

Since electrodynamic coupling constants are well understood, the electrodynamic interactions of these particles can be calculated with very great precision. As an example, one set of quantum electrodynamic calculations was verified to order α^5, (where α is the fine-structure constant, 1/137), by radio-frequency resonance measurements of the second-order Zeeman splitting of the triplet ground state of positronium (a hydrogen-like, bound system of an electron and positron), by Pond and Dicke (1952). These precision measurements have, in all cases, involved positron annihilations in gases, where a positronium atom, once formed, can be considered isolated, with negligible interaction between it and the neighbouring gas molecules.

The theoretical predictions are much less precise, however, in the case of positron annihilations in liquids and solids, due to the present lack of knowledge about the total wave-function of the electron system in the material. Thus, the suggestion has been advanced (Ferrell, 1956, and Daniel,

1957) that detailed experimental investigations of positron annihilation in these materials should be capable of extending our knowledge of the wave-functions of the electron within these materials.

In addition, discussions of the interactions of other Dirac particles, as, for example, the muon, have relied to some extent on information regarding the analagous situations involving positrons and electrons. Thus, the "mesic atom", consisting of a negatively-charged meson bound to a positive nucleus in direct analogy to normal atoms consisting of electrons bound to the nuclei, have been observed, and a study of this system has yielded much pertinent information about the nature and interactions of both the mesons and the nuclei. The highly fruitful investigations of the bound states of positrons and electrons has, as a result, led to a search for similar systems involving mesons. However, the bound system consisting of a positive meson and electron, forming a "muonium" atom, has, so far, evaded observation, partly due, perhaps, to the difficulties associated with the detection of such a system. Further studies of the more readily detectable positron-electron system may, however, suggest alternative approaches to the problem.

In summary, then, a sound experimental understanding of the nature of the annihilation process of positrons in various forms of matter promises to be of eventual assistance in the determination of electronic wave-functions in these materials, in providing further checks of the validity of quantum electrodynamics, and also in shedding more light on the analagous

problems associated with muon physics. It is possibly worth noting that the positronium atom is a system satisfying Bose-Einstein statistics, and thus may be of interest to workers in the field of solid-state who are interested in a study of bosons of electronic mass.

1. Annihilation in Amorphous Solids.

The annihilation of positrons in many solid materials is complicated by the fact that several competing processes may occur. Such a situation is evident in many amorphous materials (like teflon) by the observation of a complex decay curve which can be resolved into several components of different mean lifetimes. These decay curves usually consist of two components, a "long" component of lifetime between one and ten nanoseconds, and a "short" component of a fraction of a nanosecond (although some substances, notably liquid helium, and some gases, exhibit three well-defined decay modes). The "long" component is normally attributed to the formation of orthopositronium (the bound state in which both the electron and positron spins are aligned in the same direction), a system which has a lifetime of about one hundred nanoseconds. The positronium atom is formed when a positron of a few electron volts of energy captures an electron from a neighbouring atom. Positron annihilation generally occurs after the positron has slowed to these energies, since the probability that a positron is annihilated while in flight is only about two per cent for five hundred kilovolt positrons.[1] The annihilation of a positron with an electron can give rise, theoretically, to any number of photons, with the reservation,

1 Heitler, W., The Quantum Theory of Radiation (The Clarendon Press, Oxford, 1954), Third Edition, p. 273.

of course, that the probability of such annihilations decreases by order α for each additional photon characterizing the decay. As a result, only annihilations by one, two, or three photons have been observed in practice. Single photon annihilation can only occur when a third agent is available to carry away the excess momentum. Such a process can therefore occur when a positron annihilates with an electron bound to a nucleus, the nucleus recoiling after annihilation in order to conserve linear momentum. According to Heitler, this process is proportional to the fifth power of the atomic number of the absorber. However, even in lead, its maximum cross-section (which occurs at an energy of 10 mc^2, with a monotonic decrease in the cross-section for decreasing energy) is only twenty per cent of the two-photon cross-section at that energy. Consequently, the relative amount of single photon annihilation expected during the absorption of positrons emitted by radioactive sources like Na^{22} is negligible. Thus, the annihilation of a positron by either a direct collision with a free electron, or from a bound positronium atom, will proceed via two or more photons. Deutsch (1953) described the selection rules which have been developed to describe annihilation from various positron-electron configurations. These selection rules arise from the necessity to conserve both angular momentum and parity. During two-quantum annihilation, the two photons must be emitted in opposite directions with equal energy in the coordinate system in which the centre-of-mass is at rest. Thus, since each of the two photons has an intrinsic angular momentum of $\pm\hbar$ along its direction of

propogation, with this direction being chosen as the z-axis, then the two photons can only result from initial states characterized by z-components of angular momentum m = 0 or 2. The anti-symmetric, singlet configuration of the electron-positron pair, classically described in terms of oppositely-directed spin directions, is characterized by a zero total angular momentum and so is free to annihilate by two-quantum emission.

The symmetric configuration, on the other hand, which classically has both spin axes in the same direction, is characterized by a total angular momentum of one unit of $\hbar$, with resultant z components described by m values of 1, 0, or -1. The states with a value of $\pm$ 1 therefore cannot decay by two-quantum emission which requires the final state to have an m value of 0 or 2. Alternatively, by invoking the law of conservation of parity (or, by insisting that the initial and final states have the same rotational symmetry), it can be shown that none of these three states with different m values can decay by two-quantum emission. Thus, the pair state with an angular momentum quantum number, J, of 1 (which includes the ortho configuration of positronium) must decay by three or more photons. Finally, a complete treatment of the selection rules shows that in the absence of external fields, two- and three-quantum annihilation are possible only from states of opposite parity and therefore never compete. From order-of-magnitude considerations, then, the lifetime of ortho-positronium would be expected to be at least one hundred times ($1/\alpha$) that of parapositronium.

The "long" lifetime component of positron annihilation

in amorphous materials, however, has a lifetime less than the theoretical value for orthopositronium. It has a lifetime which is a function of the composition and temperature of the absorber, and lastly, is characterized by two-photon decay. This is interpreted in terms of orthopositronium formation followed by annihilation of the positron by a "pick-off" process involving the orbital electrons of the atoms with which the positronium collides (Ferrell, 1956). If such a collision places the positron component of the positronium atom near an oppositely-directed electron contained in an atomic orbit, then there is a significant probability for two-quantum annihilation. The observed lifetimes are thus measures of the cross-section for this type of "pick-off" process.

Additional information concerning the annihilating pair has been obtained by an experimental technique involving the measurement of the angular correlation of the annihilation gamma rays. If the centre-of-mass of the annihilating pair has a finite momentum, then, due to the appropriate conservation laws, the annihilation gamma rays must carry away the additional momentum and energy. The broadening of the mc^2 gamma line, due to a random momentum distribution of the annihilating pair has been observed by DuMond and his co-workers (1949). Furthermore, the momentum of the annihilating pair can be determined by measuring the angular deviation from co-linearity of the two gamma rays. If the energy broadening of the gamma line is small, then the momentum of each gamma ray is mc, and the momentum of the centre-of-mass resulting from an angular departure of θ from co-linearity, will be θmc. Thus, the momentum of the annihilating pair (in

units of mc) is obtained directly in a measurement of θ. In practice, the component of θ (and hence of the momentum) that lies in the particular direction defined by the experimental apparatus is the quantity that is measured. These momentum distributions have been measured in a variety of substances by several groups of workers. (Warren and Griffiths, 1951; Lang et al, 1955; and Stewart, 1957).

All the angular correlation measurements for those amorphous materials which exhibit long-lifetime components appear to be characterized by a very wide, gaussian-like distribution topped by a lower-intensity narrow peak (Stewart, 1955). Page and his co-workers (Page et al, 1955), in an analysis of their results for fused quartz, estimated the intensity of the narrow peak to be 18% of the total two-photon decay rate. The lifetime measurements, on the other hand, performed by Green and Bell (1957) show the familiar complex spectrum, with the long-lived component (of lifetime: 1.5 nsec) amounting to 50% of the total two-photon decays. If this is interpreted in terms of positronium formation as described earlier, 67% of the positrons must form a bound positronium state before annihilating, the 67% consisting of 50% orthopositronium formation, and 17% parapositronium formation, the statistical weights being 3:1 respectively (the value of the statistical weight will be discussed in greater detail later). The remaining 33% of the positrons will either annihilate during direct collisions with bound, orbital electrons in the quartz with a cross-section deduced first by Dirac (which is discussed in more detail in the theoretical section entitled "Dirac Annihilation"), or by forming a chemical bond, in which the

positron shares electrons with the oxygen ions, eventually annihilating by two-photon emission from the singlet configuration with an appropriately oriented electron.

The positrons in the orthopositronium atoms are then assumed to annihilate by the "pick-off" mechanism discussed earlier, resulting in a wide momentum distribution characteristic of positron annihilation with orbital electrons. (Berko and Plaskett, 1958, discuss the angular correlation results expected for positron annihilations with the bound electrons of copper and aluminum). All the processes discussed thus far involve annihilations between the positrons and bound, orbital electrons which have momenta of the order of αmc, contributing, therefore, to the wide, gaussian-shaped momentum distribution observed in the measurements. The remaining positrons (17%) which form parapositronium are expected to decay from this state with the theoretical characteristic lifetime of parapositronium of 1.25×10^{-10} seconds (Ore and Powell, 1949). Since the momentum distribution of the gamma rays is that of the positronium atoms themselves, a quite narrow distribution may result if the atoms have been slowed by thermalisation processes to an energy of less than an electron volt. This model is consistent with the observations of Page et al (1955) mentioned earlier, namely, the existence of a narrow (low momentum) component of the two-photon decay, of intensity 18%.

2. Annihilation in Liquids.

The annihilation of positrons in liquids follows the same general pattern as in amorphous solids in that a complex mode of

decay of equivalent relative intensities is also observed. Because of the lack of angular correlation experiments in liquids, however, there is little information available regarding the momentum distributions of the annihilating pairs. The "long" component in most organic liquids (including water) has a lifetime of between one and two nanoseconds, and an intensity, usually, of twenty to thirty per cent. The experimental evidence (Berko and Zuchelli, 1956) indicates that the lifetime of the long component can be altered (with the intensities remaining constant) by inserting small amounts of a suitable "quenching" agent in the liquid. Typically, a paramagnetic free radical, such as diphenyl picryl hydrazyl is employed, the quenching behaviour being interpreted in terms of triplet-singlet conversion of the positronium atoms via spin-exchange collisions with the spin unpaired electron of the free radical. Exchange cross-sections of the order of 10^{-17} cm^2 are obtained, of the same order of magnitude as the triplet-quenching cross-section in gases due to the addition of NO (Deutsch, 1951A). A somewhat different "quenching" process recently described by Green and Bell (1957) involves a decrease in the intensity of the long-lived component without an appreciable change in the value of the lifetime, due to the addition of either NO_2^- or NO_3^- ions to water. This process is interpreted as a decrease in the number of positrons available for positronium formation, due to the capture of some of them by the negative ions to form the chemical compounds positronium nitrate, or nitrite. These captured positrons then decay with a short lifetime in a similar manner to those

annihilating from a singlet state. It would appear then, that an investigation of positron decay processes in liquids is likely to afford a convenient basis for the study of positron chemistry.

3. Annihilation in Gases.

The annihilation of positrons in gases is, in many respects, similar to the corresponding processes in liquids and amorphous solids. The main difference, arising from the greatly reduced density of gases, is that the free 'Dirac' annihilation cross-section which is dependent on the electron density is considerably reduced, resulting in a much longer lifetime for annihilation by direct collision between the positron and the atomic electrons (Deutsch, 1953). A short period, of the order of the slowing-down time of the positrons has been detected, but not measured with significant accuracy. This mode of decay was interpreted as annihilation from the short-lived state, para-positronium. A second period, of the order of magnitude of that predicted by the Dirac cross-section, and inversely dependent on the gas pressure, is strongly suggestive of annihilation of the positron during free collisions with the atomic electrons. The third period is practically independent of pressure and corresponds to a mean life of about 0.14 microseconds, both of which are consistent with a model based on annihilation from orthopositronium atoms. The fact that the three photon yield is much increased in those gases which are characterized by a relatively intense, pressure independent, long-lifetime component is further evidence for this interpretation.

Both the relative abundances of the three components

and the lifetime of the pressure dependent component of the decay depend critically on the nature of the gas used. As an example of this, lifetime results indicate that almost every positron stopped in freon and carbon dioxide form positronium atoms, only about two thirds of them are effective in nitrogen and argon, and none of them appear to annihilate from the orthopositronium state in oxygen (Deutsch, 1951B). Again, in analogy with the case of liquids, several gases were found which had the ability to quench the three-quantum annihilation; viz. NO, NO_2, and the halogens. The quenching process due to NO was explained by Deutsch in terms of a spin flip due to electron exchange during collisions between the bound positronium positron and the unpaired electron of the NO molecule. Since the energy difference in the NO molecule associated with the change in the orientation of the unpaired electron is only thirteen millivolts, he believed the process could have the large cross-section required to be compatible with the results. The quenching effect of the halogen molecules, however, was interpreted in terms of a formation of chemical compounds between the positrons (positive positronium ions) and the halogen ions. An attempt to determine which of these processes is significant in a particular experiment should, of course, be possible by measuring the lifetimes and relative intensities of the different lifetime components of the positrons in the gas, as a function of the concentration of the quenching material (Green and Bell, 1957). A spin-exchange mechanism should result in a shortening of the lifetime of the orthopositronium, the amount of the shortening depending on the

concentration of the quenching material, without significantly altering the intensity of the component. The two-photon decay rate would also rise at the expense of the three-photon rate as the concentration of the quenching agent was increased. Quenching by chemical compound formation, however, would tend to alter the intensity of the long-lived component, rather than the value of the lifetime, the reduction being dependent on the concentration of the quenching agent. This mechanism is the same as that postulated by Green and Bell (1957) to explain their observations of such effects in liquids.

Angular correlation measurements of the annihilation radiation from various gas absorbers of positrons have been obtained by Page and co-workers (Heinberg and Page, 1956). In many of these gases (contained under about twenty atmospheres of pressure) a narrow component of the angular correlation results was observed above a wide gaussian-shaped distribution, similar to the results for many of the amorphous solids described earlier. In the case of gases, however, where the thermalization times are expected to be much longer than those for solids, and probably dependent on the nature of the gas employed, considerable variations were observed in the peakedness and intensity of the narrow component from gas to gas. In particular, argon gas yielded no significant narrow component at all. This can be explained if it is assumed that:

(i) the parapositronium atoms which are formed have too short a lifetime compared to the thermalisation time for the atoms to be slowed significantly from their original energies of

several electron volts before annihilating, and

(ii) the lack of an efficient triplet-singlet conversion mechanism in argon would result in the long-lived orthopositronium atoms (which might, indeed, have had time to "thermalize") decaying by three-quantum emission, thus entirely removing this component from observation by a two-photon angular correlation technique. On the application of a magnetic field of several kilogauss, however, a central, narrow peak became quite evident (Page and Heinberg, 1957). Since the presence of a magnetic field results in an admixture of the singlet wave function to the triplet m = 0 state (in order for the total wave function to be an eigenfunction of the new Hamiltonian - - under these circumstances, the total wave-function is no longer an eigenfunction of the total angular momentum operator), then the m = 0 fraction of the orthopositronium atoms may annihilate via two-photon emission through the singlet component of the wave function.

Thus, the application of a magnetic field serves to quench the three-photon orthopositronium annihilation. The interpretation of the angular correlation curves therefore depends on the following assumptions (Page and Heinberg, 1957):

(i) The positronium atoms are originally formed with a rather large kinetic energy, namely one to two electron volts,

(ii) The positronium atoms are "thermalised" sufficiently slowly that the singlet states, with a lifetime of the order of 10^{-10} seconds, retain a good part of this motion, resulting in a contribution towards the wide portion of the angular

correlation distribution.

(iii) The "thermalisation time" is sufficiently short that the magnetically-quenched fraction of the orthopositronium atoms whose lifetime is of the order of five nanoseconds, will have lost most of their motion, their energy being degraded to about 0.3 electron volts, by the time they undergo two-photon annihilation, thus contributing to the narrow component of the decay.

Thus, although the angular correlation distribution obtained for argon is similar in appearance to those for the amorphous solids, the interpretation of the results is quite different for the case of the gas. With argon the narrow component is ascribed to the decay of orthopositronium atoms which have been magnetically-quenched to produce two-photon emission. Annihilations from the singlet state are assumed to contribute to the wide portion of the angular correlation results, because of the relatively high energy still retained by these atoms when annihilating, whereas in solids, where the thermalisation process is faster, the short-lived parapositronium can contribute to the narrow component.

In an attempt to understand in more detail the processes involved in direct positron annihilation, positronium formation and ionisation, and the various orthopositronium quenching mechanisms, Massey and Mohr (1954) calculated the cross-sections for these processes in the idealized case of a monatomic hydrogen gas, on the basis of existing theoretical knowledge concerning the interactions of slow positrons with

matter. Meaningful comparisons of their predictions with experimental results for practical gases is virtually impossible, however, due to the strong energy dependence of most of their calculated cross-sections, and the lack of knowledge of the relative positron-electron energies in the gas absorbers after thermalisation. In fact, they state that "Experiments in which this (degree of moderation of the positronium energy) is controlled in some definite way is essential in order to compare cross-sections."

In addition, the complex nature of the annihilation of the positrons, from a number of different, competing states, hampers any detailed interpretation of the observed momentum distributions, since these are frequently composed of several completely different momentum distributions corresponding to the different annihilating states. For example parapositronium atoms in gases under twenty atmospheres of pressure appear to have kinetic energies of a few electron volts, whereas the orthopositronium atoms have, in general, been slowed to about 0.3 electron volts before annihilating (Heinberg and Page, 1956). In addition, there is a component due to the decay of those positrons which annihilate during direct collisions with the bound, orbital electrons of the gas, and the centre-of-mass momentum of these pairs is at least that of the orbital electrons; in this case, something of the order of ten electron volts.

Even in the amorphous solids (which are somewhat similar, with respect to positron annihilation, to gases under very high pressure), there is a variation in the momentum distributions of

the various lifetime components. The energy of the positrons at the time of positronium formation is of the order of an electron volt, and the momentum distribution of those positrons which annihilate by direct collisions is quite unknown, since their lifetimes (of the order of one third of a nanosecond) is almost certainly less than the thermalisation time of the positrons. In these materials, the thermalisation time is probably significantly greater than 3×10^{-10} seconds, the value estimated by DeBenedetti et al (1950) for a metal lattice, where it was assumed that positrons could lose energy by exciting lattice vibrations. In fact, rough estimates of the thermalisation time for these amorphous solids by Wallace (1955) indicate times of at least one nanosecond.

For these reasons, it would seem advisable to concentrate the experimental investigations (lifetime and angular correlation measurements) to those absorbers where the momentum distributions of the positrons and electrons are known at the time of annihilation, and, where possible, the annihilation process yields a simple exponential curve, indicating annihilation from one state only. Use of the knowledge of the electron momentum distributions that has been obtained for many solid materials from studies of low-energy X-ray interactions in those solids (Parratt, 1959) should also prove of assistance in the interpretation of the positron annihilation results. Only after the development of a sound understanding of the processes involved in these interactions can the problems involved in interpreting the complex decays be attacked in a reasonable fashion. Two such

materials which, at first sight, appear to satisfy these requirements are ionic crystals and metals. Both these substances exhibit only a short lifetime component, but whether or not this component represents a single mode of decay is uncertain, since the measured mean lifetime is shorter than the resolution times of the equipment used in the measurements.

4. Annihilation in Ionic Crystals.

No measurements have been made, nor detailed calculations presented, of the thermalisation time of positrons in ionic crystals, although Ferrell (1956) claims that there is some indication that it might be less than 10^{-10} seconds. Assuming complete capture of the positrons by the negative ions, Ferrell derived lifetime estimates and angular correlation functions that were not incompatible with the measured results. Accurate descriptions of the positron and electron wave-functions for such configurations have not been calculated to date, but Ferrell's rough calculations based on a number of simplifying assumptions yielded predictions which should be susceptible to experimental test (such as a dependence of the positron lifetime on the cube of the radius of the negative ion). Further experimental work on the determination of positron lifetimes in alkali halides is necessary before the understanding of the processes involved in these crystals will be anywhere near complete.

5. Annihilation in Metals.

DeBenedetti et al (1950) originally calculated the thermalisation time of positrons in metals to be about 3×10^{-10} seconds on the basis of energy loss of the positrons, first, by

exciting or ionizing the atoms of the absorber, then by causing inter-band electronic transitions, and eventually, when the energy is too low for this, by excitation of lattice vibrations. A modification of these calculations to include another mechanism, that of the positron energy loss involved in the Coulomb scattering of conduction electrons whereby the electrons are increased in energy and scattered out of the Fermi sea, led Garwin (1953) followed by Lee-Whiting (1955) with more accurate calculations, to arrive at a value for the thermalisation time for positrons in metals of approximately 10^{-12} seconds. Although no experimental verification of these estimates exists, it would be reasonable to expect the thermalisation time in metals to be negligible compared to the positron lifetime if the probable error of the theoretical estimates is less than a factor of ten. Assuming complete thermalisation, the positron wave-function in the metal lattice can then be regarded as constant (indicating a momentum of zero). Obviously, the positrons will have a momentum distribution of at least that corresponding to thermal excitations, but this is very small compared to the energies of the electrons in the Fermi sea. Also, the wave functions of the valence electrons in a metal can be considered from the point of view of the Sommerfeld (1928) model, to be represented by simple plane waves, the momentum distribution being determined by the density of available states in momentum space and Fermi-Dirac statistics (in other words, the normal Fermi sea of electrons). It has been suggested (DeBenedetti et al, 1950) that the wave-function of the positrons is effectively

constant in a metal except at the regions occupied by the positively-charged, metallic ion cores, where the positron wave-function is excluded and is assumed to equal zero due to coulomb repulsion of the positrons by the ions. Under this assumption, then, the positrons would annihilate only with the conduction electrons. Thus, it would appear, at least to a first approximation, that knowledge concerning the wave functions of both the electrons and the positrons in metals are available as desired for a complete understanding of the annihilation process.

This simple picture is surprisingly successful in explaining the shapes of the angular correlation functions in many metals, especially those in which the simple Sommerfeld theory should most likely apply, as, for example, in the alkali metals (Stewart, 1957; Lang and DeBenedetti, 1957). In those cases, the momentum distribution of the emitted photons fits that of the momentum distribution of electrons in a Fermi sea remarkably well. On the basis of this interpretation, the positron momentum must, indeed, be close to zero to account for the observed momentum distributions.

The results of lifetime measurements of positrons in metals have not, however, been capable of such ready interpretation. In fact, calculations of the positron lifetimes due to direct collisions with the free, plane-wave conduction electrons yielded variations of a factor of ten (approximately 0.5 to 5 nanoseconds) from metal to metal. (These calculations are outlined in more detail in the theoretical section on Dirac annihilation). Experimentally, however, DeBenedetti and

Richings (1952) found that the lifetimes of positrons in a number of metals which varied greatly in conduction electron density, were constant to an accuracy of 0.7×10^{-10} seconds. Later measurements by Bell and Graham (1952) confirmed these results, and also supplied a measure of the absolute lifetime of positrons in aluminum, 1.5×10^{-10} seconds. The constancy of these results, together with the small value for the absolute lifetime, led Bell and Graham to postulate that all positrons in metals form singlet positronium which then decays with a lifetime of 1.25×10^{-10} seconds. Garwin (1953) soon pointed out, however, that if positrons are assumed to form positronium atoms in metals, both para- and ortho-positronium should be formed, in the ratio of 1:3 respectively because of the statistical weights. A single, short lifetime could still be guaranteed, he pointed out, by assuming a rapid conversion mechanism operating between these states, such as rapid electron exchange with the conduction electrons which would produce momentum distributions the same as that for the electrons, thus giving results compatible with the angular correlation data. Such a rapid conversion system would result, however, in all four states (three triplet, and one singlet) being populated for the same lengths of time. And, since only the singlet state can annihilate by two-photon emission with the short lifetime, the resulting measured lifetime should be four times that of the pure singlet state; i.e. 5×10^{-10} seconds, a value significantly longer than that observed. Meanwhile, a succession of theoretical modifications to the free annihilation theory (as described in the theoretical

section of the thesis) based on a distortion of the plane-wave electron wave-function due to Coulomb interactions between the positron and the conduction electrons succeeded in reducing, but not eliminating, the discrepancy between the experimental lifetimes and those calculated in terms of this model. Furthermore, following publication of the measurements of Bell and Graham (1953), there appeared a succession of determinations of the absolute lifetime of positrons in aluminum by a variety of techniques, yielding results which varied from 1.5 to 2.5 x 10^{-10} seconds (Minton, 1959; Ferguson and Lewis, 1953; Gerholm, 1956; and Sunyar, 1957).

Because the processes governing positron annihilation in metals should be capable of a detailed theoretical treatment, and further, because of the confused state regarding the experimental knowledge of the lifetime of positrons in metals, it was deemed worth while to perform a thorough experimental investigation of the positron lifetimes in a large variety of metals in an attempt to resolve some of these problems and inconsistencies. The remainder of this thesis is devoted to a description of such an investigation and the results obtained.

CHAPTER II

THEORY

Three distinct mechanisms of slow positron annihilation in matter have been considered to date. These three (although, of course, there may be others) are described in some detail below:

(a) Dirac annihilation with free electrons was the first mechanism to be considered in detail, and describes the annihilation of a positron in an electron gas in which each electron is considered free. In this approximation, a substance is considered to consist of an electron gas of density NZ_e, where N is the number of atoms/cm^3, and Z_e is the effective number of electrons per atom.

(b) The experimental observations described in Chapter I regarding the complex decay modes in many substances, suggested the existence of a bound, hydrogen-like state. The lifetime for annihilation of a positron from this state would be dependent only on the density of the associated electron at the positron, and therefore not on the other electrons in the material. Reasonable agreement between the observed and calculated values of the long-life component of positron decay in gases was offered as further evidence for the existence of this process.

(c) Consideration of the existence of a positronium "atom" soon led to suggestions regarding possible chemical reactions between these atoms and those like the halogens with a valence of -1. The stabilities of such compounds were

investigated theoretically by Ore (1948, 1952). This concept of chemical compound formation has proved useful in explaining the intensity variations of the long lifetime mode of decay in liquids arising from the addition of certain solutes to the liquid (as described in Chapter I, Section 2).

1. Free Dirac Annihilation.

The probability of annihilation of a positron-electron pair with the emission of two gamma rays was first described by Dirac (1930) in terms of a second-order transition of the electron from a positive energy state, through an intermediate state, to an empty negative energy state (the "hole" in the negative energy states manifesting itself as the observable positron). The calculation was based on the assumption of positron annihilation with a free electron, neglecting the effect of any interaction between the positron and electron; in other words, a plane wave approximation was used for the electron. The total probability of annihilation was obtained by averaging over the spin directions in the initial state, and summing over all spin directions of the electron in the final state. (Explicit dependence of the two-photon annihilation probability on the relative spin orientations of the two particles as a function of their kinetic energy has recently been discussed by Page (1957), his results being in agreement with those of Dirac when the spin dependence is averaged out). The final result, after summing over all directions of the photon polarization, is the differential

cross-section:[1]

$$d\sigma = \frac{e^4 d\Omega}{4 p_o E_o c}\left[\frac{E_o^2 + p_o^2c^2 + p_o^2c^2\sin^2\theta}{E_o^2 - p_o^2c^2\sin^2\theta} - \frac{2p_o^4c^4\sin^4\theta}{\left(E_o^2 - p_o^2c^2\cos^2\theta\right)^2}\right] \qquad (1)$$

where p_o is the momentum of the initial electron in the system where the centre-of-mass of the annihilating pair is at rest,

E_o is the energy of the initial electron (in units of mc^2),

θ is the angle between the direction of the positron and one of the photons,

and $d\Omega$ is the solid angle into which a gamma ray is emitted.

Since less than five per cent of the positrons which enter a sample with a maximum initial energy of one Mev are annihilated while moving with a significant relativistic velocity[2], we are only interested in the non-relativistic limit of the above equation, i.e. $E \to mc^2$, $p \to mv$, $pc \ll E$. By this means, expression (1) reduces to:

$$d\sigma = \frac{e^4 d\Omega}{4m^2c^3v} \qquad (1')$$

and integration over the solid angle gives the total cross-section:

$$\sigma = \frac{\pi e^4}{m^2c^3v} = \pi r_o^2 \frac{c}{v}, \qquad (2)$$

where r_o is the classical electron radius: $\frac{e^2}{mc^2} = 2.82 \times 10^{-13}$ cm

Although the cross-section diverges for low relative velocity, the rate of annihilation, R, does not, since, in a substance with N electrons per unit volume, $R = N\sigma v_+ = \pi r_o^2 c N \ (sec^{-1})$. (3)

Alternatively, the transition probability can be determined

1 Heitler, W., The Quantum Theory of Radiation, (Clarendon Press, Oxford, 1954), Second Edition, p.207.

2 ibid, p.231.

directly without inserting the notion of a cross-section. In this case, as expected, the transition rate per unit electron density is: $\pi r_o^2 c$ per second. The cross-section can then be obtained by normalising to unit flux, that is, by multiplying by the factor 1/v, and so obtaining the cross-section for annihilation given by expression (2) above. Thus, on the basis of the theory of Dirac annihilation with free electrons, the mean lifetime of positrons in a substance is given by:

$$\tau = \frac{1}{\pi r_o^2 c N} \text{ sec.} \qquad (4)$$

If we assume that the number of free electrons in a metal is equal to that of the valence electrons, as indicated by the results of the angular correlation measurements of annihilation radiation (Lang and DeBenedetti, 1957), then typical results as calculated from equation (4) are as follows:

Metal	Effective Electrons/Atom	Positron Lifetime
Aluminum	3	0.75 nsec.
Sodium	1	5.2 nsec.
Copper	1	1.6 nsec.
Beryllium	2	0.55 nsec.

The annihilation rates discussed thus far are only those expected for two photon annihilation. Annihilation from a triplet spin state of the positron-electron system, on the other hand, is characterised by three-photon emission (as described in Chapter I, Section 1), a process with an annihilation rate of the order of α less than for two-photon decay (where α is the fine-structure constant). Explicitly, Ore and Powell (1949) calculated the relative annihilation rates to be:

$$\frac{\lambda_{3\gamma}}{\lambda_{2\gamma}} = \frac{4}{9\pi}(\pi^2 - 9)\alpha \qquad (5)$$

which is about $\frac{1}{8}\alpha$, or, $\frac{1}{1100}$ for three-quantum compared to two-quantum emission, where, eg $\lambda_{3\gamma}$ is the probability for annihilation by 3 photons. Although the basic annihilation rate for three photon emission is $\frac{1}{8}\alpha$ less than that for two-photon annihilation, electron-positron collisions result in the formation of a triplet spin state three times as often as the singlet state because the statistical weights for the productions of these states are 3/4 and 1/4[1], respectively. Thus, positron annihilation with free electrons should be characterised by a two photon to three photon ratio of $\frac{\lambda_{2\gamma}}{\lambda_{3\gamma}} \times \frac{1}{3} = \frac{8}{3\alpha} = \frac{370}{1}$, whereas annihilation from a system of isolated, positronium atoms, for example, would result in a ratio of 1:3.

(A) Experimental Support.

As described in Chapter I, Section 1, the momentum distribution of annihilating positron-electron pairs can be determined by measuring the angular correlation distribution of the emitted photons. In general, the measured momentum distributions in metals are very similar to those of the Fermi sea electrons, superimposed on an additional broad higher-momentum distribution. The width and intensity of this latter distribution varies considerably from metal to metal.

The close agreement between the measured momentum distributions and that of the Fermi sea electrons naturally prompted an explanation of the annihilation process in terms of a stationary positron (which is reasonable, in view of the short thermalisation time expected; Chapter I, Section 5), annihilating with the conduction electrons in accordance with the

1 Schiff, L.I., Quantum Mechanics (McGraw-Hill Book Co., Inc., 1949), First Edition, p.226.

Dirac cross-section, equation (2) (Stewart, 1957).

The measured ratio of three-photon decay to two-photon decay in aluminum is also consistent with this description. Basson (1954) obtained a value of $1/(406 \pm 50)$, compared to the theoretical value (for positrons annihilating with free electrons) of 1/370. These experimental observations are, then, consistent with a description based on the following two assumptions: (Stewart, 1959),

(a) Prior to annihilation, the positron has been completely thermalised. Estimates of this thermalisation time have been carried out by Garwin (1953) and Lee-Whiting (1955), the latter obtaining a value of about 5×10^{-12} seconds.

(b) The annihilation probability (equation 3) is essentially velocity independent over the range of velocities of the conduction electrons.

The latter assumption is perfectly consistent with the Dirac theory of annihilation with free electrons, for which case the non-relativistic annihilation probability is exactly velocity independent.

(B) Experimental Disagreement.

Before the detailed angular correlation results were obtained, the lifetimes of positrons in a variety of metals had been determined (Bell and Graham, 1952; DeBenedetti and Richings, 1952). The results of these measurements indicated that the lifetime of positrons in metals (about ten were studied) is $(1.5 \pm 0.5) \times 10^{-10}$ seconds, independent of the metal. This very short lifetime and lack of dependence on the conduction

electron density is very difficult to reconcile with a free electron theory of the type described in the above section, which, as observed from the examples on page 25, predicts lifetimes varying from 0.55 nsec in beryllium to 5.2 nsec in sodium.

2. Coulomb Enhancement of the Dirac Cross-section.

An obvious over-simplification inherent in the discussion of section (1) is the plane-wave approximation for the electron and positron wave functions, i.e. the neglect of any positron-electron interaction. DeBenedetti et al (1950) showed how the Dirac cross-section could be modified for arbitrary electron and positron wave functions provided that:

(i) the wave functions of the initial and final states are treated non-relativistically so that the spinor and spatial parts of the wave-functions are separable, and

(ii) the wave functions of the intermediate (virtual) states of the process are treated in the free particle approximation (plane waves).

If these conditions are satisfied, the expression for the Dirac transition probability factors into two parts, one being the matrix element discussed in detail in Heitler[1], which gives a transition rate of $\pi r_0^2 c$ as described earlier. The other contains the spatial dependence of the wave-functions, yielding an expression of the form: $\int |\psi_-(\vec{r})|^2 |\psi_+(\vec{r})|^2 dv$, where $\psi_\pm(\vec{r})$ are the electron and positron wave-functions, respectively. This integral, as described by Ferrell (1956), is the electron density operator at the position of the positron, averaged over the positron position. In other words, the

1 Heitler, W. loc. cit. p. 206.

normal free-electron Dirac transition probability is normalised to a new electron density at the position of the positron.

A. Simple Coulomb Enhancement:

Karpman and Fisher (1956) considered the case of a pure coulomb attraction between the positron and the electron. This coulomb attraction distorts the incoming electron plane wave, thereby increasing the electron wave-function at the positron by the factor $\frac{2\pi\alpha/\beta}{(1-\exp(-2\pi\frac{\alpha}{\beta}))}$, where β is $\frac{v}{c}$, and α is the fine-structure constant. For the electron velocities found in metals, however, the exponential term is negligible, resulting in a 1/v type of enhancement factor. As a result, the low velocity electrons are deflected more strongly by the coulomb field of the positron than are the high velocity electrons, resulting in an enhancement of the low velocity electrons at the position of the positron. The cross-section given in (2) is therefore modified to the following: $\sigma = \pi r_0^2 \frac{c}{v} \times 2\pi \frac{c}{v} \alpha = 2\alpha \left(\frac{\pi r_0^2 c}{v}\right)^2$ Thus, the probability per unit time of positron annihilation with electrons having velocities from v to v + dv at infinity, is: $dw = (\sigma v) \times 2 \times \frac{4\pi (mv)^2 d(mv)}{h^3}$

where m is the mass of the electron in the metal,
v is the velocity of the electron relative to the positron,
and the last term is the density of levels in phase space.
Integrating this equation from v = 0 to v = v_E (the velocity of the electrons on the Fermi surface), Karpman and Fisher obtained $w = \frac{\alpha^3 m}{h} v_E^2 \quad sec^{-1}$. The mean lifetime of a positron in the metal would then be given by: $\tau = \frac{1}{w} = \frac{m}{\pi^2 \alpha^3 k} \left(\frac{\pi}{3N}\right)^{2/3}$

where we have substituted for v_E an expression in terms of the density of Fermi electrons in a metal: $N = \frac{8\pi}{3}\left(\frac{m v_E}{2\pi\hbar}\right)^3$ Thus, this form of coulomb enhancement reduces the E dependence of τ from N^{-1} to $N^{-2/3}$, still a marked dependence, however. The theoretical estimates of the lifetime of positrons in metals, with this enhancement factor included, are: Al (0.61), Cu (0.96), Ag (1.6), and Au (1.6) where the values in parentheses are in units of 10^{-10} seconds. The positron lifetimes are therefore reduced by this method to values near those determined experimentally, except that a variation of a factor of three still exists between the various calculated values. Furthermore, the direct interpretation of the angular correlation data in terms of the momentum distribution of Fermi electrons requires a positron annihilation probability essentially independent of the electron velocity, as results, for example, in the free Dirac annihilation treatment. For these reasons, the simple coulomb enhancement modification given above, with its inverse velocity dependent annihilation rate, has been regarded by most as an unsatisfactory explanation of the short positron lifetime in metals.

Similar values for the lifetimes were calculated by Daniel (1957) who used a screened potential of the form $\frac{1}{r} e^{-qr}$ in determining the enhanced electron density at the positron. By performing a detailed numerical calculation of the electron enhancement in copper, he obtained a value of: 0.7×10^{-10} seconds for the positron lifetime. A more approximate method

of calculation provided the following results: Na(2.0), Al(0.8), and Cu(1.1) in units of 10^{-10} seconds. Since this enhancement depends on a screened potential, its effect on distant electrons is attenuated to a much greater degree than the pure coulomb attraction discussed earlier. As a result, the density enhancement of the low-velocity electrons would probably not be as strong as that of the earlier model, although the actual velocity dependence of the annihilation rate was not discussed by Daniel. The dependence of the lifetime on the electron density is still too large to be consistent with the experimental results, however.

B. Coulomb Enhancement of the Entire Fermi Sea.

The more complicated case of considering a screened coulomb interaction between the positron and all the electrons, not only the annihilating pair, has been discussed by Ferrell (1956). He considers all the electron wave functions to be modified, relative to plane waves, by the factor $1 + Ce^{-\frac{r}{a}}$, which is practically unity for all values of r greater than about 2a. The constant C determines the enhancement factor, $(1 + C)^2$, of the electron density at the positron. The parameters, C and a, are then determined by a variational approach, namely that of minimizing the total correlation energy. His results for such an analysis indicate a value for C of: $0.66\ V_s^{\frac{1}{4}}$, where V_s is a measure of the volume per conduction electron in the material (i.e. a volume of 1/N, where N is the conduction electron density) in units of $\frac{4}{3}\pi r_o^3$, the volume of a sphere of radius equal to the Bohr radius, r_o, (V_s is equal to r_s^3 in

Ferrell's notation). Thus, for a free Dirac lifetime of $\frac{V_s}{12}$ nsec., the enhanced value becomes $\frac{1}{(1+0.66V_s^{1/4})^2}\frac{V_s}{12}$ nsec. The enhanced lifetimes for a few examples, are: Na(6.3), Al(1.6), Cu(2.8), where the values are again given in units of 10^{-10} sec. Again, the introduction of an enhancement factor increases the annihilation rate, bringing the lifetimes into closer agreement with the experimental values. The theoretical values, however, are close to the experimental ones only for those metals with fairly high conduction electron densities, as in the case of aluminum, for example.

This form of enhancement is, in addition, consistent with the angular correlation data, since, according to Ferrell, the annihilation rate for the fastest electrons in a metal is only ten to twenty per cent greater than for the slowest. According to this model, the density of the faster electrons is more enhanced at the positron because the Pauli exclusion principle allows only the electrons near the top of the Fermi band to have properties similar to those of classically free electrons.

In summary then, positron annihilation rates in metals can be substantially increased over those predicted by the Dirac free electron theory by several models of electron enhancement at the positron. Some of these, however, lead to strongly velocity-dependent annihilation rates which are incompatible with the interpretation of angular correlation data in terms of Fermi electron momentum distributions. An exception to this statement is the enhancement model, deduced by a variational approach involving a screened coulomb interaction between the

positron and all the electrons, yielding an annihilation rate which varies by less than twenty per cent for the different electron velocities in the Fermi sea. Even the latter form of enhancement, however, is unable to explain the constancy of the lifetime of positrons from metal to metal.

It should perhaps be pointed out here that the velocity-independent nature of the annihilation rates calculated by the last theory described above results primarily because of the initial form of enhancement assumed for the positron-electron wave-function. That is, the same enhancement factor, $(1 + Ce^{-r/a})$ is assumed to apply to <u>all</u> the plane-wave electron wave-functions of various momenta. Removal of this somewhat drastic assumption would probably result in an electron enhancement somewhat intermediate in nature between that calculated by Daniel and Ferrell. In other words, the constant, free-electron wave-function should probably be enhanced first by a method similar to that of Daniel (1957), which is based on the screened coulomb potential outlined in Mott and Jones, 1936, (pg. 87), before performing a Fourier decomposition in order to determine the momentum distribution of the electrons described by the wave-function.

3. <u>Annihilation From Bound Positron-electron States</u>.

Ferrell (1956) attempted to limit the maximum lifetime of positrons in metals of low conduction electron density by invoking the formation of positronium ions (a system consisting of two electrons bound to a positron) in these metals. The stability of such a system was checked by Hylleraas (1947) who deduced a binding energy of about 0.2 electron volts.

Thus, if there is room in the crystal lattice for the formation of these large atoms (a question raised and discussed to some extent by DeBenedetti et al, 1950), electron capture by the positron would not stop with the formation of the positronium atom but would continue until the full quota of two electrons was captured by the positron. Ferrell assumed that in a normal metal (like aluminum) the conduction electron density is so high that a negative potential energy (of greater magnitude than the binding energy of the positronium atom) attributed to positron-electron correlations prevents the formation of bound states in which the positron is correlated strongly with only one or two electrons rather than all of them. On reducing the electron density, and hence the magnitude of the correlation energy, the point is eventually reached where the correlation energy is about the same as that of the binding energy of the positronium atom. Under these conditions the positron is assumed able to capture particular electrons, correlating strongly with them, thus forming positronium ions.

A. Characteristics of Positronium Ion Decay.

A two-parameter estimate of the wave function of the positronium ion has been shown by Hylleraas (1947) to be of the form:

$$\Psi(r_1, r_2) = C_0 e^{-\frac{r_1+r_2}{2C_3}} \left[1 + C_2\left(\frac{r_1-r_2}{C_3}\right)^2\right]$$

where the constants C_j are functions of two parameters, varied to minimize the total energy of the system. Using this wave function for the ion, Ferrell (1956) calculated the lifetime of the positrons in this configuration to be about 3.25×10^{-10}

seconds, with a possible error of ten to twenty per cent, depending on the accuracy of the trial wave function.

Since the Pauli principle requires the two electrons to have opposite spin directions in the ground state of the positronium ion, annihilation of the positron with one of them (spins parallel) would always result in three-quantum annihilation, whereas annihilation with the other (spins oppositely directed) would be from a state consisting of the three-photon emitting triplet state half the time, and the two-photon emitting singlet state the other half, (since $\alpha_- \beta_+ = \frac{{}^0\varphi_0 + {}^0\varphi_1}{\sqrt{2}}$ where α_- and β_+ are the two oppositely-directed spinors of the electron and positron, respectively, and ${}^0\varphi_0$ and ${}^0\varphi_1$ are singlet and triplet wave-functions of zero m value, respectively). This is substantiated by a more detailed treatment, where the wave-function of the ion, ${}^m\psi_j$, diagonalized with respect to the total angular momentum and the various m values, is expanded in terms of ${}^0\varphi_0$ and ${}^m\varphi_1$, the spin functions for the electron-positron pairs. If we take, for example, $J = \frac{1}{2}$, $m = \frac{1}{2}$,

$$ {}^{\frac{1}{2}}\psi_{\frac{1}{2}} = \frac{1}{\sqrt{2}} \beta_2 {}^1\varphi_1 - \tfrac{1}{2} \alpha_2 {}^0\varphi_1 - \tfrac{1}{2} \alpha_2 {}^0\varphi_0 $$

as shown in Appendix (D), where α_2 and β_2 are the two spinor functions describing one of the electrons (the recoil electron, say). It is seen that the probability coefficients of the final state spinor functions agree with those given in the earlier rough estimates. Since the total annihilation rate, R, is:

$R_{ion} = \frac{1}{2} R_{3\gamma} + \frac{1}{4} R_{3\gamma} + \frac{1}{4} R_{2\gamma}$ where $R_{3\gamma}/R_{2\gamma} = 1/1100$ (p. 26)

then, $R_{ion} = \frac{R_{2\gamma}}{4}\left[(1)_{2\gamma} + 3\left(\frac{R_{3\gamma}}{R_{2\gamma}}\right)_{3\gamma}\right]$ which indicates three-quantum annihilation of an intensity 1/370 that of two-quantum annihila-

tion, a situation indistinguishable from free positron annihilation with randomly oriented electrons, and hence, in agreement with observation (Basson, 1954). Following the annihilation of the positron and one of the electrons, the remaining electron can not be left in any arbitrary momentum state because of the Pauli exclusion principle, but must enter a vacant momentum state in the Fermi sea. In other words, if the positronium ion has been slowed to thermal energies before annihilation (by the same processes as those which govern the thermalisation of a positron, Garwin, 1953; and Lee-Whiting, 1955), the annihilation gamma rays must carry off a momentum equal and opposite to that carried away by the remaining electron. Since there will exist at least two vacant states formed by the capture of the two electrons from the Fermi sea by the positron, it might be expected that the momentum distribution of the recoil electron (and hence of the annihilation gamma rays) would be that of the Fermi sea of electrons.

An explanation of the type given here, however, is ruled out because of the very short relaxation times of the electrons in the Fermi sea. A consideration of the relaxation process involved in collisions of the Fermi electrons with the crystal lattice, for example, yields an estimate of the relaxation time in a metal of the order of 10^{-14} seconds.[1] On the other hand, calculations of the time involved in the filling of a positive valence hole by Auger processes have indicated possible times of

1 Kittel, C., Introduction to Solid State Physics, (John Wiley and Sons, Inc., N. York, 1953), First Edition, pg. 247.

the order of 10^{-16} sec (Landsberg, 1949). Thus, the relaxation time is far too short for an explanation of the annihilation gamma-ray angular correlation results by the simple model described earlier. If a rapid, electron exchange mechanism between the positronium ion and the conduction electrons is assumed, however, of a rate at least that of the relaxation of the valence electrons, vacant states would still be available in the conduction band at the time of annihilation of the ion. The collision rate between a positronium atom and the conduction electrons in a typical metal is of the order of: $\pi r_o^2 \times vN \sim \pi r_o^2 \alpha c N$, (Gerholm, 1956), where r_o is the Bohr radius; thus giving, for N of about 10^{22} electrons/cm^3, a rate of $\sim 10^{15}$ exchanges/sec, a value of the same order as the estimated relaxation time of the valence band holes. This rate is, however, calculated on the basis of conduction electron collisions with an isolated solid sphere of a radius equal to that of a hydrogen atom. An exchange rate greater than this value should occur in reality, however, due to the expected overlap between the electronic wave-functions of the positronium ion and those of the valence electrons from the neighbouring metal atoms. A significant overlap would indicate a substantial sharing of these electrons between the two systems, resulting in an enhanced electron exchange rate probably of sufficient magnitude to exceed the Fermi electron relaxation times, and so result in a momentum distribution of the positronium ions at the time of annihilation equal to that of the electrons in the Fermi sea.

Problems concerned with the stability of the weakly-

bound positronium ion under bombardment by energetic electrons in the Fermi sea, are also simplified when the effects of the Pauli exclusion principle are considered. Since an incident electron cannot change its momentum if the neighbouring momentum states are occupied (as they are in a Fermi sea), anything other than exchange collisions with the positronium ion are forbidden.

If the above assumptions concerning the formation and decay of positronium ions in metals are admitted, the resulting observable effects are consistent with the experimentally determined results, viz:

(a) a three-photon to two-photon ratio of 1:370.

(b) a short lifetime of about 3×10^{-10} seconds.

(c) a constant lifetime from metal to metal, because the electron density at the positron is determined only by the wave-function product within the ion, independent of the conduction electron density in the metal.

(d) a consistency with the interpretation of the annihilation angular correlation data in terms of the momentum distribution of electrons in a Fermi sea.

B. Characteristics of Positronium Atom Decay.

In a similar way, the annihilation of positrons from positronium atoms is also consistent with the experimental data if the assumption of rapid electron exchange is introduced. Such an assumption is necessary to insure a simple exponential decay function, as outlined in Chapter I, and also to produce the three-quantum to two-quantum ratio of 1:370 as observed experimentally. If, as suggested by Ferrell, collisions of the

conduction electrons with the positronium atoms results in a transfer of the positron from one electron to another, the momentum distribution of the positronium atoms will be just that of the Fermi electrons. The rapid electron exchange, therefore, produces a lifetime for the system which is four times that of a free atom in the singlet state, (as discussed in more detail in Chapter I, Section 5), that is, 5×10^{-10} seconds.

Thus, in terms of positron annihilation from bound states, consistency with the usually-accepted interpretation of the angular correlation results no longer requires a velocity independent annihilation probability, but, instead, requires that the momentum distribution of the annihilating positron-electron pairs be the same as that of the conduction electrons.

C. Formation of Positronium Atoms and Ions in Metals.

There are two major problems involved in the hypothesis of the formation of and the existence of positronium atoms (or ions) in metals. The first involves the question of sufficient "room" for the existence of a bound state in the metal structure, and the second involves the time required for the formation of such a state.

Although the general problem of the stability of such a bound positron-electron state within a metal lattice has not been treated in detail, several aspects of the problem have been discussed by various authors. One of these is concerned with the volume available for the positronium atom within the crystal lattice. This question was discussed to some extent by

DeBenedetti et al (1950), who considered the positronium atom in a crystal in terms of an atom confined within an impenetrable sphere. As an example of this, it was pointed out that the binding energy of a hydrogen atom becomes positive if it is enclosed in an impenetrable sphere of diameter less than 1.84 times the diameter of the isolated hydrogen atom Bohr orbit. This argument is probably applicable in many types of ionic crystals where the atoms are closely packed. In metals, however, the metallic ion cores frequently represent a rather small fraction of the volume of the unit cell, being less than about fifteen per cent for the metals Lithium, sodium, beryllium, magnesium, aluminum, germanium, tin, bismuth, calcium, barium, zinc, cadmium, and lead (Lang and DeBenedetti, 1957). In aluminum, barium, calcium, and lead, for example, consisting of face-centred cubic and body-centred cubic lattices, the maximum interstitial volume available in the lattices would contain a sphere of diameter a-2b, where a is the lattice constant, and b the ionic radius. These values, calculated for the above metals, range from 3.58 A^{o} for calcium, to 2.31 A^{o} for barium, most of them well in excess of the diameter of the positronium atom, viz 2.1 A^{o}. The existence of analogous bound systems in many semi-conductors, such as electrons bound to impurity atoms, and the formation of bound electron-hole systems (excitons) suggests that the relative volume of the ion cores is frequently not too large for stable binding.

The other aspect considered in the formation of positronium in metals is the effect of the high conduction electron density. This question was discussed by Karpman and Fisher (1956) and

Ferrell (1956). Karpman and Fisher regarded the high electron density to be sufficiently effective in screening the coulomb potential of the positron that the formation of a bound state was impossible. Actually, the effective screening distance (corresponding to the Debye-Hückel screening radius considered in the theory of electrolytes) of the potential of an isolated point source due to the surrounding conduction electrons is $\gtrsim 2A^{o}$ (Mott and Jones, 1936, pg.88) for most metals. If a bound state could be formed, they concluded that the screening effect would reduce the binding and smear the wave function out over a larger volume. Such a screened potential, however, is similar to that employed in the analysis of the "exciton" structure[1], described earlier.

Ferrell, on the other hand, chose to consider the problem in terms of a correlation binding energy due to many-body interactions between the positron and all the electrons, according to a collective interaction formulation outlined by Bohm and Pines (1952). Ferrell estimated that for the electron densities found in most metals, this correlation energy is more negative than the positronium binding energy by a factor of between two and three, thus preventing the formation of a bound state. Because of the drastic nature of the assumptions involved in the form of the enhancement factor (as discussed in greater detail on pg 33), however, a detailed comparison of the relative magnitudes of the correlation energy and the positronium binding energy is probably

1 Kittel, C., Introduction to Solid State Physics, (John Wiley and Sons, Inc. N.Y.) Second Edition, p.505.

unwarranted at the present time.

The second question mentioned earlier, regarding the formation time of positronium atoms, has been discussed in some detail by Bég and Stehle (1959). These authors point out that the cross-section for ordinary radiative capture of a free electron into a bound state is about an order of magnitude smaller than the observed annihilation cross-section of the positron. They indicate, however, that in a free electron gas, the capture rate is considerably increased by means of Auger transitions of a third electron to an energy greater than the Fermi energy of the gas. Thus, their analysis is restricted, essentially, to the formation of bound states in metals. The results of their calculations indicate that the capture rate involved in the formation of positronium atoms is of the order of 10^{15} per sec for thermalised positrons. This result should be most accurate in the case of low electron density, N, (such as in the alkali metals), where their approximations are most applicable. The rate would increase with N, though not as fast as N^2, since, with increasing Fermi energy, the low-lying electrons cannot participate in the process. However, their approximations, as well as the assumption of a hydrogenic ground state for positronium, get progressively worse for increasing N. Although they did not discuss the equivalent process for the formation of the positronium ion, it would seem that their description would probably apply in this case too, with, perhaps, a capture rate somewhat less than the 10^{15} per second, given above.

4. Consistency with Experimental Results:

The various measurable properties of the annihilation process as predicted by the two main types of theory (i.e. annihilation during collision versus annihilation from a bound state) were examined in order to determine which of the suggested models has the strongest experimental support:

(a) Shape of Decay Curve: Both types of model yield a pure exponential decay curve if the thermalisation time of the positrons can be considered negligible (and there exists strong theoretical support for this expectation). The condition under which the bound-state model leads to a single simple exponential decay is described in the previous section: i.e. a rapid electron exchange mechanism is required for the positronium atom, but is unnecessary for the positronium ion.

(b) Angular Correlation Results: In those metals characterised by large lattice spacings (see pg 133), the measured angular correlations of the annihilation gamma rays implies a momentum distribution of the annihilating positron-electron pairs equal to that of the particular conduction electrons concerned. This observation is predicted by both theories if the following restrictions are assumed:

(i) Annihilation during Collision: Both the free Dirac annihilation theory and the modified form involving correlations between the positron and the electrons are compatible with this observation, but that described by pure coulomb enhancement of the annihila-

tion cross-section is not.

(ii) Annihilation from Bound States: Annihilation from both the positronium atom and the ion configurations are compatible with this result if rapid electron exchange collisions are assumed.

(c) Two-Photon: Three-Photon Yield: Both theories yield the same theoretical value of 370:1.

(d) Absolute Positron Lifetime in Aluminum: The lifetime results listed here (in units of 10^{-10} seconds) are those calculated on the basis of annihilation with the conduction electrons of aluminum only, as necessitated by the results of (b) above. The reasons for the choice of aluminum as an example were twofold: First, aluminum is one of the metals of DeBenedetti's Group A classification, (see pg133), indicating an angular correlation distribution of the type described above. Also, it is the metal for which most of the absolute lifetime determinations have been performed, and so should be known most accurately. The free Dirac annihilation theory predicts a value of: 7.5 (x 10^{-10} sec). Simple coulomb enhancement yields a value of: 0.61 - 0.8.

The Ferrell many-particle correlation model gives: 1.6

For the bound-state models we have:

Positronium atom with rapid, electron exchange: 5.0

Positronium ion with or without electron exchange: about 3.0

(e) Positron Lifetime Dependence on Conduction Electron Density, N: Both bound state models indicate annihilation

rates which are independent of the conduction electron density, to first order. A marked deviation from hydrogenic orbits under high electron density would naturally have an effect on the annihilation lifetime of the state. All the collisional-annihilation processes, on the other hand, yield a significant dependence. The free-electron Dirac annihilation process yields an annihilation rate proportional to N. The Ferrell correlation model yields a first-order dependence on N, with correction terms of higher-order, and the simple Coulomb enhancement theory predicts a dependence on $N^{2/3}$.

(f) Metal Structure Effects: Possible effects attributable to environmental conditions in the neighbourhood of the positron should also be considered as a means of distinguishing between the various suggested mechanisms for positron annihilation.

(i) The Collisional Annihilation Process:

Since a collisional annihilation process is only dependent on the conduction electron density, variations in the structure of the metal should exhibit a relatively minor effect. Thus, changes in the phase of the material (e.g. solid to liquid), and the structural changes involved in different lattice configurations, should have no effect on the positron lifetime, providing the metallic density (and hence the density of the conduction electrons) remains unaltered. On the other hand, changes which alter the physical

density significantly, as, for example, marked temperature changes, should affect the annihilation rate to approximately the same extent.

(ii) Annihilation from a Bound State: In the case of positron annihilation from a bound state, however, quite different dependences would be expected. Since the annihilation of a positron in a bound positron-electron system is dependent on the detailed nature of the wave-function of the system, and therefore on the volume available in the interstitial regions of the metal, the characteristics of the lattice structure should be much more significant for this case than for that of the conduction electron density. Thus, a dependence of the annihilation rate on changes in the lattice configuration (especially for the various allotropic forms of a particular metal), and the phase of the metal (liquid to solid) should result, independent of the conduction electron density. In other words, the effect on the lifetime due to a density change resulting from a change of the allotropic form, or the phase of the metal, could well be more significant than that due to an equivalent density change resulting from a change in temperature or pressure. The dependence of the lifetimes measured in this work on the structural form of the absorber is discussed in some detail in Chapter VII.

(g) Magnetic Effects: Although, at first sight, it might

appear that annihilation of a positronium ion might be distinguishable from that of a positronium atom by a difference, say, in the relative triplet-singlet state admixture in response to the application of a magnetic field, the effects of such admixtures are completely obscured by the very rapid electron exchange mechanism assumed. In other words, the magnetic enhancement effect can only be detected when observing a "complex" decay, with two distinct lifetime components, by its effect on the relative intensities of the two lifetime components. If an exchange process exists which is sufficiently rapid (as is assumed in the case of metals) to quench completely the long-lived component, then it is obviously meaningless to discuss the possibilities of any further quenching by an applied magnetic field. Thus, for positron annihilation from bound states, no apparent effect should result from the application of a magnetic field.

For the case of collisional annihilations, however, a slight dependence of the ratio of two-photon to three-photon annihilations may occur depending on the direction of the applied magnetic field (Hanna and Preston, 1958). Since the positrons emitted by Na^{22} which enter an absorber are actually polarized along their direction of motion (Page and Heinberg, 1957), the relative probabilities of occurrence of triplet and singlet states during positron-electron collisions is then a function of the direction of the alignment of the relative spins of the electrons and positrons, and the direction of the electron orientation can be controlled to an

extent by the application of an external magnetic field. Small two-photon enhancement effects of this sort have been observed and described by Hanna and Preston,(1958). Such effects, then, could be expected for those annihilations resulting from collisional processes such as those described by the free, Dirac annihilation process, and "pick-off" annihilations between positrons in bound states and polarized electrons from a neighbouring atom. For collisional positron annihilations in a Fermi sea of electrons, however, only the few electrons at the top of the sea are capable of any net polarization (Mott and Jones, 1936, pg 184). Thus, only positron annihilation with oriented core electrons (such as can occur in the transition metals) should possess any marked effects of the type described above.

A consideration, now, of the available experimental data yields the following checks:

(a) The decay curve describing positron annihilation in metals has been assumed exponential in shape (although no experimental verification exists due to limitations in the instrumental resolution available).

(b) With suitable restrictions applied to the models (as mentioned in (b) above) both forms of theory are compatible with the angular correlation data.

(c) The experimental value for the ratio of the two- tothree-photon yield from metals has been found to agree with the theoretical one within the experimental error (Chapter II,

Section 1).

It is obvious that the most sensitive tests of these theories are those labelled (d) and (e), both dependent on lifetime measurements. Experimental determinations of the lifetime of positrons in aluminum have ranged from 1.5 to 2.5 x 10^{-10} seconds. These values can be considered consistent with both the Ferrell correlation model and possibly the positronium ion model, without further modification. If the lifetime of the positronium atom is assumed to be different in a metal to that resulting from annihilation in free space (or if the theoretical calculations are fundamentally incorrect), then compatibility between the experimental results and that predicted by the positronium atom model might be possible.

It is in the comparative lifetimes for different metals that we have perhaps the most stringent test of the theories. The results of these measurements suggest that the lifetime of positrons is the same in all metals (measured to an accuracy of 0.7 x 10^{-10} seconds). Assuming possible variations in these lifetimes of an amount allowed by these limits, we find a possible variation of a factor of two in lifetime (if the lower limit of the absolute value in aluminum is accepted), whereas the collisional annihilation process with the least dependence on conduction electron density (viz. proportional to $N^{2/3}$) still yields an expected variation of about 4.5 for the electron density range considered. The predictions of the bound state model are clearly consistent with the results as far as independence of lifetime on electric density are concerned.

Since the lifetime results appear to represent an important measure of the validity of the various theoretical approaches, a more detailed analysis of the reliability of the various existing measurements will be presented.

5. Previous Experimental Results.

A. Sources of Systematic Error.

Because the lifetimes of positrons in metals are smaller than the resolving times of existing instruments, a determination of the lifetime from the measured delayed coincidence curve requires for analysis some form of comparison to an instrumental "prompt" curve. Ideally, the prompt curve should be obtained from a measurement of a source of radiation identical in all respects to that being investigated, except that the coincident radiations are simultaneous. Deviations from this ideal in actual measurements can give rise to a number of systematic errors, the most significant of which is that introduced when the radiations emitted by the prompt source differ in energy from those of the comparison source. The reason for this is the following. Assuming that the front edge of the light pulse (which decays with a characteristic time-constant, T) in the scintillator portion of the detector occurs immediately after the detected radiation is incident upon the crystal, then, as each of the photons strikes the photocathode surface of the photomultiplier, a photoelectron is ejected with a certain probability; usually less than ten per cent. The time resolution of the whole instrument, then, has as its ultimate limit

the uncertainty in the time of ejection of the first photoelectron. Post and Schiff (1950) derived an expression for the mean time delay for the ejection of the first photoelectron of the form: $\bar{t} = \frac{T}{R}\left(1+\frac{1}{R}\right)$, where R is the total number of photoelectrons in the pulse. For practical values of T and R, (T about five nanoseconds, and R a value less than one hundred), this uncertainty becomes comparable with the lifetimes to be measured. Although T is fixed for a given scintillator, R is linearly dependent on the intensity of the scintillations, and hence on the energy dissipated by the radiation in the crystal. Thus, an energy-dependent instrumental time shift develops, which is undoubtedly the major systematic error involved in the measurement of short lifetimes.

B. Methods for Measuring Positron Lifetimes.

In the measurement of positron lifetimes several methods have been employed for obtaining the prompt and delayed resolution curves.

(a) Positron lifetimes may be determined by measuring the time interval between the emission of the 1.28 Mev nuclear gamma ray of a Na^{22} positron source surrounded by a positron absorber and the 0.51 Mev gamma ray emitted by the annihilating positron. This method (employed by Ferguson and Lewis, 1953, Minton, 1954, and Gerrholm, 1956) actually determines the difference between the mean lifetimes of the positrons, and the 1.28 Mev gamma rays. Thus, it is a useful method for the determination of the positron life-

times only if the lifetime of the 1.28 Mev gamma ray is short compared to 10^{-10} seconds. Recent experimental evidence for such a short lifetime is discussed on page 90 . The absolute lifetime of the positrons in the absorber can then be determined by comparing the resulting coincidence resolution curve with a prompt resolution curve obtained using a source of pairs of coincident gamma rays. Although a "prompt" source yielding gamma rays of similar energies to those from Na^{22} would be desirable to minimize the energy-dependent, instrumental time shifts, such sources are extremely difficult to find. Thus, Co^{60}, which has a mean time interval between the two gamma rays (of energy, 1.33 and 1.17 Mev) of $(1.1 \pm 0.2) \times 10^{-12}$ seconds (Metzger, 1956) has been employed almost exclusively as the prompt source. To eliminate the type of systematic error described above, which tends to result from the use of a prompt source of gamma rays of these energies, workers using this method have employed differential pulse-height selectors in the system to ensure that the only coincidences that are counted are those produced by scintillations of similar intensity (and similar intensity distribution over the selected range) for both sources. In other words, only the fast coincidence pulses corresponding to the selected portions of the Compton spectra of the incident gamma rays are recorded.

(b) As an alternative approach, Bell and Graham (1952) measured the time interval between the detection of a pulse produced

by the energetic positron passing through a thin crystal of a scintillation counter, and the detection of the annihilation gamma ray in a second counter, emitted when the positron decayed in a sample material. The two counters were able to be separated in space because a beta-ray spectrometer was used to define the momentum (and hence the transit-time) of the accepted positrons. The delayed coincidence curve was obtained by allowing the selected positrons to be stopped in a positron absorber placed directly in front of the second scintillation counter. A prompt resolution curve was obtained, on the other hand, by removing the positron absorber, and allowing the selected positrons to impinge directly on the crystal of the second scintillation counter. The difference between these curves is then due to the lifetime of the positrons in the absorber, the transit time of the positrons in the spectrometer subtracting out.

(c) Comparisons of the lifetimes of positrons in various materials is facilitated by comparing only the resulting resolution curves, thus yielding the differences in the lifetimes for the various absorbers. In this way, possible systematic errors due to differences in spectral shapes, and differences in counting rates, are completely eliminated.

C. Numerical Results of the Positron Lifetime Measurements.

(a) Absolute Lifetime Determinations.

The numerical values obtained for a number of metals (in units of 10^{-10} seconds), and a discussion of the

technique involved in the measurements, is given below.

(i) Aluminum: Bell and Graham (1953) by the method involving the use of a beta-ray spectrometer, obtained a value of: 1.5 ± 0.3

The following workers used Co^{60} as a prompt source.

Ferguson and Lewis (1953) obtained the value: 1.6 ± 0.6

Minton (1959), on the other hand, measured a lifetime of: 2.4 ± 0.6

Gerholm (1956) stated a similar result: 2.5 ± 0.3

(ii) Gold: Bell and Graham also measured the absolute lifetime of positrons in gold, using the same technique as that described for aluminum. Their result for this material was: 1.2 ± 0.3

(iii) Lead: Using a "diode" time-sorter, similar to that described by Jones (1955), Sunyar (1957) measured the lifetime of positrons in lead. The nature of the prompt resolution curve used in his analysis was not reported.

The result he obtained was: 1.6 ± 0.15

Gerholm, however, found no difference (to $\pm 0.3 \times 10^{-10}$ sec) between his values for lead and aluminum (from the comparative results described later in this section).

It is interesting that the determinations of the absolute lifetime of positrons in aluminum (and lead) show such a large variation, and also appear to be segregated into

two principal groups, one centred at about 1.5 x 10^{-10} sec, and the other at 2.5 x 10^{-10} sec. Since the major portion of the quoted errors were probably statistical in nature, it is felt that the major causes of the disagreement in these values are due to the existence of systematic errors due to: (1) energy-dependent time shifts of the type described in part (a) of this section, and (ii) variations in the count-rates between the two comparison sources.

In an attempt to minimize systematic errors of type (i) above, Bell and Graham set their spectrometer to select positrons of 220 Kev, an energy near the mean of the range of the annihilation Compton spectra selected by the side channel discriminator (viz. 150 - 340 Kev). With this arrangement, they estimated the difference in time delay between the sample-out and sample-in conditions to be less than 0.2 x 10^{-10} sec. Although the means of the two energies are similar, Gerholm (1956) suggested that the lack of similarity in the spectral shapes under the two conditions could give rise to changes in the instrumental delay of the order of 10^{-10} seconds. Several other possible contributing sources of error in the lifetime determinations of Bell and Graham are also discussed by Gerholm.

Gerholm, on the other hand, attempted to minimize this instrumental time shift by employing a comparison source of similar gamma-ray energies to those of Na^{22}, viz. Pb^{207}, which emits several gamma rays, the two predominant ones (of energies 1.06 and 0.57 Mev) being in cascade. A Bi^{207} source was therefore employed, which, following decay by electron capture to the 1.63 Mev state of Pb^{207}, de-excites through the 0.57 Mev

level to the ground state, thus emitting the two gamma rays mentioned above. The mean lifetime of the 0.57 Mev level was first determined by Stelson and McGowan (1955) by a measurement of the transition probabilities involved in a Coulomb excitation of the level, resulting in a value of $(1.0 \pm \frac{0.4}{0.2}) \times 10^{-10}$ sec. A determination by delayed coincidence techniques (Sunyar, 1957), yielded a value of: $(1.1 \pm 0.15) \times 10^{-10}$ sec.

With one side channel window set to detect the top portion (about forty per cent) of the annihilation gamma ray Compton spectra, and the other adjusted to detect everything above 500 Kev of electron energy, Gerholm (1956) found that the lifetime of positrons in aluminum was longer than the mean lifetime of the first excited state of Pb^{207} by $(1.1 \pm 0.3) \times 10^{-10}$ sec, indicating a positron lifetime greater than the 1.5×10^{-10} sec measurement of Bell and Graham.

Gerholm then measured both positron-in-aluminum and Pb^{207} lifetimes using Co^{60} as a prompt source, both measurements being performed under identical conditions. His results were then calculated by averaging the measurements for both "normal" and "inverted" modes of operation of his instrument. By an "inverted" mode of operation is meant that mode which results when the settings of the two side channel analysers are interchanged, so that the detector which normally detects the "delayed" pulse, would, under the inverted mode of operation, detect the "prompt" (or zero time) pulse. The final results quoted by Gerholm are: $(2.5 \pm 0.3) \times 10^{-10}$ seconds for the lifetime of positrons in aluminum, and $(0.9 \pm 0.3) \times 10^{-10}$

seconds for the lifetime of the 0.57 Mev state of Pb^{207}. The good agreement between his value for the first excited state of Pb^{207} and the values quoted earlier adds to the reliability of his result for the lifetime of positrons in aluminum.

It is clear from this collection of measurements, that a more accurate determination of the lifetime of positrons in metals, associated with a thorough quantitative investigation of the systematic errors involved in these measurements is required before attempting to establish the detailed nature of the positron decay processes.

(b) Comparative Lifetime Measurements:

The results of the comparison measurements described in Section B (c) of this chapter will be given next. An interesting observation regarding these values is the degree of consistency between the results of different workers. This would be expected if the deviations in the absolute value measurements were due to the type of systematic error which subtracts out in the comparison measurements.

(i) Comparisons With an Aluminum Reference:

DeBenedetti and Richings (1952) found that the differences in the mean lifetimes of positrons in the metals: lithium, sodium, potassium, silver, lead, and copper, as compared to aluminum, were $(0 \pm 0.7) \times 10^{-10}$ seconds.

Bell and Graham (1953) determined that the mean positron lifetimes in aluminum, beryllium, copper and mercury (liquid) were constant within 0.4×10^{-10} seconds.

Minton (1954, 1959), however, detected a significant

difference between the mean lifetimes of positrons in lead and aluminum, yielding an increased lifetime in the lead of $(0.5 \pm 0.3) \times 10^{-10}$ seconds.

Gerholm, on the other hand, detected no difference (within 0.3×10^{-10} sec) between the mean lifetimes of positrons in lead, copper, and iron.

(ii) Comparisons with a Lead Reference:

Ferguson and Lewis (1953) found that the mean lifetimes of positrons in aluminum, magnesium, and iron, were the same as in lead to an accuracy of 0.5×10^{-10} seconds.

Although the results of the comparative measurements listed above have been interpreted as indicative of a constant positron lifetime, independent of the nature of the metal absorber (Bell and Graham, 1953), it is evident that measurements of greater accuracy are required in a larger number of metals before any conclusions about the nature of positron annihilation in metals are justified.

CHAPTER III

DEVELOPMENT OF A FAST TIME SORTER

1. Introduction.

Equipment used for measuring short time intervals in the range 10^{-11} to 10^{-6} seconds is generally one of the following two types: either a "delayed coincidence circuit" or a "time sorter". The delayed coincidence circuit is a single-channel time-measuring device, in which voltage pulses from two detectors are counted when they are coincident in time. In practice, a coincidence is counted when the pulses arrive within a short time interval of each other, this time interval being termed the electronic resolution time of the instrument. When measuring short lifetimes with this form of apparatus, coincident count rates are normally recorded as a function of the amount of time delay inserted in one of the detector circuits. Such circuits (and their application in the measurement of short lifetimes) have been fully described by Bell (1954, 1955). Multichannel coincidence circuits, or "Chronotrons", have also been designed (Ticho and Gauger, 1956), but have not found wide acceptance because of their complex mechanical design and inflexible time characteristics (the time channel width, for example, is fixed by the mechanical design).

The "time sorter", another form of multichannel time-measuring device, consists of a circuit capable of producing voltage pulses whose amplitudes are a measure of the time interval between the pairs of input pulses. This "time-to-

pulse-amplitude converter" may then be followed by a conventional kick sorter (multi-channel pulse amplitude analyser) to complete the instrument. The advantage of increased capacity for data collection afforded by such a multi-channel instrument more than compensates for the slightly increased electronic complexity.

A form of time sorter which has seen fairly widespread use employs a 6BN6, gated-beam tube with two control electrodes in the time-to-pulse-amplitude converter, and was first described by Neilson and James (1955). This circuit, however, failed to achieve the resolution times attainable with the delayed coincidence circuit of Bell et al. (1952). This was partly attributable to the necessity of developing larger pulses for operation of the 6BN6 converter than was necessary in the circuit of Bell et al., which employed a crystal diode in the coincidence detector. The loss of bandwidth associated with the higher gain required for the 6BN6 circuit thereby reduced the intrinsic resolution time of the instrument.

Since good resolution (hence, a high bandwidth) linearity of response in the nanosecond range, and high electronic stability were desired for the measurements described in this thesis, it was considered desirable to utilize a modified form of the time sorter described by Jones and Warren (1956) in which a crystal diode was used as the sensitive element in the converter circuit. Since microwave diodes have a higher operating bandwidth and require smaller signals for operation than do vacuum tubes of the 6BN6 type, a time sorter circuit based on these

components was developed.

The basic circuit and operation of the type of time sorter to be discussed in this section was described by Warren and Jones, 1958, as having the following characteristics:

(a) An intrinsic electronic resolution time of less than .05 nsec.

(b) A resolution time, using prompt gamma rays from Co^{60}, of 0.8 nsec.

(c) An electronic stability of better than 1% (i.e. less than .05 nsec.) over the course of a day.

(d) Linear time calibrations in the range of one to ten nanoseconds.

2. Description of the Time Sorter.

A standard fast-slow coincidence system (Bell et al, 1952) was employed as shown in fig.1, with limiters or equalizers following the scintillation counters to produce the necessary step voltage pulses for operation of the time sorter itself. The operation of the time-to-amplitude converter circuit is similar to that described by Jones and Warren (1956) and is described briefly as follows (fig. 2):

(a) Upon detection of a gamma-ray of sufficient energy, the limiter produces a step voltage (rise-time estimated at less than one nsec), which, after a flat plateau of about one microsecond, recovers with a longer time-constant (about one hundred nanoseconds).

(b) Upon reaching the time sorter, this step is clipped by a

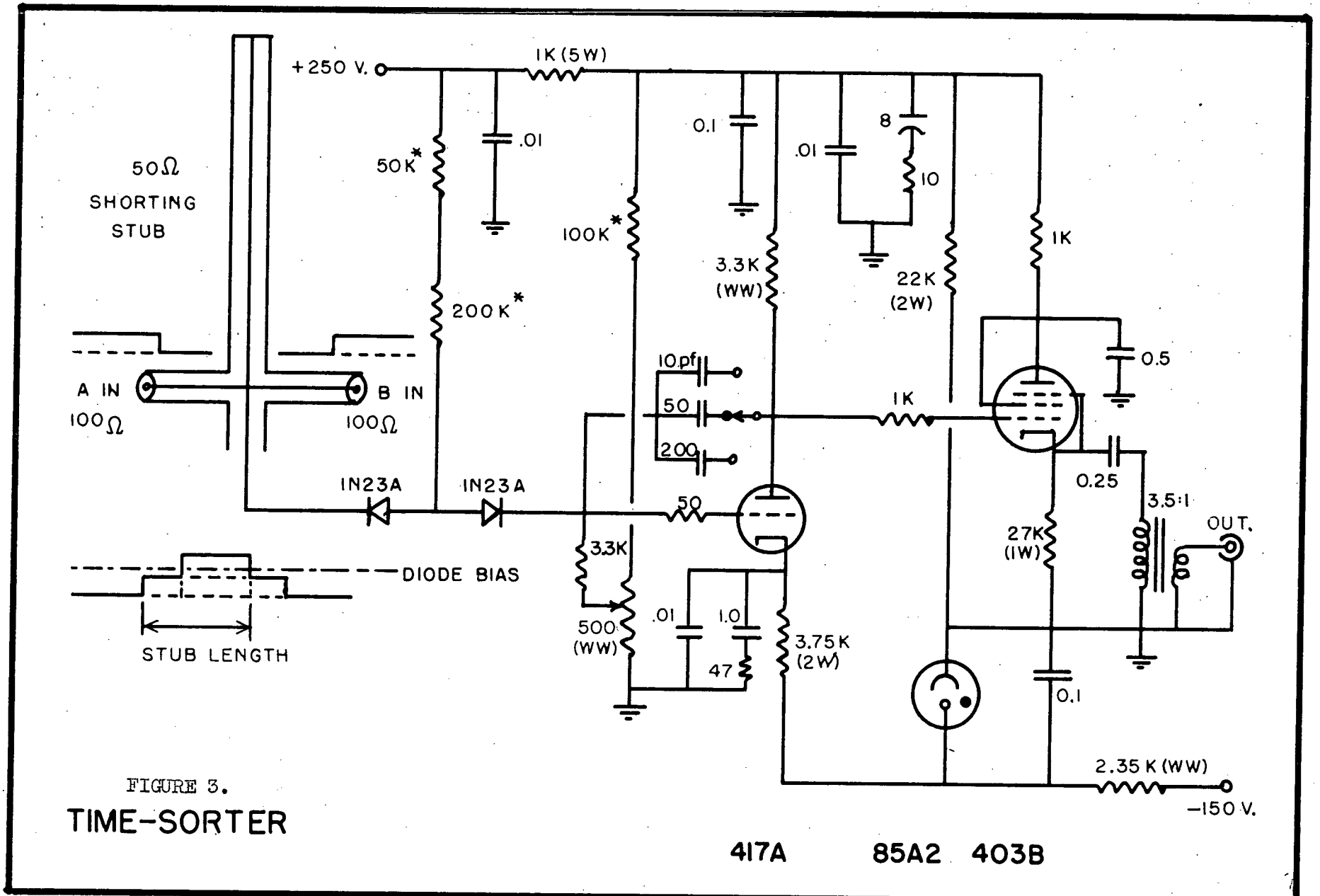

FIGURE 3.

TIME-SORTER

shorting stub to a fixed length, τ_o (about fifteen nanoseconds).

(c) If a pulse is produced by the second limiter within a time τ_o of activation of the first limiter, a linear superposition of the two waveforms occurs at the input to the shorting stub. If the converter is biased to the level shown, only the overlap portion of the pulse will be transmitted into the integrator circuit.

(d) In the time sorter a fast diode switch is operated by the overlap pulse, and a fixed current is integrated for a time determined by the length of the overlap. After amplification, then, a pulse of the form shown in fig. 2(d) is obtained.

The purpose of the ancillary apparatus shown in the block diagram, fig. 1, is adequately described by Jones (1955).

3. Detailed Description of Individual Units.

(A) Time-to-Pulse Height Converter:

The circuit diagram of the converter is given in fig. 3. The circuit is simply a fast current switch consisting of two microwave diodes followed by a Miller integrator.[1] Preceding the diode switch is a shorted stub clipping line, used in the same manner as that described by Bell et al (1952). In contrast to the 6BN6 time sorter system (Neilson, 1955) in which separate clipping lines are incorporated into each limiter, this system utilizes a

---

1 Farley, F.J.M., "Elements of Pulse Circuits", (Methuen Monograph), Methuen and Co., Ltd., England (1956), p. 76.

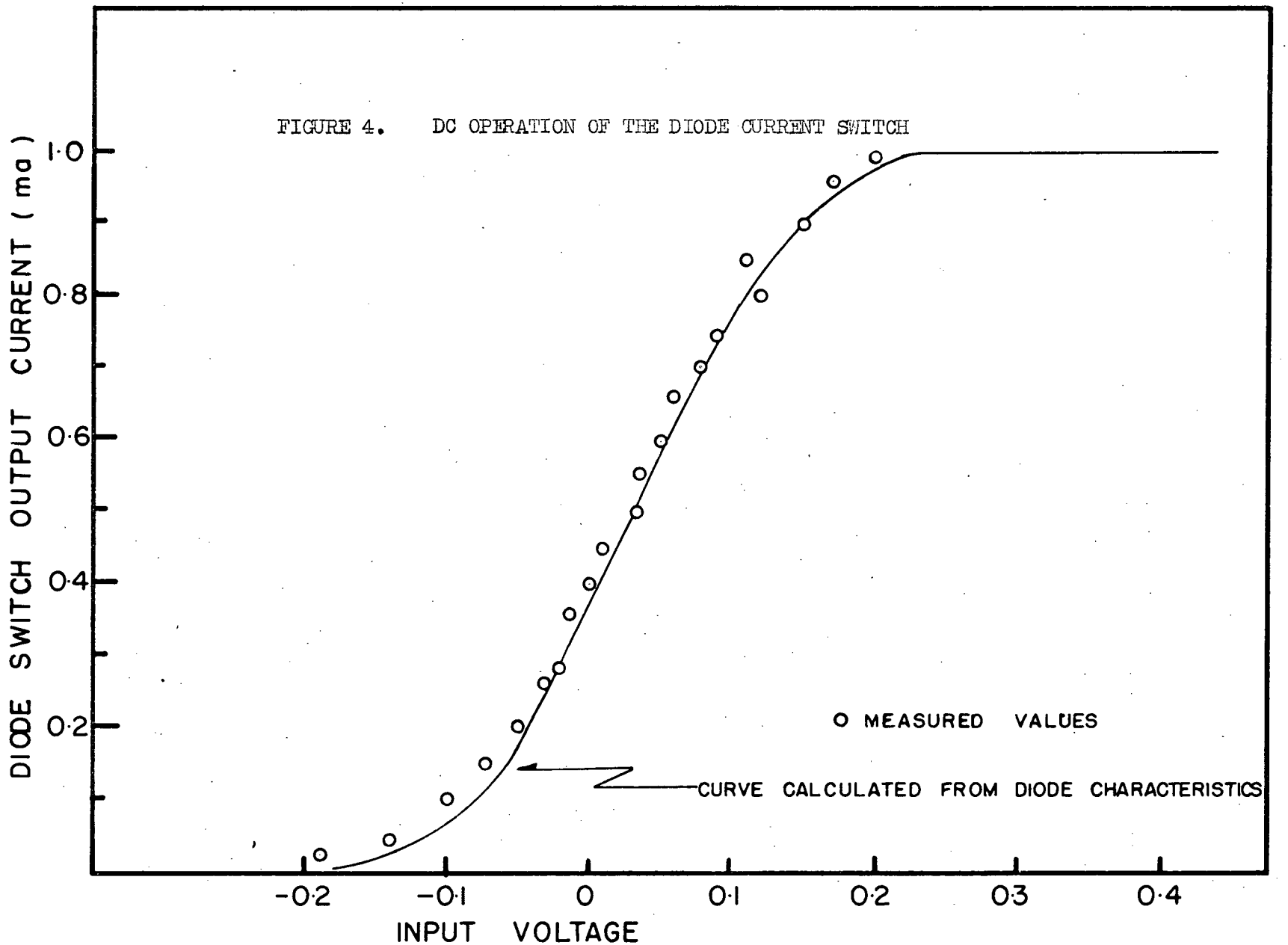

FIGURE 4. DC OPERATION OF THE DIODE CURRENT SWITCH

single shorting stub for both channels. In the quiescent state, the input diode conducts a constant current of one milliampere to ground (from the 250 kilohm resistor to the positive 250 volt line), while the second diode is biased off by about 0.7 volts.

The presence of a single pulse at the input merely causes a rise in voltage at the diode junction, with the second diode remaining cut-off. Superposition of two coincident pulses, however, causes the voltage at the junction of the two diodes to exceed the bias voltage, thus switching the constant current into the integrator as the first diode cuts off. Since the input diode is cut off during this time interval, the loading effect of the time sorter on the incoming pulses is small (one milliampere of the incident forty milliamperes being required for the initial switching).

This idealized description of the apparatus is not strictly realized in practice, however. Since the characteristics of the diode switch are not infinitely sharp, there is a small current conducted by the second diode during a single pulse or during the pedestal surrounding a partial overlap. The d.c. switching characteristics of these microwave diodes is illustrated in fig. 4, in which the output d.c. current is plotted as a function of an input d.c. voltage, with no bias applied to the second diode. As is indicated in the diagram, a limited pulse of amplitude greater than 0.4 volts is required to switch the output from zero to full current. Also, to prevent

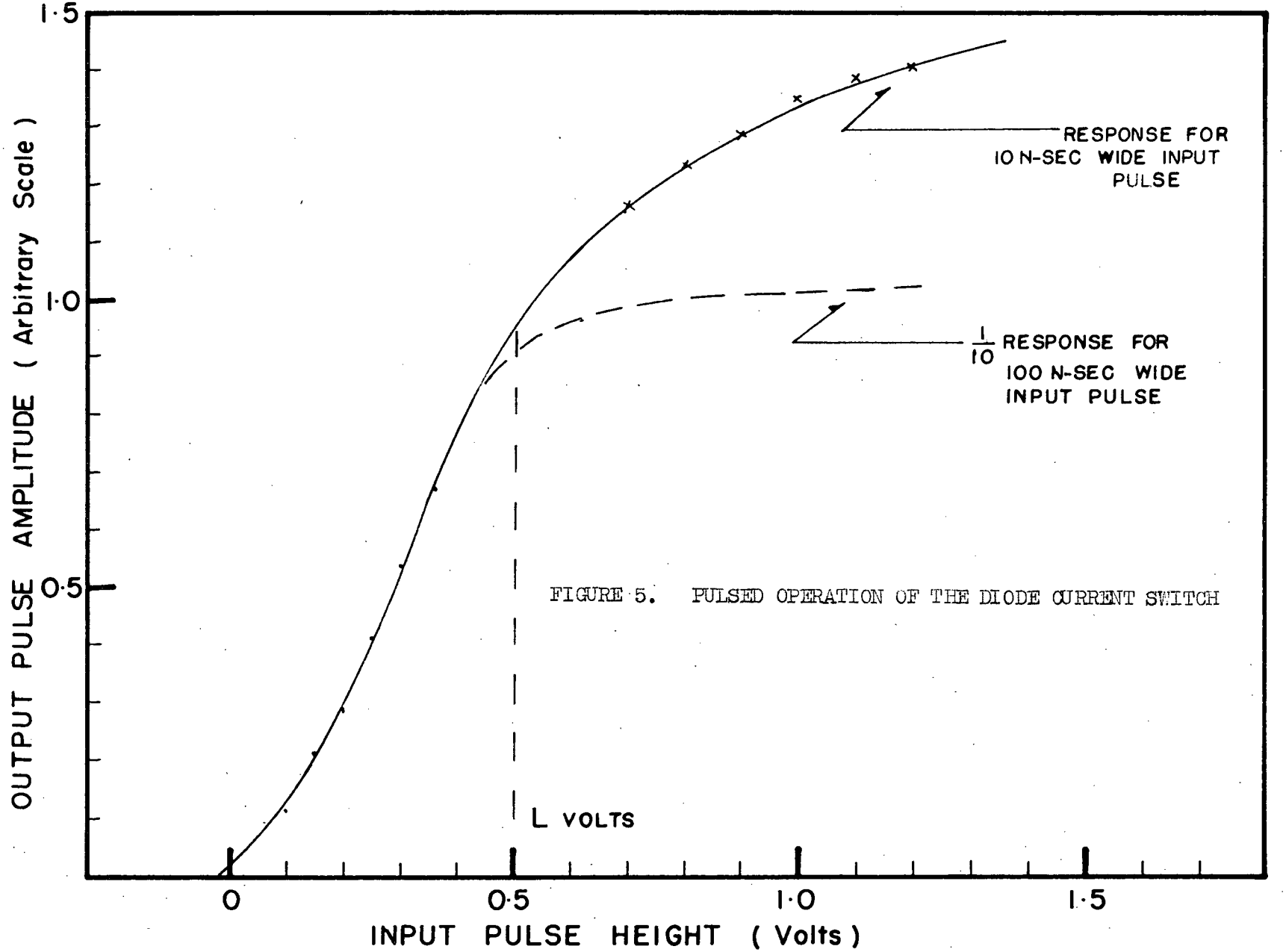

FIGURE 5. PULSED OPERATION OF THE DIODE CURRENT SWITCH

conduction during the single pulses, a bias of about 0.25 volt more than the limited pulse amplitude must be selected. The value of 0.47 volts for the limited pulse amplitude (given in section 3(c)) should therefore produce satisfactory switching, and would also indicate a bias level of at least 0.72 volts. By operating the circuit in this manner, a doubles:singles ratio of greater than twenty:one is easily realized.

(a) Hole Storage Effects:

If the d.c. characteristics of the current switch shown in fig. 4 are also assumed to apply to the fast pulses, the operation of the time-to-amplitude converter would be expected to be independent of the input amplitude (providing the pulses were large enough for complete switching of the current), thus greatly simplifying the design of the limiters. With practical diodes, however, such operation is not obtainable, due, primarily, to hole storage effects. The result of these effects is shown in fig. 5 which illustrates the switching characteristics of the diode circuit during pulsed operation. The ordinate is the amplitude of the integrated output pulse, and the abscissa is the amplitude of the clipped input pulse. The d.c. bias for the diodes was set to a convenient, arbitrary value and kept constant for both measurements. The deviation in the amplitude of the integrated output pulse for the ten nanosecond input pulse from that expected (on the basis of the integrated output being 1/10 of that obtained with a 100 nsec pulse) is attributed to minority carrier conduction (in the reverse direction) in

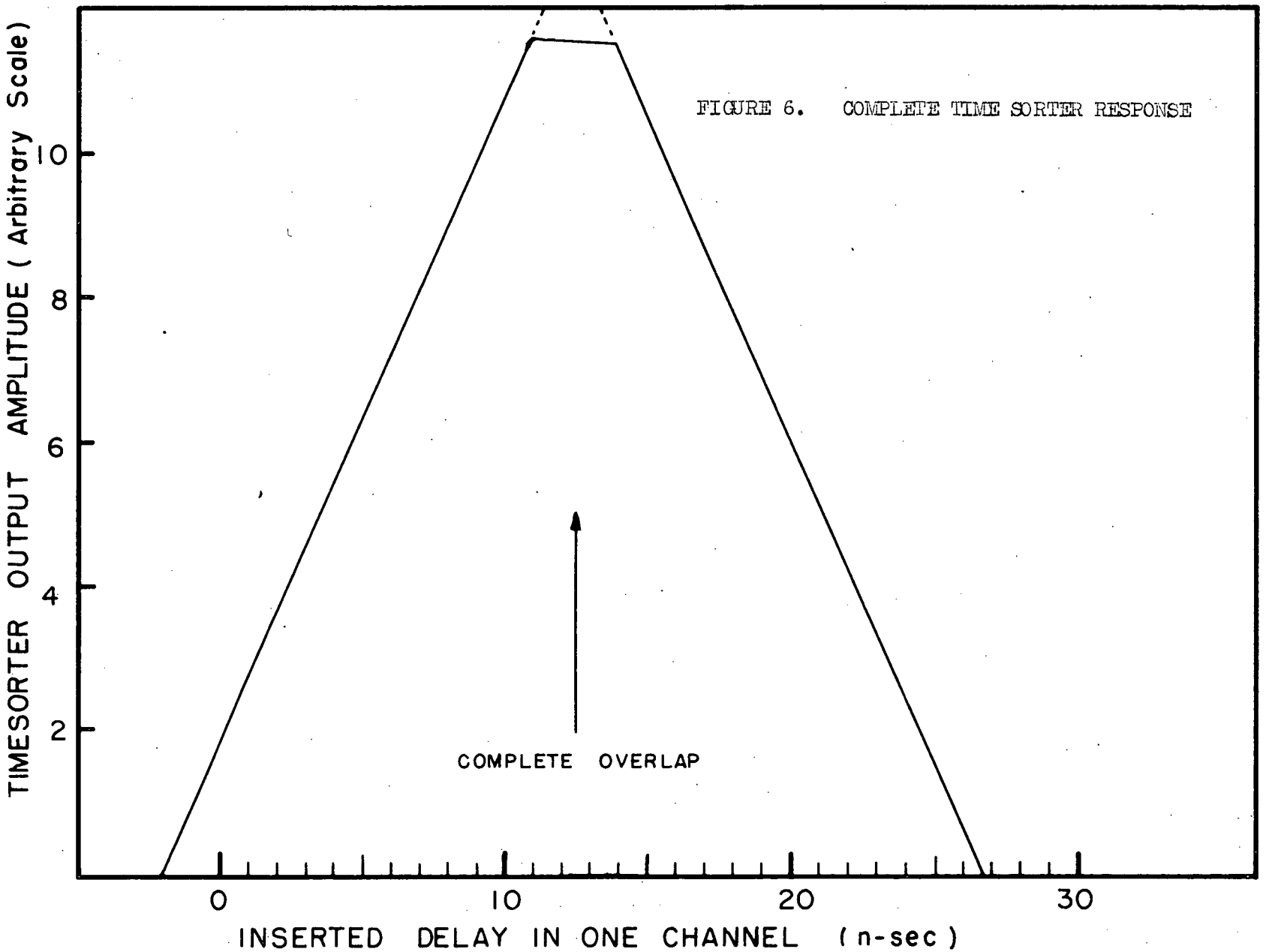

FIGURE 6. COMPLETE TIME SORTER RESPONSE

the first diode during the period when it is supposedly cut off. Since the relative amount of minority carrier conduction is strongly dependent on the input pulse width, the linearity of response is also dependent on this parameter. As is seen from the diagram, however, this effect is small if the bias is adjusted so that the current switched by the overlap pulse is about 95% of the maximum (corresponding to the operating point indicated by the voltage L in fig. 5). Under these conditions the linearity is good down to overlap pulse lengths of a few nanoseconds. Such operating conditions increase the stability requirements for the limiter circuits.

Minority carrier conduction in the second diode tends to remove some of the switched current from the integrator when the input signal returns to ground level. Since the minority carrier lifetime is expected to be in the nanosecond range for microwave diodes, this effect can be reduced by preventing the input signal from returning to ground for a period of several nanoseconds after the overlap signal. This was accomplished by using (for the lifetime measurements described herein) a shorting stub length of fourteen nanoseconds and a relative channel delay of nine nanoseconds, which, for coincident pulses, resulted in an overlap length of five nanoseconds, and a pedestal length (on both sides of the overlap pulse) of nine nanoseconds, during which time the second diode was able to recover. The results of this effect can be observed in fig. 6 which is a plot of the measured output pulse from the time sorter as a function of the delay inserted in one of

the channels. The loss in output pulse amplitude (resulting in non-linear response) near complete overlap (and hence zero pedestal length) is attributed to this effect.

The choice of the diodes in the diode switch was governed by three factors, viz. good high frequency response (thus indicating a short minority carrier lifetime), high back resistance (to lessen the temperature dependence of the switching circuit by reducing the magnitude of the strongly temperature-dependent reverse leakage currents), and high forward conduction (in order to produce a sharp switching action). Associated with the high frequency response, is the desirability of a fast turn-on time for the diode. Of the several commonly-available microwave mixer diodes examined, the 1N23A was selected on the basis of the above requirements. It is designed for use as a microwave mixer up to 9000 mc. In addition, it has a reverse current of less than twenty microamperes at a voltage of one volt (room temperature), and a forward conduction of about fifteen milliamperes at one volt. With regards to possible improvements in this portion of the circuitry, some recently developed diodes such as the Bell Telephone 1N696 Varistor should be investigated. The 1N696, for example, has the following characteristics: a reverse leakage current of .001 microamperes at one volt, a forward conduction of twenty five milliamperes at one volt, and a recovery time of less than five nanoseconds on switching from ten milliamperes forward to ten milliamperes reverse current. This recovery time will be correspondingly shorter for smaller

forward conduction currents.

The value of 1ma for the constant-current employed in the fast, diode switch was chosen for the following reasons. The voltage range required to switch from zero to full current is a function of the amount of current switched. For example, the voltage range required to switch from 5% to 95% of the current was calculated to be 0.25 volts for a current of 0.5 milliamperes and 0.6 volts for a current of five milliamperes. Since the amount of stored minority carriers is also a function of the current, a good switching characteristic requires the use of small currents. Thus, sharp switching and the use of small voltage signals are both facilitated by using small currents. These benefits tend to be offset, however, by the finite time required to charge up the junction of the diodes, thus producing an undesired delay between the time the first diode switches off and the second diode switches on. Since even a one milliampere current requires a time of one nanosecond to charge up a capacity from the junction to ground of only two picafarads (stray plus diode capacity) by 0.5 volts, the use of still smaller current was not considered advisable. Thus, a value of one milliampere was regarded as a satisfactory compromise.

The integrating circuit was supplied with a variety of integrating capacitors that could be switched in when desired. By this means, a variety of operating ranges could be obtained; a 0-200 millivolt range of output pulse amplitudes for pulse overlaps of zero to fifteen nanoseconds for the ten pf range,

120 nsec for the 250 pf range, and about 400 nsec for the 750 pf range. A fifty foot, shorted length of RG17, a high-frequency 52 ohm coaxial cable, was obtained to enable time measurements to be made in the one hundred nanosecond range, using square pulses of 150 nsec length. Still larger time intervals could no doubt be measured if larger shorting stubs were used.

(B) Gamma-Ray Detectors:

The gamma-ray detectors consisted, as mentioned earlier, of scintillation counters followed by limiter tubes used for pulse shaping. In order to obtain good time resolution with the instrument, serious consideration was given to the selection of the two components of the scintillation detector, viz. the scintillation crystal, and the photomultiplier tube. As pointed out on page 51, the mean time delay for the appearance of the first photoelectron from the photocathode of a scintillation counter, is: $\bar{t} = \frac{T}{R}\left(1+\frac{1}{R}\right)$, where T is the mean life of the scintillation in the phosphor, and R is the total number of photoelectrons produced during the pulse. Since R is proportional to the light output from the crystal, it is strongly dependent on such factors as the nature of the optical coupling of the crystal to the photomultiplier, etc. Thus, the achievement of short resolution times requires care in the selection of the components to minimise $\bar{t}$. It should be noted, however, that the formula given above only considers that portion of the scintillation counter consisting of the crystal and photocathode, and is the ultimate limit in

the resolution time of the instrument only if the spread in transit-time of the electrons in the photomultiplier structure itself can be considered negligible compared to $\bar{t}$, and if the photomultiplier is capable of sufficient gain for the detection of single electron pulses from the photocathode.

The photomultiplier tube chosen for this work was the 1P21, selected for its short transit-time spread and high gain (Bell, 1954). Since the photocathode-first dynode electron transit-time spread is generally much greater than that between successive dynodes because of poorer focussing, the 1P21, by virtue of its internal photocathode, has a much shorter transit-time spread than the conventional end-window tubes. The recently-developed, curved photocathode tubes (designed with spherical geometry as the objective), such as the RCA 7264, are much superior to the flat end-window tubes regarding transit-time spreads (Widmaier, 1958) and facilitate much better optical coupling to the crystal than the internal photocathode tubes such as the 1P21. The choice of the scintillator should depend, as indicated by the formula of Post and Schiff (pg. 51), on having as small a ratio of decay time to intensity of light pulse as possible. Of the commercially-available organic crystals, diphenylacetylene appears to be superior (Jones, 1955) with a decay constant of four nanoseconds, and a light yield for beta particles, relative to that of anthacene, of 0.8. NE102 (a plastic scintillator manufactured by Nuclear Enterprises, Pembina St., Winnipeg, Canada) has somewhat poorer characteristics, a decay time of the same value, but a relative

light output, compared to anthacene; of 0.6. Since the plastic phosphor can be readily machined, however, it was felt that suitable shaping of the phosphor to assist in focussing the light pulse on the photocathode of the 1P21 might improve the effective light-coupling sufficiently to make this assembly superior to that using diphenylacetylene. The results of this investigation were somewhat inconclusive, however, with no significant difference in resolution observed between the two assemblies.

(a) Assembly:

The 1P21 tubes were first silvered on the outside by the Brashear process to reduce tube noise (MacKenzie, 1953). The phosphors were glued to the sides of the tubes with R313[1], and then covered with MgO for good light reflectivity. The complete mount was then wrapped with black scotch electrical tape and painted with black enamel to ensure light tightness. A total of four counters were constructed, two consisting of diphenylacetylene crystals of size: 1" x 3/8" x 3/8", with one longitudinal face machined to fit the photomultiplier tube, and the other two with shaped NE102 phosphors, of approximate size: 1" x ½" x 5/8". The best two scintillator-photomultiplier combinations (one being a diphenylacetylene counter, and the other a plastic phosphor counter) were then selected from these four and used in the subsequent measurements.

The photomultiplier dynode voltages were determined by a resistive bleeder chain placed across a regulated, electronic

1 R 313 Bonding Agent, Carl H. Biggs Co., 2255 Barry Ave., Los Angeles 64, California.

high tension supply, the resistor values being given in fig. 8. Capacitive decoupling was used on the later dynode stages to reduce capacitive degeneration of the output pulses. Small damping resistors were inserted in series with the condensers, however, to reduce the tendency for high frequency ringing (Jones, 1955).

(C) Limiters:

The requirement of high stability in the operation of the time sorter described in this thesis resulted in several stringent conditions for the limiter circuit. Firstly, the limiter tube had to be a sharp cut-off tube, capable of producing an anode pulse with a rise-time of less than one nanosecond. The tube had to be capable of conducting a dc plate current of about twenty milliamperes in order to produce the desired one volt output pulse across the effective plate load of fifty ohms. Further, the circuit had to be characterised by a high degree of dc stability, so that the limiter output pulse amplitude would be constant for the reasons described on page 65. Finally, it was desired that the circuit should be count-rate insensitive, so that the amplitude of the output pulses would be uniform and independent of count-rate. The data given on page 86 indicate that the total fluctuations in the limiter current must be less than 0.3% if time measurements to an accuracy of $\pm$ 0.1 x 10^{-10} seconds are intended.

The time sorter described by Warren and Jones (1958) (an improved version of that described by Jones, 1955) contained limiters designed about a secondary-emission pentode, the

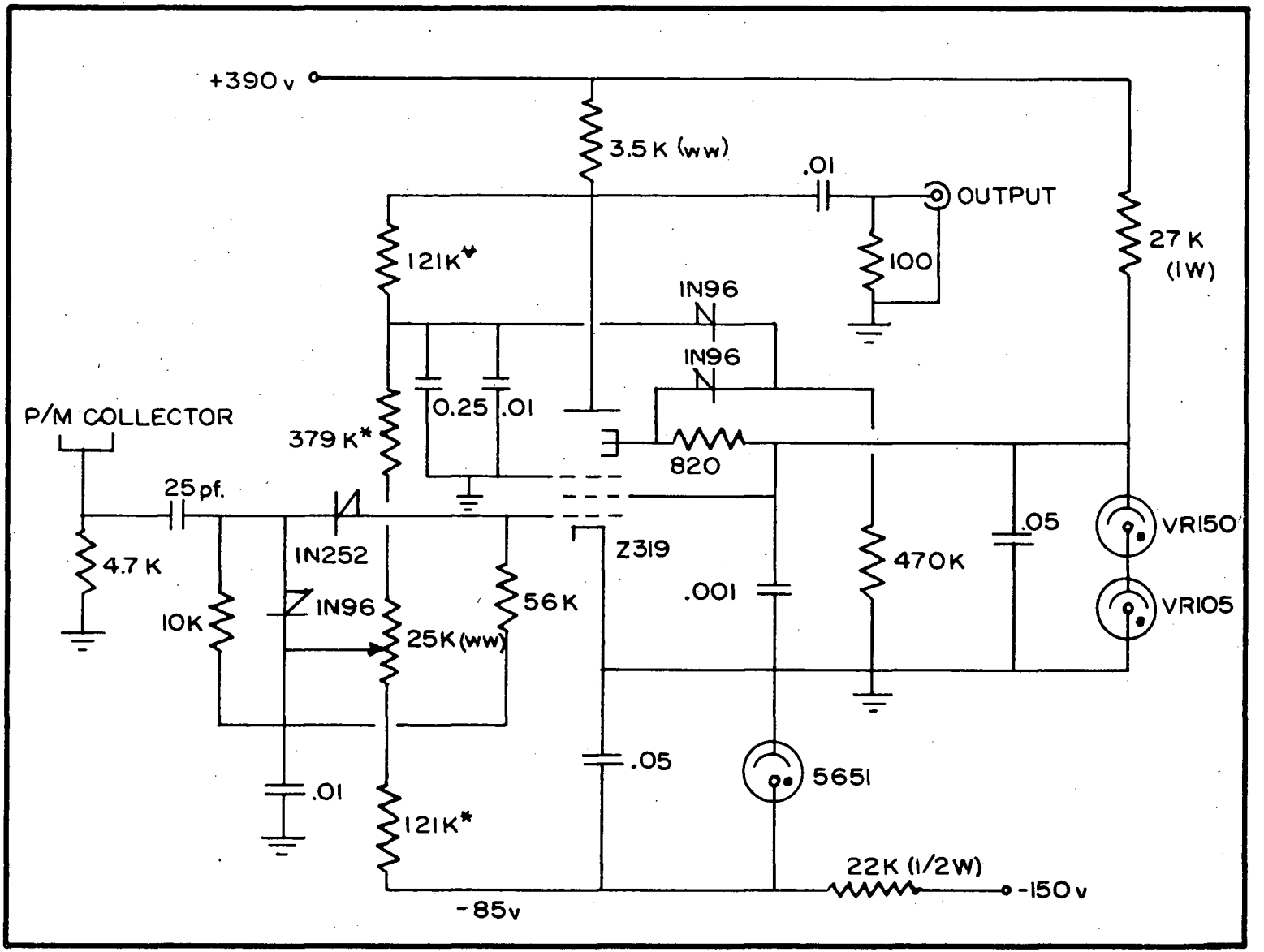

FIGURE 7. SECONDARY-EMISSION PENTODE LIMITER CIRCUIT

Z319[1], with both dc and count-rate compensation feed-back loops to improve the stabilisation (as shown in fig. 7). Use of this circuit was discontinued, however, when difficulties involved in attempting to reduce random shifts occurring in the time measurements led to the discovery that these tubes had the characteristic that large negative input pulses failed to turn off the tubes completely. It appeared that after the initial warming-up period, the dynode continued to emit electrons thermionically for some time after a negative, cut-off pulse was applied to the grid. This temperature-dependent, residual current thus introduced a limitation to the constancy and uniformity attainable for the amplitude of the output pulses. For this reason, attention was directed to recently-developed high-gain, high current pentodes. Two pentodes were found suitable in overall characteristics, and able to handle a continuous dc current of twenty milliamperes; the E180F (a Philips tube, marketed in North America under the number 6688) and the 404A (a Western Electric pentode). Since the 404A tubes were obtained first, the limiters employed in the equipment described herein were constructed with these tubes. The circuit is sufficiently insensitive to tube characteristics, however, that the E180F can be used with but a few minor alterations in the screen voltage supply (Prescott, 1959), and use of this tube rather than the 404A is advised, since it is cheaper than the 404A by a factor of three.

---

1 EMI Research Labs., Ltd., Hayes, Middlesex, England.

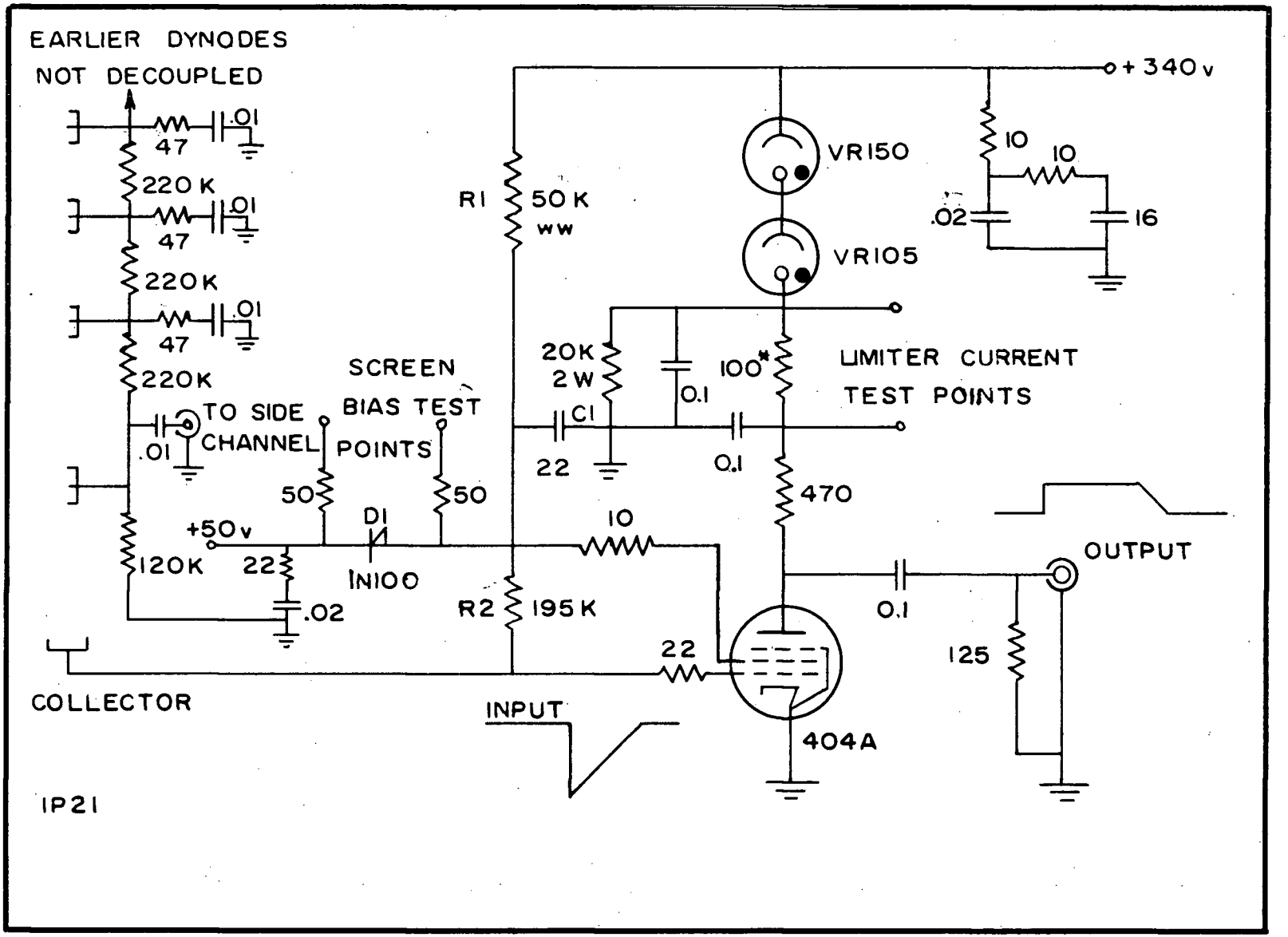

FIGURE 8. 404A PENTODE LIMITER CIRCUIT

The circuit diagram of the final limiters is given in fig. 8. Considering, first, the dc operation of the circuit, it is to be noted that both the grid and screen are operated under "clamped" conditions (Millman and Taub, 1956, pg 126), to minimise the changes in the plate current resulting from contact potential changes in the cathode-grid structure. Thus, assuming that the grid (and screen) captures a geometrically-defined fraction of the current that is emitted by the cathode, then, if the grid (and screen) current is forced to attain a constant value by external means, the grid and screen voltages must adjust themselves to be compatible with these currents, therefore ensuring that the resultant plate current is well-defined and constant at least to a first approximation.

An additional benefit is obtained by connecting the grid supply resistor to the screen. If the screen current tends to decrease (indicating reduced tube conduction and decreased plate current), then the screen voltage rises, automatically increasing the grid current and so increasing the total tube conduction. In this way, additional negative feed-back is introduced. The screen voltage supply is adjusted to be a few volts more positive than the screen itself, so that the diode, D1, is cut off in the dc state. Since the grid is biased positively, the screen voltage will be low (about sixty volts) if a plate current of only twenty milliamperes is to be produced. By employing a low plate voltage also (about ninety volts), the power dissipations of both the

screen and the anode are kept well within their rated maxima.

The operation of the circuit under pulsed conditions is as follows: When the tube is cut off by a negative input pulse applied to the grid, a current of close to ten milliamperes is delivered to the external load as desired, and the screen voltage rises as the decoupling condenser, C1, charges up. When this voltage reaches the screen supply voltage, the diode D1 comes into conduction and clamps the screen voltage to this value. When the tube returns to its conducting state, the diode D1 turns off as the screen current increases, and the screen voltage drops to its normal value with a time-constant of R1C1 which is $20 \times 10^{-12} \times 50 \times 10^{3}$ = 1.0 microsecond. Thus, by keeping the decoupling condenser C1 small, the screen voltage is able to recover to its dc level within a few microseconds, thus assisting in reducing the count-rate effects to a minimum. Since the value of C1 is at least ten times larger than the expected 404A plate-to-screen capacity, less than 1/10 of the seven milliamperes screen current will flow in the plate circuit when the tube is cut off, and this is less than five per cent of the total plate current. Thus, if the variations in the screen current are kept below two per cent, the capacitive contribution to the front edge of the output pulse will vary by less than 0.1%.

The value of the grid supply resistor, R2, was chosen to recharge the grid circuit to its nominal value of 0.5 volts within a time interval of approximately one microsecond after photomultiplier conduction. An important advantage of this

method of grid clamping is that an approximately constant value of recharge current is supplied to the capacity of the grid circuit to ground after the grid has been charged negatively by the current pulse from the photomultiplier. Thus a waveform of the type shown at the grid point in fig. 8 is produced, rather than the usual exponential recovery which approaches the baseline slowly, a poor characteristic from the point of view of count-rate insensitivity. The use of a negative photomultiplier HT allows direct coupling between the anode of the photomultiplier and the grid of the limiter tube, thus enabling another frequent source of count-rate shifts, the coupling condenser, to be eliminated. The value of R2 given for this circuit was found to be much too small for a one microsecond recovery when using photomultipliers which are characterised by less after-pulsing than the 1P21 (Prescott, 1959), and in those cases, a larger value is required. D C monitor points were supplied for measuring the screen voltage, D1 bias voltage, and the plate current. The D1 reverse bias voltage was normally adjusted to about two volts. Monitoring of the plate current also affords a convenient method for determining the total limiter count-rate, since the fractional decrease in the mean dc plate current is equal to the fractional mark-to-space ratio (to first order). The cable used to transmit the limit pulses to the time sorter was a 100 ohm type with good high-frequency characteristics, Telcon AS48[1],

---

1 T.C.M. Co. Greenwich, London, England.

which has a semi-air core contained within a polythene dielectric.

(D) The Shorting Stub:

The shorting stub is a coaxial line constructed of brass, with a 3/16" brass rod mounted within a 7/16" inner diameter ($\frac{1}{2}$" outer diameter) brass tube. With an air dielectric, this ratio produces a characteristic impedance very close to fifty ohms, the value required for matching the impedances between the stub and the two, effectively parallelled, 100 ohm cables to the limiters (Bell et al., 1952). In this way, the shorting stub is terminated in its characteristic impedance, thus preventing the occurrence of multiple reflections of the voltage pulses within the shorting stub. The use of a low impedance stub of this sort does result, however, in a mismatch of the individual limiter cables, the terminating impedance of these cables being the parallel combination of the shorting stub and the other cable: $\frac{50 \times 100}{50 + 100} = 33\ \Omega$. Thus, a reflection of an amount: $\frac{100-33}{100+33} = 50\%$ occurs when the limiter output pulse strikes this junction. For a typical limiter output pulse of 0.94 volts (9.4 ma into 100 ohms) this results in a pulse amplitude of 0.47 volts being transmitted into the shorting stub, a value shown in section 3(a) of this chapter to be sufficient for satisfactory operation of the time sorter proper.

A dielectric constant very close to that of air was obtained by packing the tube with a homogeneous spacer consisting of hollow cylinders of styrofoam. The outer tube

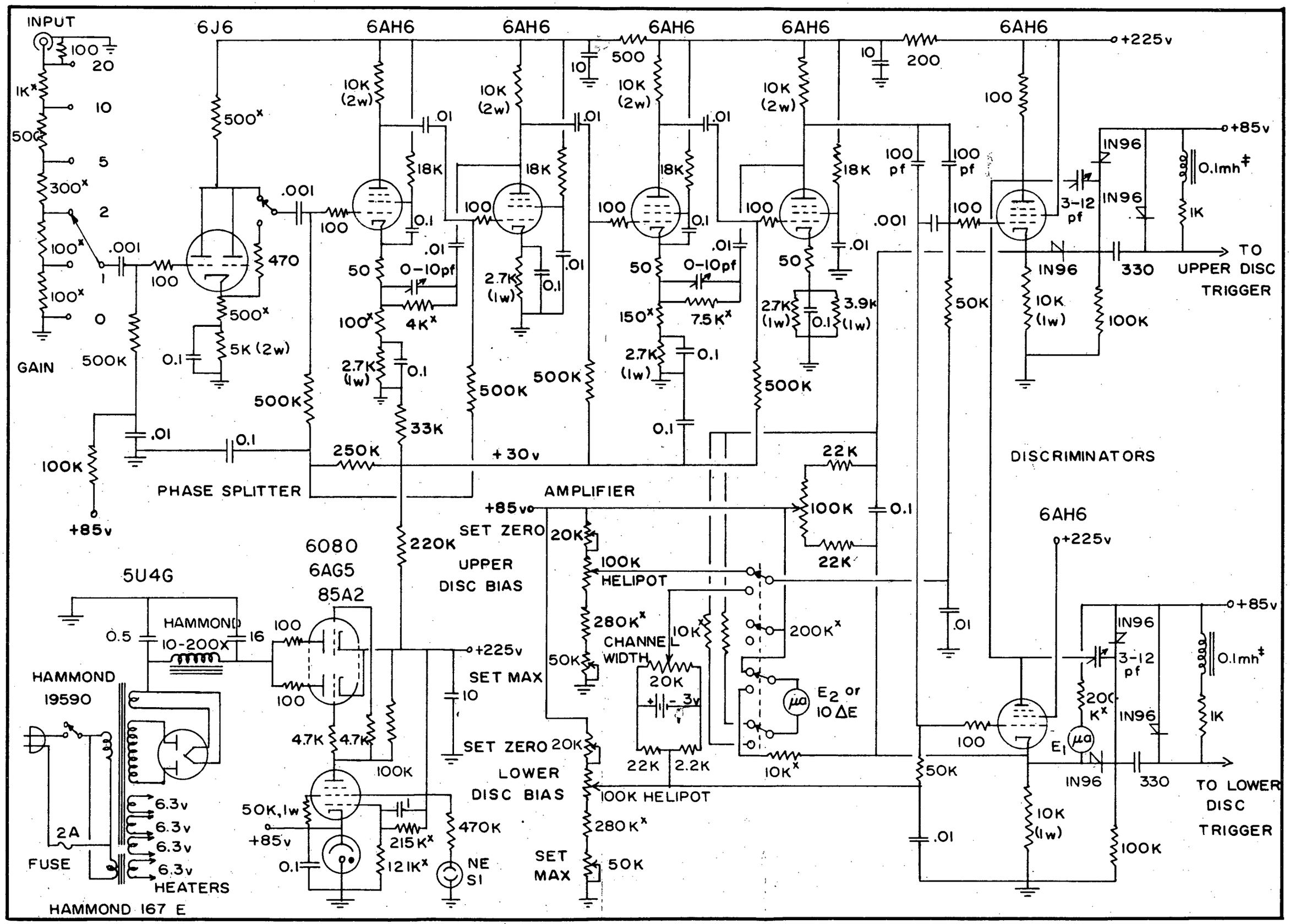

FIGURE 9A. SINGLE-CHANNEL PULSE HEIGHT ANALYSER

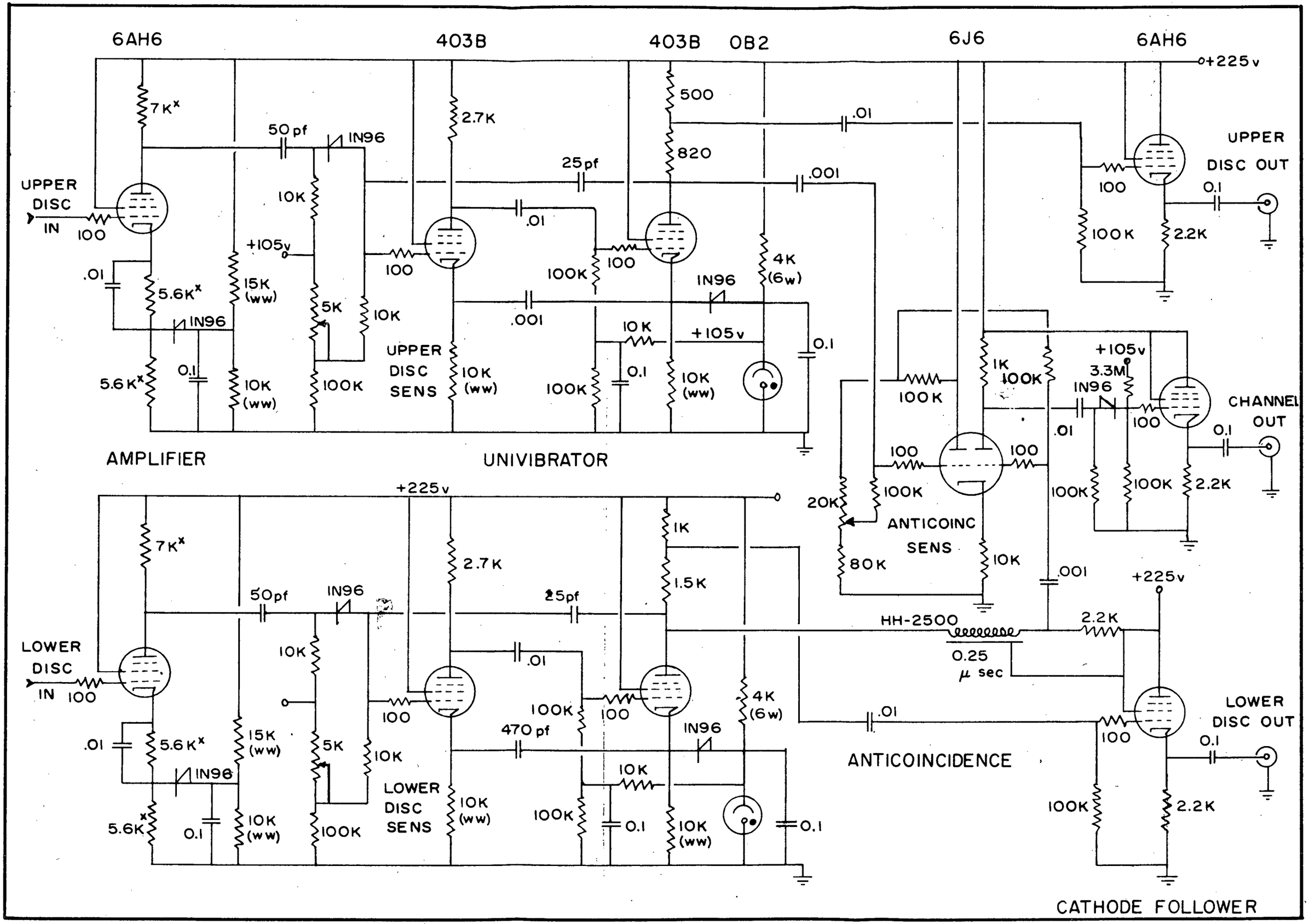

FIGURE 9B. SINGLE-CHANNEL PULSE HEIGHT ANALYSER

contained slots at 1/2 nanosecond intervals into which shorting bars could be inserted to produce clipped pulses of lengths varying from three to fourteen nanoseconds in one nanosecond steps. Time calibrations, obtained by varying the clipped pulse length (thus altering the overlap pulse lengths) were readily performed with this type of shorting stub. The shorting stub was terminated at the far end by a forty seven ohm carbon resistor, to absorb secondary reflections and prevent them affecting the behaviour of the line.

Throughout the fast pulse portion of the circuitry, type N constant impedance (75 ohm) Amphenol connectors were employed.

(E) Ancillary Equipment:

The power supplies used throughout were standard, electronically regulated, "Lambda"-type power supplies (Lambda Electronics Corp., Corona, New York, model 28), except for the limiter supply, which was a high stability, Lambda model C282. All the power supplies were supplied with Sola-stabilized mains voltage.

The side-channel, single-channel, pulse amplitude analysers were designed at UBC but are similar in block diagram to those designed by R.E. Bell and R.L. Graham at AECL, Chalk River. Standard circuitry was employed in their design, the circuit diagram being given in fig 9. Their count-rate characteristics were determined using a General Radio pulse generator (Type 1217A), producing 0.1 microsecond wide pulses of sixty millivolts amplitude. It was found that the effective gain of the analysers (determined by noting the lower discrimi-

nator setting just required for triggering the discriminators) increased by about 3½% from 200 pps to 100,000 pps. The dead-time of the instrument was found to be equal to the width of the output pulse, viz. one microsecond, when the pulses were significantly larger in amplitude than that corresponding to the lower discriminator level. For pulses just greater than this lower level, a dead time of about five microseconds was obtained, which decreased rapidly as the pulse amplitude was increased above the lower discriminator level.

The slow coincidence unit is a standard diode coincidence circuit (Millman and Taub, 1956, pg 398) followed by a transitor emitter-follower used to drive the 100 ohm cable leading to the biased amplifier. The resolving time of this unit is also one microsecond, determined by the length of the input pulses from the analysers.

The time sorter pulses, after preliminary amplification in the time sorter itself, were further amplified in a wide-band pulse amplifier (Northern Electric amplifier, type AEP1444). The time sorter output pulses of about sixty millivolts amplitude (for a five nanosecond overlap, eleven pf integrating capacity) were amplified to about 200 mv by a pulse transformer (used primarily to match the 100 ohm cable to a 1000 ohm delay line) before entering the 'Moody' pulse amplifier. The 1000 ohm delay line of length 0.5 microseconds in series with the signal path compensated for the delays inherent in the "slow" gate pulses. The 1000 ohm input impedance connection of the Northern Electric amplifier was used in order to terminate the

delay line. The second ring only of the Northern Electric amplifier was used to amplify the input pulses to a twenty volt level, corresponding to a gain of about one hundred. These pulses were then delivered to a gated, biased amplifier prior to being recorded in the kick-sorter.

The biased amplifier is one which was designed and constructed at UBC and described by P.J. Riley (1958). The gate pulses from the gate pulse generator were nominally set to about one microsecond width. The shaped output pulses from this unit were then connected to either the thirty channel Marconi kick-sorter (Pulse Amplitude Analyser, type #115-935), or the one hundred channel C.D.C. instrument (Computing Devices of Canada Kicksorter, type AEP2230). Typical settings for these instruments (for a pulse overlap of five nanoseconds) were as follows:

Northern Electric Amplifier: Attenuation, 3 db; Top Cut, 4; Bottom Cut, 5.

Biased Amplifier: Gain 4; Bias, about 3.

4. Operational Characteristics of the Time Sorter.

The total response of the equipment as a function of the time delay inserted in one channel is illustrated in fig 6. This curve was obtained by using an electronic pulse generator (Epic, Electrical and Physical Instrument Co., N.Y., Model 200) to drive both limiters, one output passing through a cable delay of about twenty nanoseconds before operating the limiter, and the other passing through a tapped, helical delay line before operating the other limiter. This system was found useful for

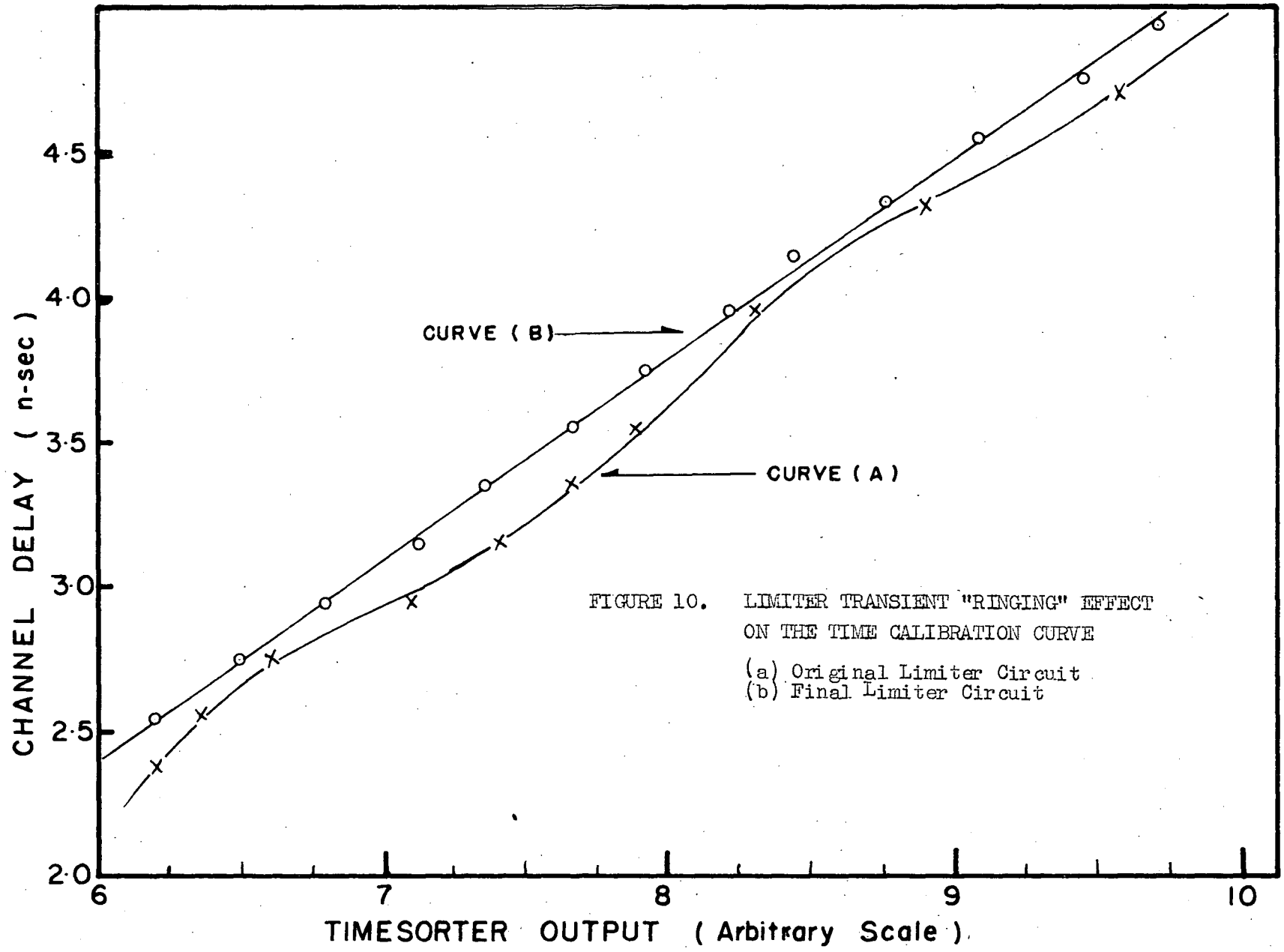

FIGURE 10. LIMITER TRANSIENT "RINGING" EFFECT ON THE TIME CALIBRATION CURVE

(a) Original Limiter Circuit
(b) Final Limiter Circuit

initial checks of the system, but was not used for performing time calibrations because of difficulties associated with the elimination of reflections and other matching problems in the helical delay line and associated cables. An example of a circuit fault detected with this system was one associated with "ringing" of the limiter pulses. If both limiters produce a transient ring superimposed on the limited square pulse, then, since the time sorter response is also somewhat amplitude-dependent, a system response similar to that shown in fig 10(a), which indicates the observed response of the original limiters, would be expected, with the time sorter output being a function not only of the relative time delay between the input pulses, but also of the relative phases of the transient rings. The principal frequency component of this ring, as estimated from the periodicity of the points in fig 10(a) was about 500 mc. Since this frequency was too high to be observed directly with equipment in our laboratory, visual verification of the rings on the limiter pulses was never obtained. These rings were effectively eliminated for overlaps of practical interest, however, by performing some modifications in the limiter circuits, viz. the insertion of damping resistors in all sections suspected to be capable of ringing, and the alteration of the physical lay-out to reduce lead lengths. Fig 10(b) indicates the equivalent calibration curve obtained after these modifications were completed.

(A) Measurement of Velocity of Pulses in Limiter Cables:

The velocity of nanosecond voltage pulses was measured in

the Telcon AS48 cable using the system arrangement described above. The time delay for a fixed length of the cable (when inserted between the pulse generator and the one limiter) was determined relative to the calculated time delay of the pulses in the helical line (in which the velocity of the pulses was assumed to be equal to the velocity of light, since the line possesses an air dielectric). By this means, a value of $(2.48 \pm .05) \times 10^{+10}$ cm/sec was obtained, a value in good agreement with that of Neilson (1955): 2.40×10^{10} cm/sec, and that of Rupaal (1959): $2.50 \times 10^{+10}$ cm/sec, determined by measuring the resonant frequencies of open- and short-circuited lines.

(B) Time Calibrations of the Equipment:

Time calibrations of the equipment could be obtained in either of the following ways. Variations in the time delay in one channel, obtained either by inserting calibrated cable lengths, or by moving a source of coincident gamma rays between the two counters, afforded a direct method of calibration. A second method, which was generally easier to perform, consisted in placing a fixed source of coincident gamma rays between the counters, and measuring the time sorter pulse amplitude as the shorting stub length was varied. Since the shorting stub method was only capable of producing time increments in units of one nanosecond, the former calibration procedure was usually employed if the range desired in the time measurements was only a few nanoseconds or less. Thus, for the measurements described in this thesis, which normally con-

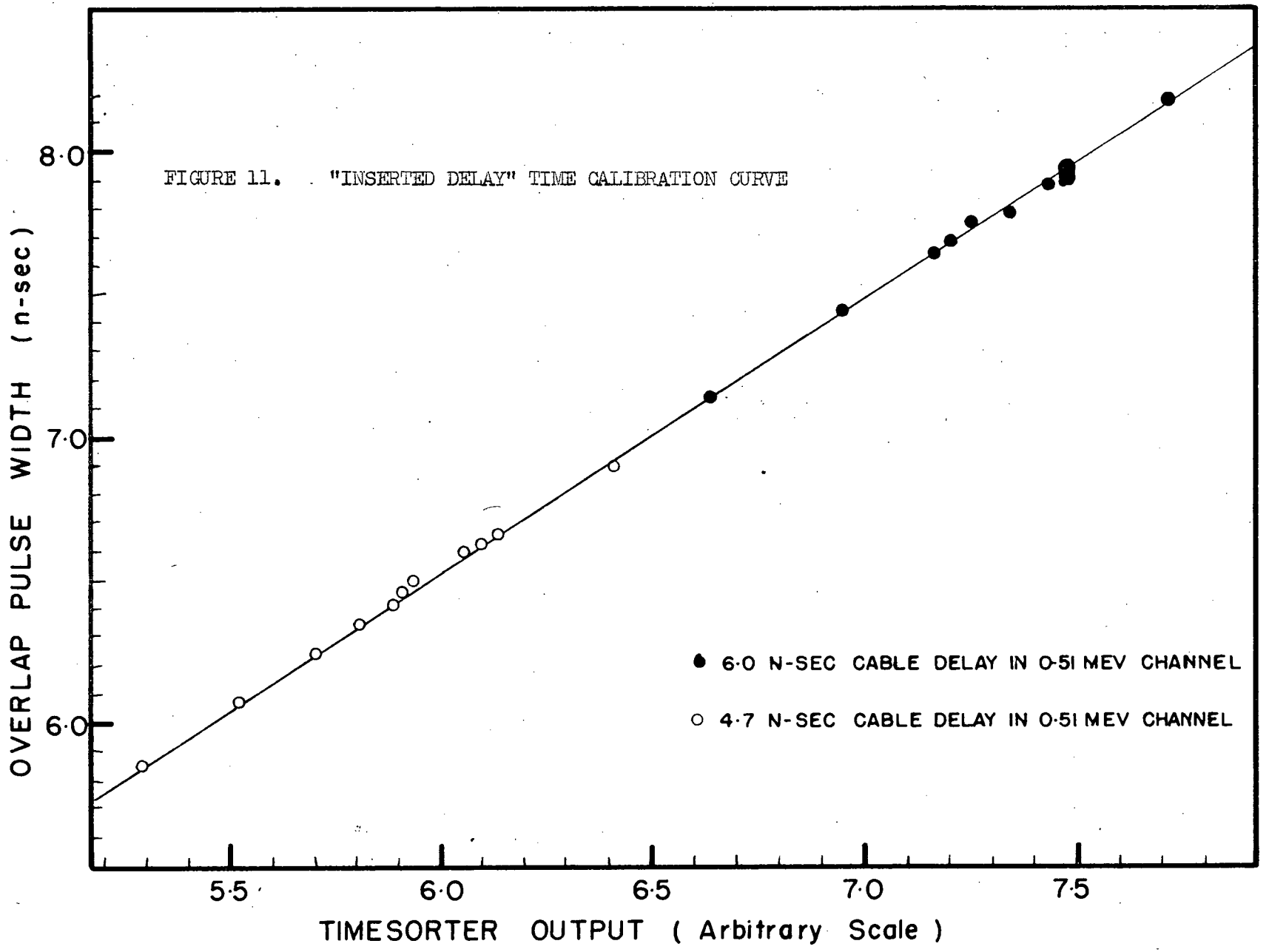

FIGURE 11. "INSERTED DELAY" TIME CALIBRATION CURVE

sisted of comparisons between two resolution curves separated by less than one quarter of their width at half-height, a time calibration curve was obtained for an interval of two to four nanoseconds, using the variable delay technique. One such calibration curve is illustrated in fig 11. As indicated on the diagram, the calibration consists of two sets of points, each group consisting of gamma-ray time-of-flight calibrations covering an interval of one-half to one nanosecond, the two different groups being associated with different cable delays introduced into the limiter circuits. These delays were in turn calculated using the measured value of the pulse velocity in the cable (2.48×10^{10} cm/sec). The linear relationship existing between the two sets of points is further evidence of the internal consistency of these measurements.

The gamma-ray time-of-flight calibrations were obtained in the following manner. After separating the counters by a distance of about twenty inches, a Na^{22} source of 0.4 mc strength was aligned between them, so that the two scintillation counters and source were colinear. This was accomplished by adjusting the position of the source in a plane perpendicular to the line joining the two counters until a maximum coincident count rate was obtained. During these measurements the two single-channel analysers were set to accept a major portion of the 0.51 Mev Compton spectrum of the annihilation gamma rays. Coincidence resolution curves were then recorded for various positions of the source

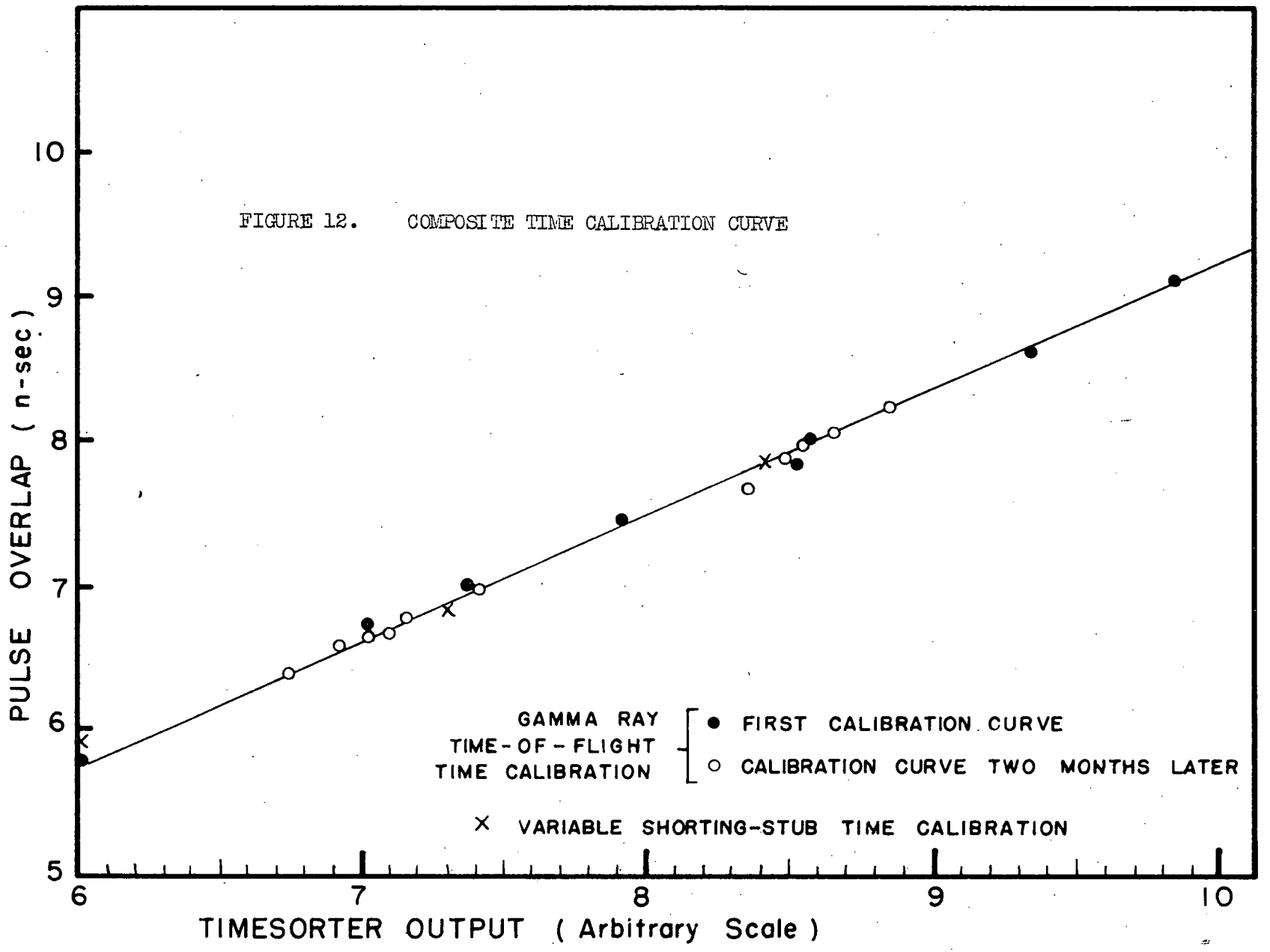

FIGURE 12. COMPOSITE TIME CALIBRATION CURVE

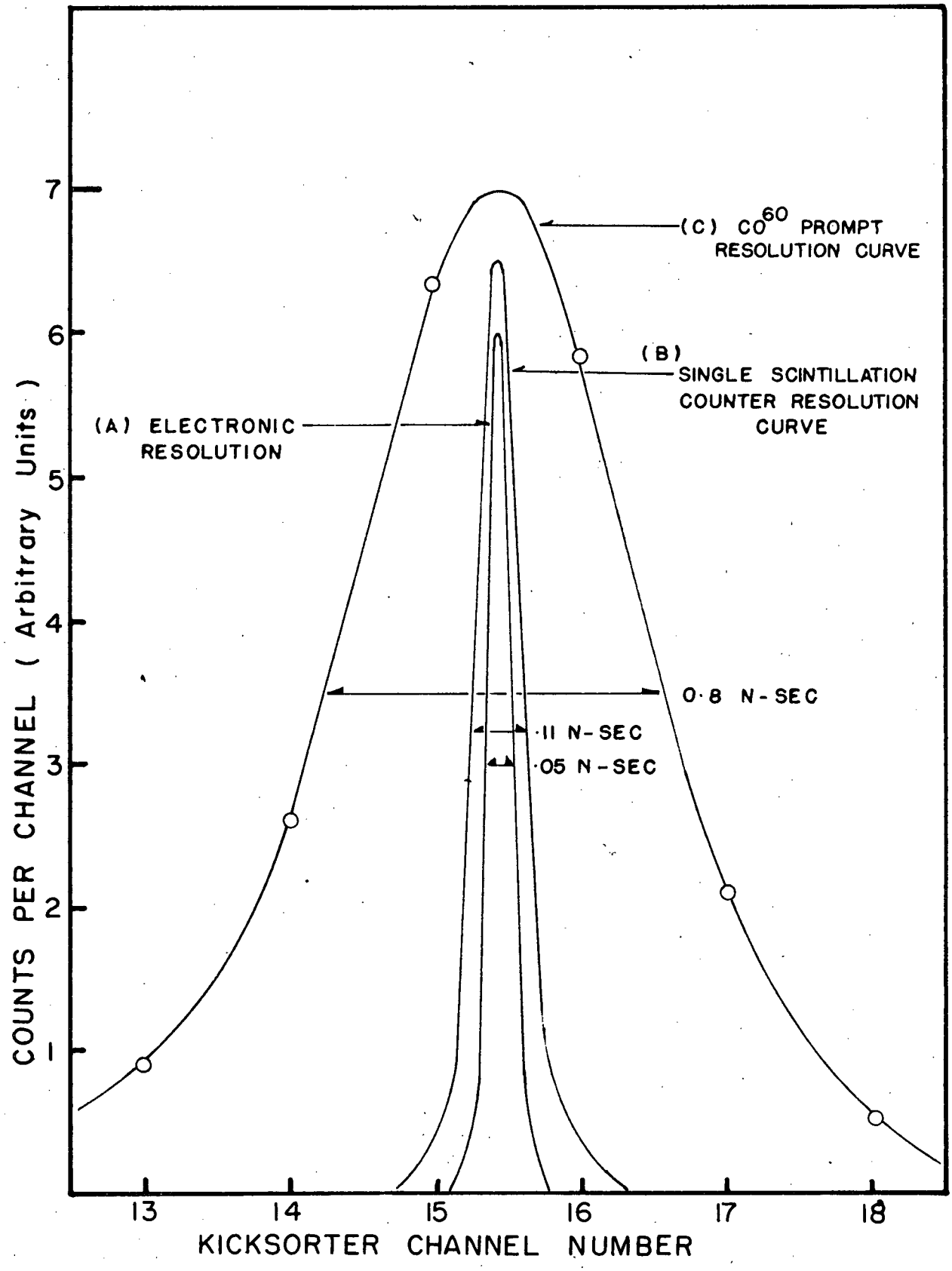

FIGURE 13. PROMPT RESOLUTION CURVES

along the line joining the two counters. The time co-ordinates of the calibration curve were calculated from the flight time of the gamma rays, and the time sorter output amplitudes determined from the positions of the centroids of the corresponding resolution curves on a kicksorter. In this way, a detailed calibration curve was obtained, enabling a check on the linearity and insuring that no periodic fluctuations of the sort described on page 80 were involved. That the "variable shorting stub" method of time calibration is consistent with that of varying the time delay is illustrated in fig 12, where the two calibrations are superimposed.

(c) Resolution and Stability:

Figure 13(a) illustrates the intrinsic electronic resolution of the apparatus when it is driven by artifical "prompt" pulses produced by the Epic mercury pulse generator. The value of .05 nanoseconds is much smaller than that resulting from a prompt gamma ray source. Figure 13(b) is the resolution curve obtained when both limiters are driven by the same scintillation counter. The increased width of this curve over that of curve (a) illustrates the effect of prompt pulses of various rise times and various amplitudes (although identical in both counters) on the resolution surve. The resolution curve for Co^{60}, shown in fig 13(c) is characterised by a resolution time of 0.8 nsec, and thus serves to illustrate that the limit in time resolution for gamma-ray detection is strictly one of the radiation detectors at the present time

A semi-logarithmic plot of a Co^{60} resolution curve is

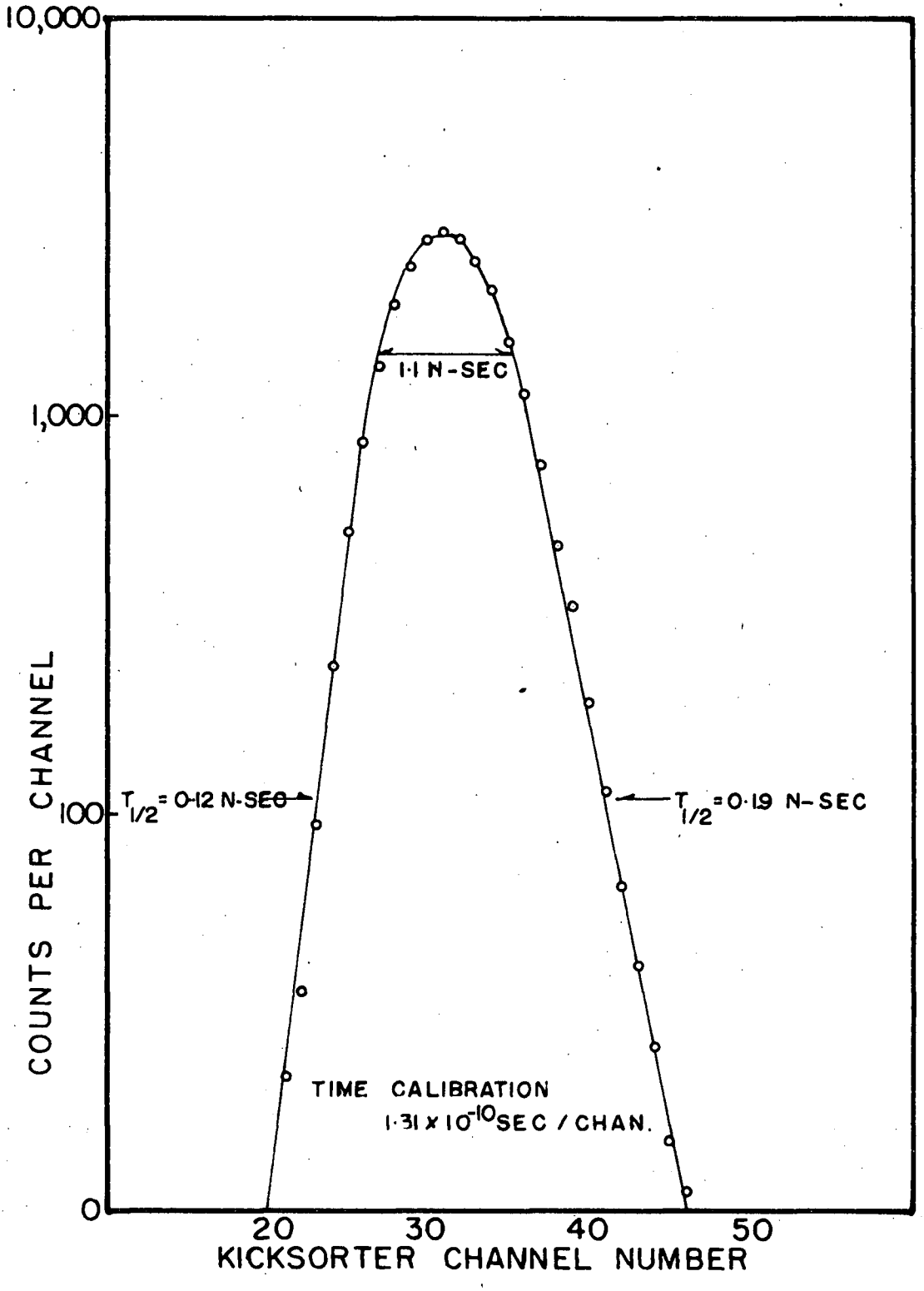

FIGURE 14. COBALT-60 PROMPT RESOLUTION CURVE

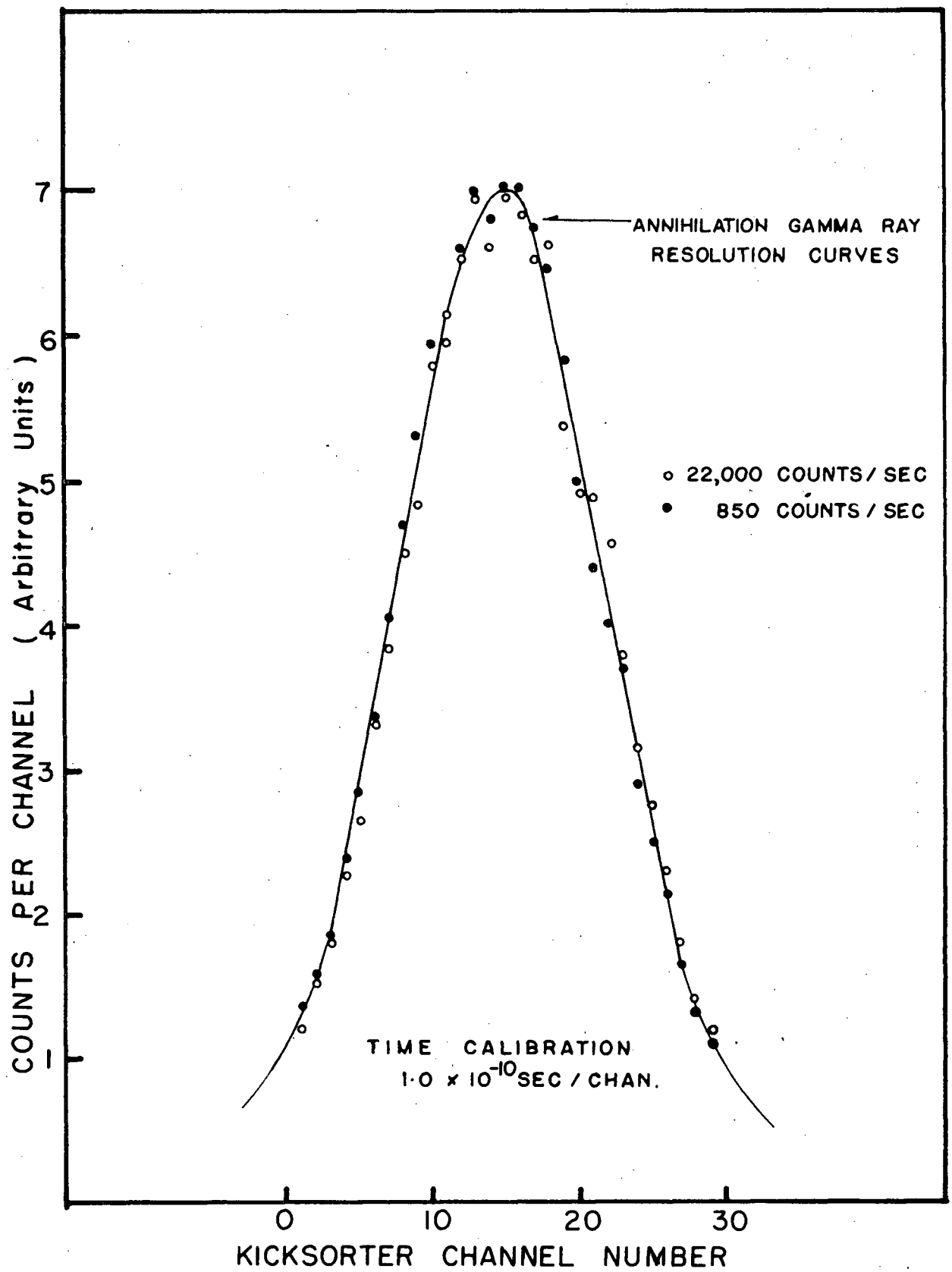

FIGURE 15. COUNT-RATE EFFECT ON RESOLUTION CURVES

illustrated in figure 14, recorded with one side-channel analyser biased to detect gamma-rays of energy greater than about 700 Kev, and the other analyser set to cover the top third of the 0.51 Mev annihilation gamma ray Compton spectrum. The values of the width at half-height 11.0×10^{-10} sec. and the slopes of the sides of the curves: a factor of two in 1.2×10^{-10} sec on the left, and 1.9×10^{-10} sec on the right, are somewhat worse than those obtained by Green and Bell (1958) for a recent 6BN6 time sorter, viz: 8.5×10^{-10} sec width at half-height, and 1.4×10^{-10} sec for the slope of the right side of the curve. This difference is probably attributable to the scintillation counters used. Green and Bell employed end-window, 6342 photomultipliers (operated at 2100 volts)in conjunction with diphenylacetylene crystals. Because of the magnitude of the differences noted here, it is felt that use of the new 7264 photomultipliers may yield still further improvement in resolution. The slope of the right-hand side of the curve in fig 14 is less than that on the left because it corresponds to longer counter delays occurring during the detection of the lower energy gamma rays associated with this counter. The formula of Post and Schiff (given on page 51) indicates the inverse dependence of these counter delays on the energy loss of the detected radiation.

(D) Count-Rate Effects:

Figure 15 illustrates the count-rate effects on the resolution curves for the rates: 850 cps and 22,000 cps, these rates being those counted at the outputs of the side-channel

analysers whose biases were set just above the noise level so that most of the Compton spectra of the annihilation gamma rays were detected. It is apparent that for these rates no significant alteration of the slopes or position of the resolution curves is observed. The very small shift apparent in the figure can be attributed to somewhat different gamma-ray flight times for the two cases.

The dc current observed at the monitor points on the limiters varied by an amount consistent with these rates (about 2% decrease at the high rate).

(E) Overall Stability:

The stability of the time calibration of the whole apparatus is indicated in fig 12, where the gamma-ray time-of-flight time calibration curve is actually a composite of two sets of measurements taken two months apart. It was observed that the small changes in the experimental conditions which occurred over the course of a day generally resulted in a small shift in the position of the time calibration curve rather than a change in slope.

A detailed study of the stability of the complete system was performed by varying the operating conditions of each of the various portions of the instrument in turn, and observing the corresponding time shift of the resulting resolution curves. These measurements were obtained while driving both limiters with one scintillation counter, thus producing a narrowed resolution curve of the type shown in figure 13(b).

(i) Variations in the rise time of the scintillation pulses

as a result of variations in the photomultiplier gain resulted in time shifts of less than .01 nsec for HT variations of less than $\pm$ 50 volts in 1850 volts. This is a somewhat over-optimistic estimate of this dependence, however, since in actual practice two counters were employed, and the differences in the characteristics of the two counters would result in different gain variations for the two photomultipliers, which, in turn, would produce greater time shifts than would be observed for just the one counter.

(ii) AC mains variations of $\pm$ 10% resulted in time shifts of less than .02 nsec.

(iii) Stability of the time sorter power supply to $\pm$ 1 volt corresponded to a time stability of $\pm$ $\frac{1}{2}$% ($\sim \pm 0.25 \times 10^{-10}$ sec)

(iv) The temperature of the diode unit in the time sorter must be kept constant to $\pm$ 0.8°C. for errors of less than .005 nsec in the time measurements.

(v) For a time uncertainty of less than $\pm$.01 nsec the limiter current had to be constant to $\pm$ 0.15%.

For the measurements described in the next chapter the operating conditions of the equipment were restricted to the following limits:

(i) Photomultiplier HT variations of less than 10 volts were ensured.

(ii) The effects of AC mains variations were reduced by using a Sola regulator.

(iii) A regulated power supply was employed for the time sorter.

(iv) The room temperature was normally kept constant to about one degree Centigrade. Temperature lagging of the fast diode assembly was also introduced by mounting the diode unit in a styrofoam-insulated box.

(v) The limiter currents, determined by frequent monitoring, were observed to remain constant to $\pm$ 0.2% over the course of a day. A slow decline in the limiter current of about 6% occurred over the course of one half year of continual operation.

It would appear, therefore, that a significant improvement in the time stability would require a limiter and time converter system of still higher quality. Either a limiter system of greater stability than the 0.2% mentioned above, or a diode switch assembly with less amplitude dependence would be required. Achieving the former while still retaining a high degree of count-rate stability is a difficult problem. The latter might be the more promising approach considering the advent of the new diodes with low hole storage and fast recovery, as described on page 66. The possibility of obtaining a narrower resolution surve by using the newly-developed photomultipliers (see page 69) should also be investigated, since such curves would greatly improve the accuracy involved in the analysis of the results. In summary, the characteristics of the time sorter described in this section were considered to be satisfactory for the accuracy desired in the measurements of positron lifetimes in metals.

CHAPTER IV

MEASUREMENT OF POSITRON LIFETIMES IN ALUMINUM

1. Comparison with a Cobalt-60 Prompt Source.

A. Experimental Difficulties and Sources of Error:

A determination of the absolute lifetime of positrons in aluminum was obtained by a method similar to that used by Minton (1954), and Gerholm (1956) (as outlined earlier on page 52). The method consists essentially of a mathematical comparison of the coincidence resolution curves resulting from the Na^{22} positron annihilations in aluminum and those from a Co^{60} prompt source. The use of appropriate side-channel energy selection ensures that only one of the limiters detects the high-energy gamma rays (the 1.28 Mev gamma ray for the case of Na^{22}) allowing the other limiter to detect one of the lower-energy coincident (within the lifetime of the positron) annihilation gamma rays. The accuracy of the final results is very much dependent on the following three factors:

(i) lifetime of the Co^{60} gamma rays;

(ii) lifetime of the Ne^{22} 1.28 Mev state; and,

(iii) systematic errors due to lack of energy similarity between the two sources.

(i) Although these lifetime measurements should, in principle, be obtained by a comparison of the resulting resolution curves to those from a truly prompt source of coincident gamma rays, an approximation to such a prompt source is all that

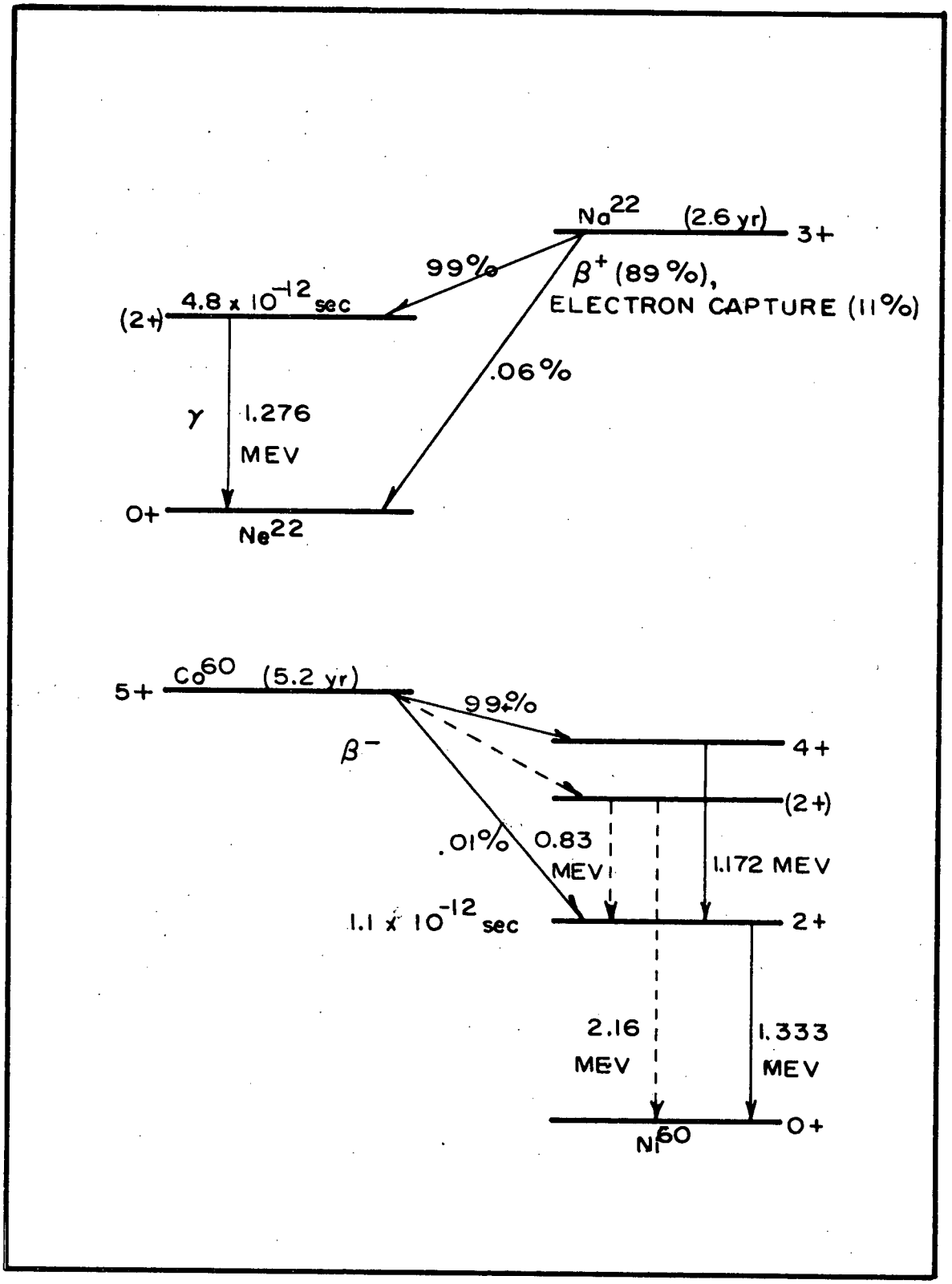

FIGURE 16. SODIUM-22 AND COBALT-60 DECAY SCHEMES

can be expected in practice. Cobalt-60 has frequently been employed as a prompt source because of the following characteristics (Strominger et al, 1958).

The nuclear decay of Co^{60} as shown in fig 16, is free of any detectable positron decay, an obvious requirement for a reference source used in positron lifetime determinations.

The de-excitation of the daughter product, Ni^{60}, occurs predominantly by the emission of two cascade gamma rays. Possible complication of the interpretation of the resolution curves due to the existence of other cascade gamma rays emitted in coincidence (as occurs in many other sources) is thereby eliminated.

Thirdly, the lifetime of the second gamma ray, the one emitted from the 1.33 Mev level of Ni^{60} is short compared to the lifetime of the positrons, a necessary characteristic if Co^{60} is to be a satisfactory approximation to a true, prompt source. Numerical estimates of the lifetime of the first excited state of Ni^{60} have been obtained by several methods. Bay et al (1955) found that the mean lives of both excited states of Ni^{60} are less than 10^{-11} seconds by measurements with a fast coincidence apparatus. By a similar method, Coleman (1955) obtained the value of $(0.8 \pm 0.5) \times 10^{-11}$ seconds for the mean life of the 1.33 Mev level. Using a resonance fluorescence self-absorption technique, Metzger (1956) determined a lifetime of $(0.11 \pm .02) \times 10^{-11}$ seconds from the measured transition probabilities. Thus, the lifetime of this state is less than a few per cent of the mean lifetime of positrons in a metal.

The effect of such a lifetime is reduced, of course, in an arrangement where both gamma rays are detected with equal facility in both scintillation counters. In this case, a finite lifetime for the 1.33 Mev state would merely widen the coincidence resolution curve (i.e. an increase in the value of the variance), rather than alter the centroid of the resolution curve. Since an analysis of the results by means of higher moments than the first was desired, however, a short lifetime for the 1.33 Mev state was definitely required.

(ii) Measurements of positron lifetimes obtained when Na^{22} is used as the source of positrons actually determine the mean time interval between the emission of the 1.28 Mev nuclear gamma ray shown in the decay scheme, fig 16, and the annihilation of the positron. In order for this value to be a reasonable measure of the positron lifetime, the nuclear gamma ray lifetime must be small.

Alkhazov et al (1959) obtained an estimate for the lifetime of the 1.28 Mev level of Ne^{22} by measuring the Coulomb excitation cross-section for this state. In this way, the reduced transition probability, and hence the lifetime (which is the reciprocal of the transition probability) of the radiative transition was calculated. The lifetime that Alkhazov et al quote for this level is 4.8×10^{-12} seconds. Since this value is only of the order of two per cent of the mean lifetime of positrons in metals, use of the 1.28 Mev gamma ray to indicate the instant of formation of the positron is justified.

(iii) When using Co^{60} as a prompt source for these measure-

ments, the possibility of a systematic error arising from the energy-dependent, instrumental time shift described in detail on page 51 must be considered. Since the gamma rays interact with organic and plastic phosphors primarily by means of the Compton effect, a full spectrum of pulses of various amplitudes (up to a maximum determined by the energy of the incident radiation) is produced. Thus, by employing side-channel energy selection with coincidences between both side channels used to gate the time-sorter pulses, only those time-sorter pulses originating from photomultiplier pulses of the same amplitude range (for both sources) are recorded. By this means, the energy-dependent systematic error can be reduced to zero in the limit of zero window width in the low-energy side channel. The high-energy side channel may, of course, be set to detect any energy above 0.51 Mev since the 1.28 Mev gamma rays from Na^{22}, and the 1.17 and 1.33 Mev gamma rays from Co^{60} all produce similar pulse amplitude spectra.

B. Method of Analysis of Resolution Curves.

The mathematical comparison of the resulting resolution curves was performed by calculating the first few statistical moments of the curves and then using the methods described by Newton (1950), and Bay (1955), to determine the corresponding moments of the unknown positron annihilation distribution function. Because of the decreased statistical accuracy of the higher moments, only the first two moments were used in the lifetime calculations described in this chapter.

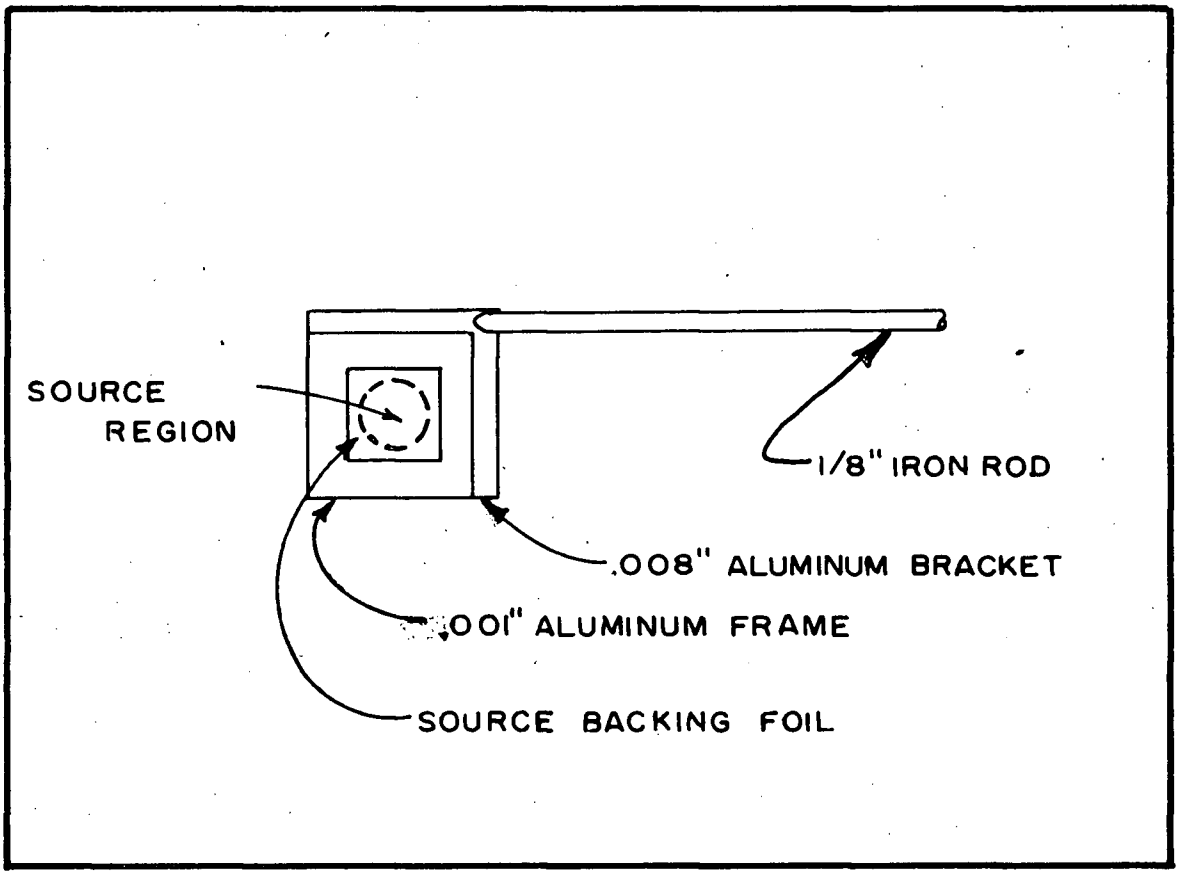

FIGURE 17. SOURCE CONSTRUCTION

In summary, then, the lifetime of positrons in aluminum was determined by performing a series of measurements in which the resolution curves for a positron source (Na^{22}) imbedded in aluminum were compared to those of a prompt source (Co^{60}).

C. Preparation of Sources:

(a) Sodium-22 Source:

Three Na^{22} sources were constructed as shown in fig 17. The source occupied a diffuse region of about 1/4 inch in diameter in the centre of the $\frac{1}{2}$ inch x $\frac{1}{2}$ inch central, thin source backing. The backings for a total of three sources were prepared by covering four .001 inch aluminum frames with .00023 inch (1.6 mg/cm^2) aluminum sheet, and two frames with 0.5 mg/cm^2 collodion films. The thin aluminum was glued to the .001 inch frame with metal lacquer (India Paint and Lacquer Co., type 46-A). The collodion films were produced by mixing Collodion (reagent grade) with an equal volume of amyl acetate and dropping about thirty five drops of the mixture on to distilled water in a four inch Petri dish. The evaporated film was then removed from the water on a seven centimeter (diameter) copper wire ring. Two lacquered aluminum frames were then laid on the collodion film and cut loose with a razor blade when dry.

The Na^{22} source was obtained from an aqueous solution of activated sodium chloride of total strength 0.8 mc, kindly supplied to the UBC Van de Graaff group by Professor W. E. Burcham, Physics Dept., University of Birmingham. About 0.16 mc of this solution was concentrated by slow evaporation in a crucible using a heat lamp, until the activity was about .010

mc per drop. Then one drop of the solution was deposited on one of the aluminum-covered and one of the collodion-covered frames. These were then evaporated to dryness using the heat lamp. One drop of five per cent collodion (in amyl acetate) was then added to the aluminum-backed source, to hold the sodium chloride deposit in place. Another aluminum-covered frame was then placed on top of this source and the edges glued with R313. Before gluing the other collodion frame on to the collodion-backed source, a piece of .001 inch tungsten wire was laid across the source to aid in removing the accumulating charge. A stronger source was prepared by depositing two drops of more highly concentrated solution from the crucible on one of the remaining aluminum-covered frames. On drying, it formed a fairly-thick, heterogeneous deposit of about ½ inch in diameter with a large number of small crystals in evidence. This was then covered with the last aluminum frame in the manner described above. The rest of the source components were mounted together using the R313 as glue. The source strengths, as calibrated using a NaI scintillation counter, and one of the UBC Van de Graaff group standards as comparison, were found to be:

(i) Collodion source: .0081 mc.

(ii) Weak Aluminum source: .0063 mc.

(iii) Strong Aluminum source: .0600 mc.

Since these sources were intended to be used to measure the lifetime of positrons in other materials, it was desired to have as few positrons absorbed in the source material as

possible. An estimate of the amount of positron loss in the source was made as follows:

(i) Geometrical loss in the .001 inch aluminum frames. The mean distance from the source to the frame was about 0.2 inches. Therefore the loss due to the solid angle subtended by the frame was about $\frac{2\pi r \Delta r}{4\pi r^2} = \frac{\Delta r}{2r} = \frac{2 \times .001}{2 \times 0.2} = 0.5\%$;

(ii) Foil Absorption: Fig 32, Appendix A, shows that a sandwich source of the form described above, with an aluminum foil thickness of .00023 inches would absorb about nine per cent of the positrons when a teflon absorber is placed around the source. It is expected that the collodion backing, being about one third as thick (by weight) as the aluminum, would absorb two or three per cent of the positrons. Thus, it would appear that the geometrical loss estimated in (i) is insignificant compared to the loss involved when the positrons traverse the backing foils. A dependence of the actual fractional loss of the positrons on the nature of the positron absorber placed around the source would also be expected, since the amount of backscattering of positrons is dependent on the atomic number of the surrounding material (Seliger, 1955).

The estimate of the positron loss given above is in agreement with that assumed by Bell (Green and Bell, 1957), but is significantly less than the ($18 \pm 5\%$) loss determined by Hatcher et al (1958) for .0002 inch aluminum foils. Since the method employed to determine the positron loss described in

Appendix A is identical to that described by Hatcher et al, it is difficult to explain the large discrepancy between the two values unless they used a single aluminum window (their geometry was not described) in which case their quoted value for the loss would also include the positrons backscattered from the sample.

(b) Cobalt-60 Source:

The Co^{60} source was prepared by imbedding a short piece (about 1/8 inch) of activated cobalt wire in an aluminum sandwich, formed of .008 inch aluminum sheet. The source was formed in this fashion to simulate the positron-in-absorber sample as far as geometry is concerned. In order to minimise possible errors in the lifetime measurements due to differences in count-rates from the two sources, the size of the Co^{60} wire was chosen to produce a source strength of about .008 mc.

D. Time Calibrations:

Time calibrations were performed as described on page 82, and were repeated several times during the course of the measurements. The curve shown in fig 11 is one such calibration. A value of $(1.10 \pm .02) \times 10^{-10}$ seconds per kicksorter channel width was obtained when the equipment was set up according to the conditions described on page 79.

E. Experimental Procedure:

(a) Source-Counter Geometry:

During the measurements, the two counters were aligned at an angle of 180° with respect to the source, and, for the sake

of coincidence efficiency, the distances between the source and the phosphors were kept small (less than one-half inch). To eliminate the possibility of detecting coincidences between the 1.28 Mev gamma rays detected in the "high-energy" counter, and the same gamma-rays, which, after recoiling from the first counter are sufficiently degraded in energy that they may be detected in the 0.51 Mev counter, a 180° alignment of the source and counters was employed, so that any back-scattered gamma rays incident on the second counter would be so degraded in energy that they could easily be distinguished from the 0.51 Mev annihilation gamma rays. Because of the significant solid angles involved in the geometry of the source-counters arrangement, the possible detection of photons back-scattered by angles between 180° and 110° were considered when determining the side-channel bias levels required. Since the energy of the back-scattered gamma ray is strongly dependent on the angle of reflection, being a minimum (212 Kev) for a back-scattering of 180°, and still only 300 Kev for a scattering angle of 110°, the alignment of the counters and source as described above enabled discrimination against the "back-scattered" coincidences by biasing the 0.51 Mev side-channel analyser above 300 Kev. Thus, only the upper portion of the 0.51 Mev annihilation Compton spectrum was utilised. The degree of removal of this prompt background was checked by measuring the coincidence resolution curve for a Zn^{65} source which produces a single gamma ray of 1.11 Mev energy (Strominger, 1958). Although 1.5% of the nuclear decays are characterized by positron

emission, all of these are ground state transitions, with the result that no true coincidences between the 1.1 Mev gamma rays and the positron annihilations would occur. The coincidence count rate obtained with this source was found to be less than one per cent of that with the Na^{22} source.

Another method considered to eliminate the possibility of recording "back-scattered" coincidences involved aligning the counters at 90° with respect to the source, and placing a lead absorber between the two counters. Adequate shielding of the two counters from each other, however, required a substantial increase in the source-counter distances. Thus, in order to retain practical coincidence counting rates, a stronger source would be required and this would result in a correspondingly larger random coincidence background. Because the 180° alignment method appeared to give quite satisfactory performance, and was free of the counting-rate difficulties inherent in the alternate method, it was decided to adopt this geometrical arrangement for the absolute lifetime measurements.

A second source of extraneous prompt coincidences was also considered. The co-linear alignment of the source and detectors could result in the recording of extraneous prompt coincidences due to random coincidences between the gate pulses generated by the slow coincidence circuit and time sorter pulses resulting from the coincident detection of two annihilation quanta. This effect was expected to be a very minor one, however, since the random count-rate would be given by $2N_aN_c\tau$, where N_a is the annihilation-pair "fast" coincidence

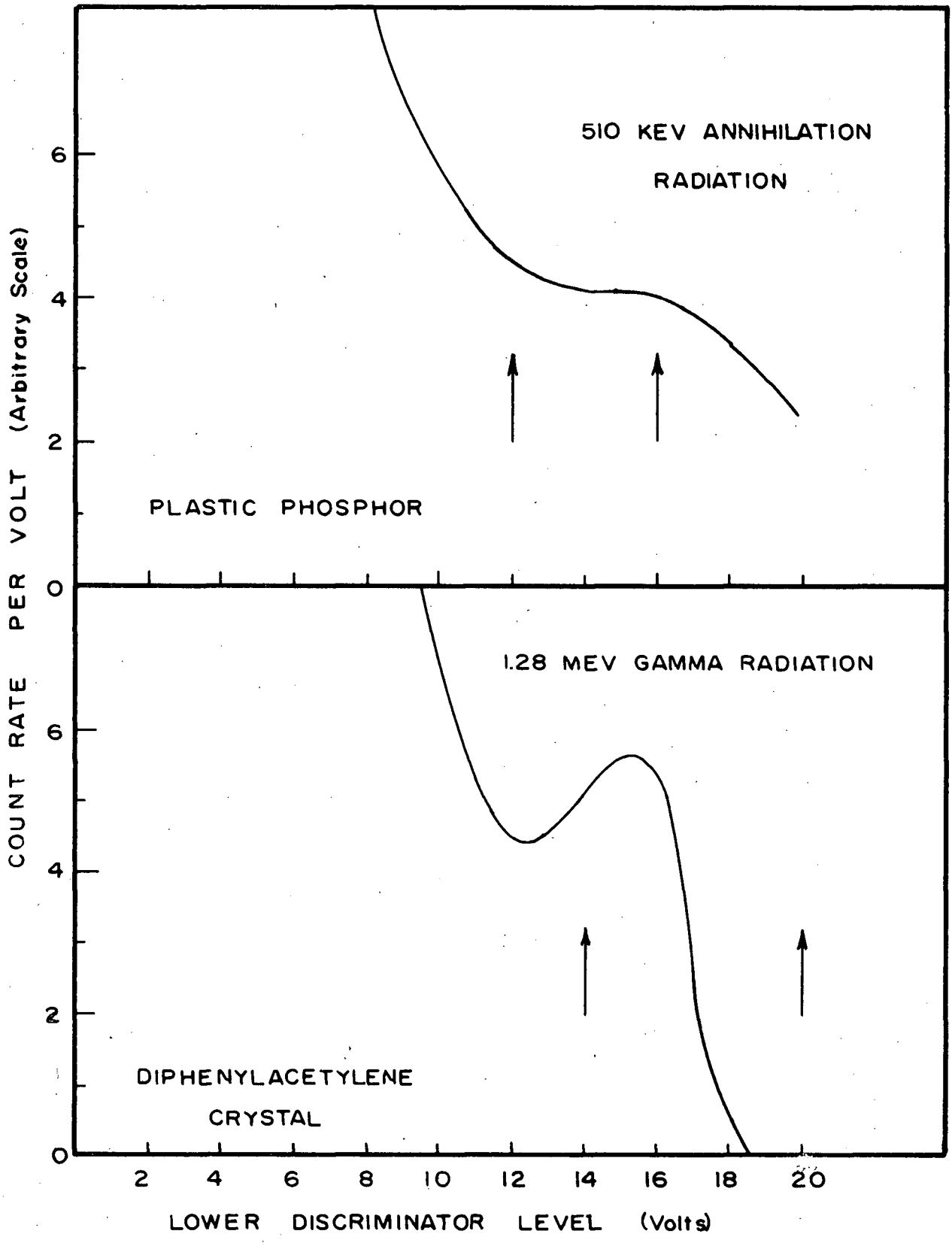

FIGURE 18. SCINTILLATION SPECTRA OF GAMMA-RAY DETECTORS

count-rate, N_c is the side-channel "slow" coincidence count-rate due to 1.28 Mev - 0.51 Mev coincidences, and τ is the coincidence resolution time of the system (in this case, equal to the gate pulse width of one microsecond). Since the true coincident count rate recorded on the kicksorter is about N_c (actually N_c may be a factor of about two higher than the true coincidence rate due to the increased number of random coincidences in the slow coincidence system), then the fraction of recorded coincidences contributed by this prompt background is $2N_a\tau$. The coincidence count rate, Na, for the annihilation gamma rays was measured by resetting both side-channel analysers to cover the majority of the annihilation gamma ray Compton spectra. Typical rates under these conditions were thirty to fifty counts per second. If one hundred counts per second is taken as an upper limit, the fractional contribution from this effect is then $2 \times 100 \times 10^{-6} = 2 \times 10^{-4}$, a background effect of negligible proportion.

(b) Side Channel Settings:

As mentioned earlier (pg 88), the side-channel, pulse-amplitude analysers were set so that one analyser was biased to trigger only for that portion of the 1.28 Mev Compton spectrum above the annihilation spectrum, and the other was set to accept a range of pulses near the top of the 0.51 Mev Compton spectrum. The discriminator levels normally employed in these measurements are indicated on the spectra (fig 18) obtained for the two counters by using the side-channel analysers as single-channel instruments with a one volt window. The counter with the best

resolution was employed in the 1.28 Mev channel to insure positive discrimination against the 0.51 Mev pulses. A check was made of the upper limit of the 0.51 Mev pulses by plotting the coincidence count rate for the colinear arrangement of the counters and source as a function of increasing lower discriminator level for the 1.28 Mev analyser. The turning-point between a rapid decrease in coincident count rate and a low level plateau indicated the maximum 0.51 Mev pulse heights. A discrimination level greater than this value was employed in the subsequent measurements. The lower limit of the 0.51 Mev analyser was normally restricted to about 2/3 of the full energy to insure discrimination against back-scattered 1.28 Mev photons.

(c) Nature of Experimental Measurements:

A series of coincidence resolution curves (each about 1½ hours in duration) were then obtained in alternate fashion for the Co^{60} source imbedded in aluminum and the collodion-backed Na^{22} source in an aluminum absorber. The aluminum samples surrounding the Na^{22} source were about .060 inches thick, sufficient to stop the positrons, about 5/8 inches square, and polished and cleaned with ethyl alcohol on the side which faced the source. A spring wire clip, glued to the backs of the samples with rubber cement, was used to hold the aluminum samples firmly against both sides of the source. Care was exercised in attempting to place the two sources in the same physical position since a difference of 0.15 cm in the source-counter distances could result in an error in the lifetime measurement of 0.1×10^{-10} sec, of the same order as the

accuracy desired.

A number of similar curves were then obtained with the settings of the two side-channel analysers interchanged. Thus, the former 1.28 Mev channel was set on the 0.51 Mev range, and vice-versa. By this means, the "fast" coincidences that were selected were those resulting from detection of the 1.28 Mev gamma rays by the former 0.51 Mev scintillation counter, and detection of the 0.51 Mev gamma rays by the other, formerly 1.28 Mev counter. Whereas the former experimental arrangement (with added time delay in the 1.28 Mev channel so that, at the time sorter, the 1.28 Mev square pulses appeared near the end of the 0.51 Mev square pulses) resulted in an increased pulse size for increased delay in the 0.51 Mev channel, the latter arrangement resulted in a decreased pulse size. Reproducibility of the two sets of results would therefore be considered to be a good check of their validity and of the operation of the apparatus.

A check of possible count-rate effects was also obtained by performing a series of measurements with various source-counter distances, and also by changing the strength of the Co^{60} source by a factor of two during one series of runs.

An experimental estimate of the effect of differences in the accepted range of the spectral distribution of pulses (as viewed by the 0.51 Mev analyser) for the Na^{22} and Co^{60} sources, was determined from a set of curves for which the width of the 0.51 Mev channel window was varied, so that an extrapolation of the results corresponding to the ideal case of zero window

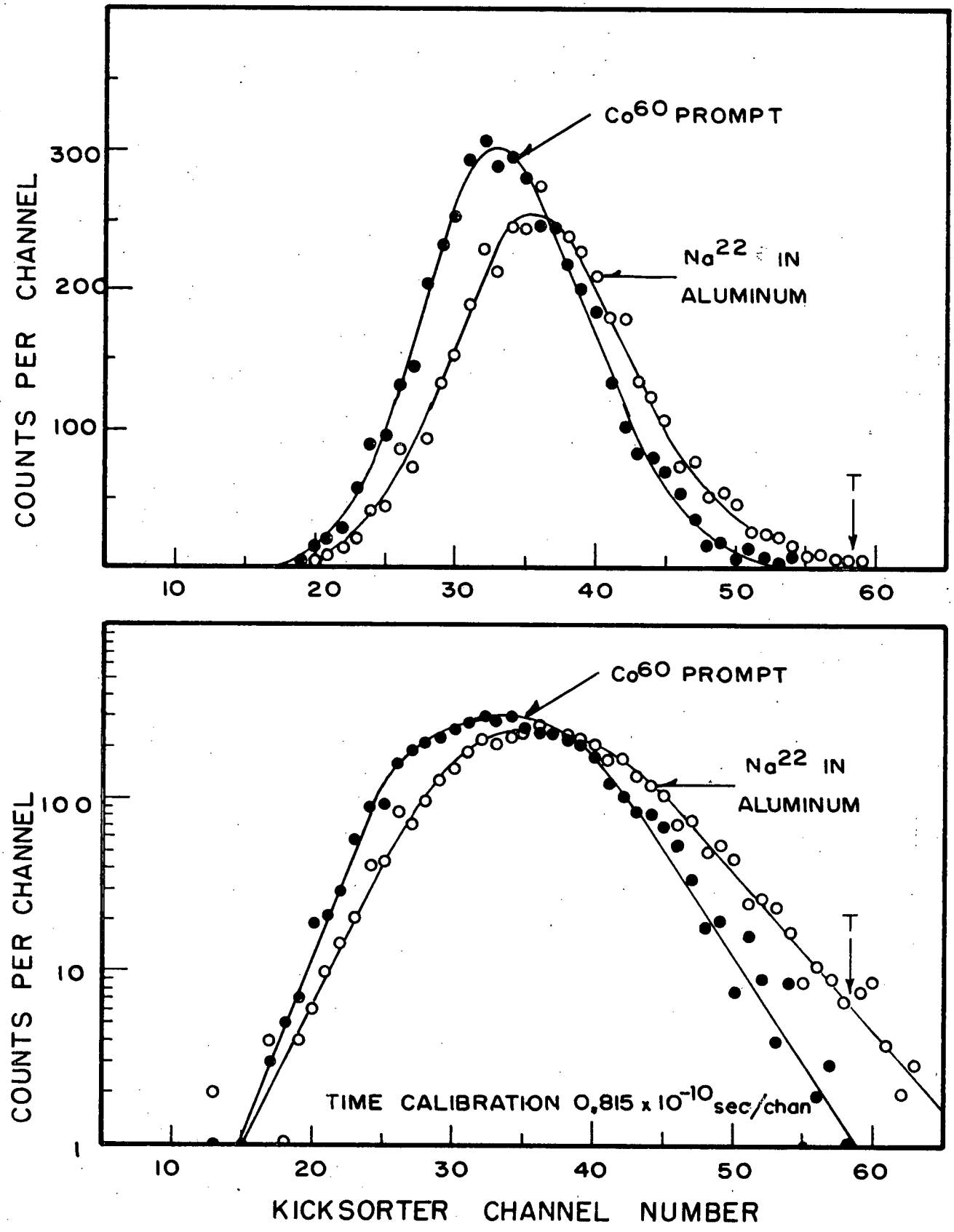

FIGURE 19. DELAYED COINCIDENCE RESOLUTION CURVES FOR SODIUM-22 IN ALUMINUM AND COBALT-60.

width could be obtained.

Although most of the results were obtained using the thirty-channel pulse-amplitude analyser, several curves were obtained using the 100-channel instrument to check, primarily, the possible existence of a long-lived component of the positron decay which was reported by Gerholm (1956).

F. Results:

(a) Method Employed for Determining the Lifetime:

Typical resolution curves obtained for the two sources are shown in fig 19 for both linear and logarithmic scales. The curves shown are the experimental data without background subtraction. As described in Appendix C, the mean lifetime, τ, of the positrons is determined by the difference in the first moments (means, or centroids) of the positron resolution curve and the Co^{60} prompt resolution curves. In addition, the variance of the positron annihilation distribution function is given by the difference in the variances of the two resolution curves. Since the square roots of the variances have dimensions of time, this measure of the positron annihilation distribution function is termed, in this thesis, the "rms lifetime" and is denoted by the symbol, τ'.

The moments analyses of the experimental resolution curves described above were performed using the UBC Alwac III E digital computer, the program used for the analysis being given in Appendix H. The random coincidence background rates were sufficiently small that their contribution to the values τ and

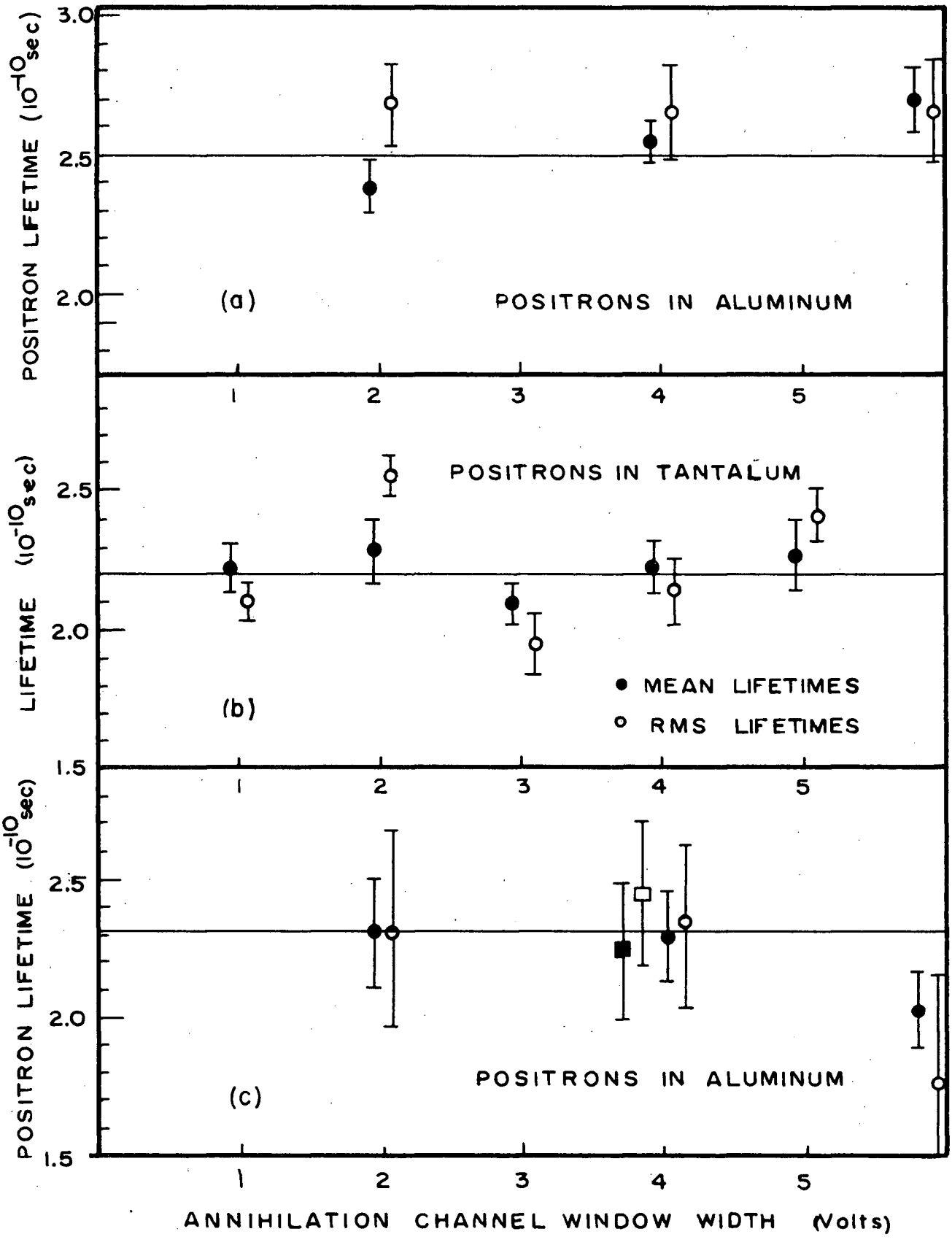

FIGURE 20. LIFETIME DEPENDENCE ON ANNIHILATION CHANNEL WINDOW WIDTH.
(a) and (b): 'Normal' Mode of Time Sorter Operation
(c) : 'Inverted' Mode of Time Sorter Operation

τ' have been neglected in the results quoted below. Analyses of several runs in which the backgrounds were subtracted indicated that their inclusion resulted in an error in the centroid determination of less than two per cent, and an error in the rms lifetime determination of less than five per cent. One reason that the backgrounds were neglected was due to the difficulty in estimating the total random coincident background over the time range involved. Since this total background was normally less than fifty counts (as estimated from the random rate outside the resolution curve) for the curves that were obtained in these measurements, an exact estimate of their effect on the results was impossible due to statistical fluctuations both in their total number and in their distribution within the time range involved. Consequently, the results were analysed without background subtraction. Instead, an estimate of the uncertainties introduced by neglecting these random counts was included in the errors quoted for the results.

(b) Results for Inverted Operation:

The results obtained using the 100-channel kicksorter showed, as expected, that inversion of the mode of operation of the apparatus had negligible effect on the measured values of the lifetime. This is indicated in fig 20(c), where two pairs of measurements are indicated corresponding to an abscissa of four volts (a window width of 25% of the upper level). Each pair consists of a determination of the mean lifetime, τ, and the rms lifetime, τ', of the positron annihilation distribution function. The two pairs of measurements were obtained

under equivalent conditions, except that the mode of operation of the apparatus was reversed (as described in greater detail on pg 100).

(c) Zero Window-Width Extrapolated Results:

Fig 20 illustrates the dependence of the results on the window width of the side-channel analyser in the annihilation radiation channel. (a) and (b) were obtained under similar operating conditions, with the equipment arranged so that an increased delay in the annihilation channel yielded an increase in the time-sorter output pulse, whereas (c) was obtained with the equipment operating in the reverse mode. An aluminum absorber was used in curves (a) and (c), and a tantalum one for (b). A lack of any onvious dependence of the results on the window width indicates that, for the window widths employed, variations of the shapes of the pulse amplitude spectra between the Co^{60} and Na^{22} soucres within the windows, had negligible effect on the lifetime determinations. As a result, measurements correct to $\pm$ 0.1 x 10^{-10} seconds are indicated for measurements with a window width as large as four volts.

(d) Count Rate Effects:

The tests conducted to determine a count-rate dependence of the results by varying the source-counter distances failed to yield any such effect, as indicated in fig 15. An additional check was obtained by changing the strength of the Co^{60} source by a factor of two in the middle of a set of runs. Again, no effect was observed.

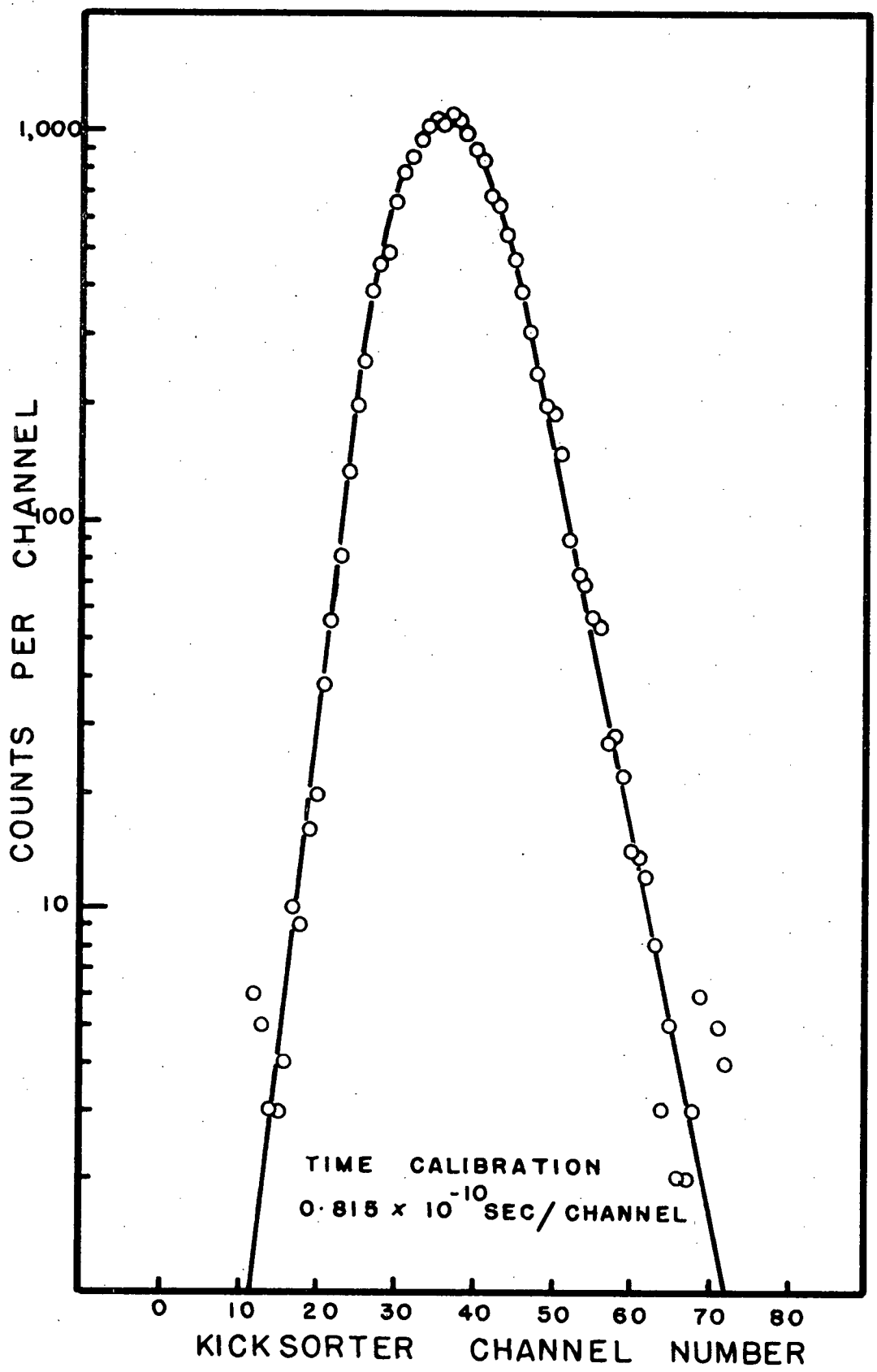

FIGURE 21. DELAYED RESOLUTION CURVE FOR POSITRON ANNIHILATION IN ALUMINUM

(e) Investigation of the Possible Existence of a Long-Life Component in Positron Annihilations:

In fig 21 is shown a semi-logarithmic plot of a resolution curve with better statistics than those shown previously for positrons annihilating in aluminum. No evidence of a long-lived component of the decay was observed over a range of at least three decades, in contrast to the results of Gerholm (1956) which seemed to suggest the existence of such a component by a change in the slope of the right-hand side of the resolution curve in the second decade from the top.

(f) Compilation of Lifetime Results:

Besides the lifetime results mentioned earlier, a series of additional measurements were obtained using the thirty-channel Marconi kicksorter, and annihilation gamma-ray window widths of both two and four volts. Because of the restricted number of channels available for these runs, due partly to a desire for a channel width of about 10^{-10} seconds, it was found that about one per cent of the true coincidences from positron annihilation in aluminum were occurring outside the range of the kicksorter. These were monitored, however, in the overflow channel at the top of the kicksorter. The true coincidences (above the random background) were estimated by subtracting from the top channel counts of a Na^{22} curve, the corresponding counts obtained from an appropriately-normalized Co^{60} curve, for which only random coincidences were detected in the overflow channel. This "truncation loss" could be allowed for by applying the correction factors described in Appendix B. For a typical truncation loss of one per cent, for example, this

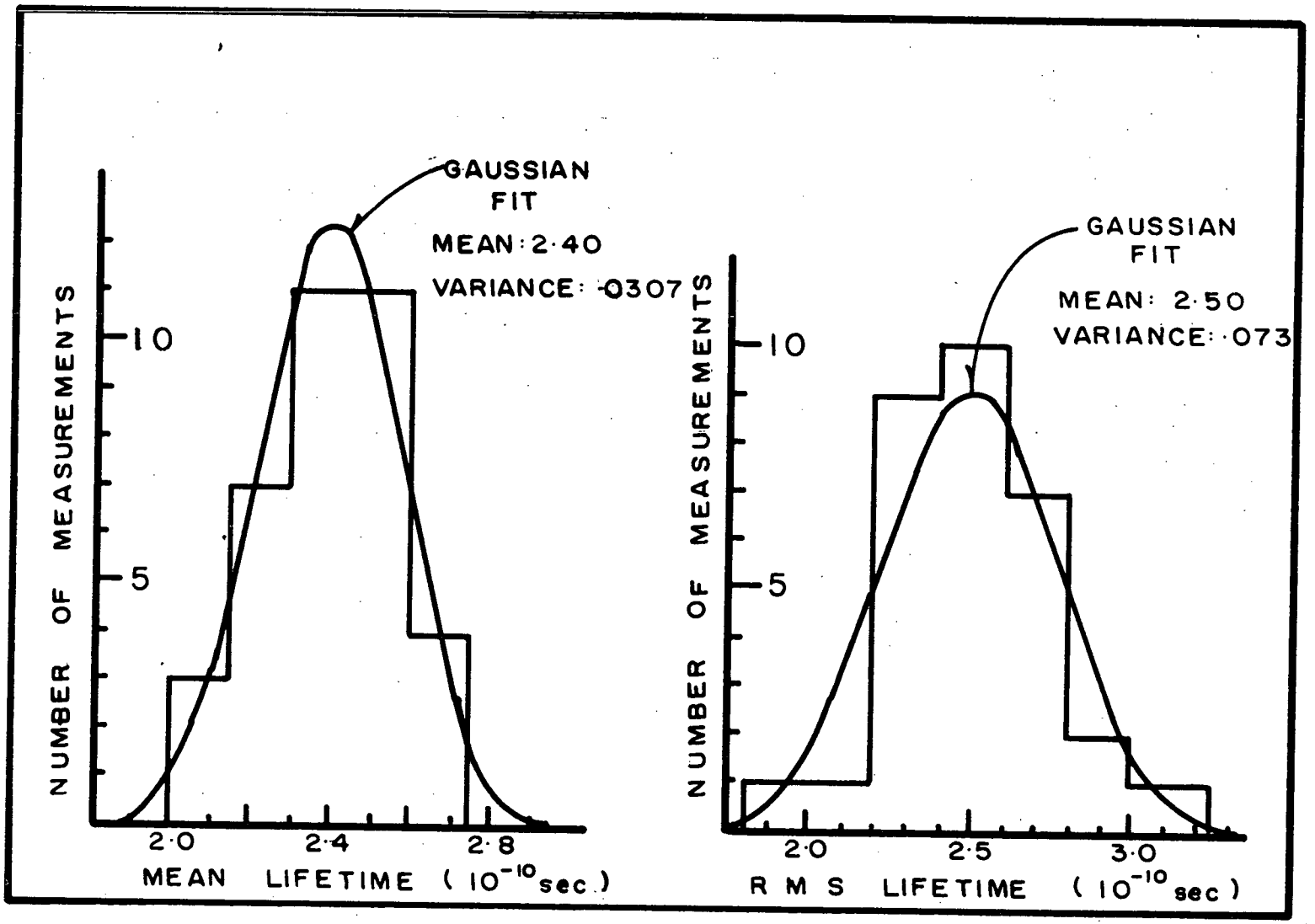

FIGURE 22. DISTRIBUTION OF RESULTS

correction factor was about five per cent for the centroid estimate, τ , and about fourteen per cent for the rms lifetime result, τ' . The results from an analysis of twenty four curves for which the Co^{60} and the Na^{22} in aluminum sources were alternated, yielded a mean value for the mean lifetime, τ , of 2.45×10^{-10} seconds, whereas the mean value obtained from all the one hundred-channel kicksorter runs, a total of twelve curves in all, was 2.30×10^{-10} seconds. Analysis of the complete set of thirty six runs for both τ and τ' yielded the distributions of results shown in fig 22, in which are also indicated gaussian curves with the same means and standard deviations.

The experimental estimates of τ, the first moment of the positron annihilation probability function were found to be distributed about a mean value of 2.40×10^{-10} seconds, with a standard deviation of 0.175×10^{-10} seconds. The values of τ' , the 'rms' measure of the positron annihilation function were distributed about a mean of 2.50×10^{-10} seconds with a standard deviation of 0.27×10^{-10} seconds. These statistics indicate a standard error of the mean of $.04 \times 10^{-10}$ seconds for τ , and $.06 \times 10^{-10}$ seconds for τ', where the standard formula was used for the estimates of the error: $t_f \frac{s_\tau}{\sqrt{n}}$, where s_τ is the observed standard deviation of the results, n is the number of lifetime determinations (given by one half the number of curves; thus, n = 18), and t_f is obtained from Student's t distribution, about one for a value of n as large as eighteen.

(g) Discussion of the Errors: Statistical and Systematic.

The standard deviation of the mean lifetime distribution, 0.175×10^{-10} seconds, consisted mostly of the statistical uncertainty in the mean of an individual resolution curve. With a standard deviation for a typical Na^{22} in aluminum resolution curve of 5.5×10^{-10} seconds and a total number of counts contained in the curve of 3600 (a typical value), the standard deviation of the distribution of means should be: $\frac{5.5 \times 10^{-10}}{\sqrt{3600}} = .09 \times 10^{-10}$ seconds. Since this estimate would only be strictly true if the resolution curves were of gaussian form, the practical case is described by a standard deviation of the means somewhat larger than the above calculation indicates. Finally, the standard deviation of a distribution of differences of such means would be $\sqrt{(.09)^2+(.09)^2} \times 10^{-10}$ seconds, or 0.13×10^{-10} seconds. This estimate of the standard deviation is too small for several reasons, viz:

(i) the non-gaussian nature of the resolution curves;

(ii) additional fluctuations due to the random contribution, and

(iii) variations in the positioning of the sources.

As mentioned earlier (page 99), variations of 0.15 cms in the positioning of the sources would result in changes of $\frac{2 \times 0.15}{3 \times 10^{10}} = 0.1 \times 10^{-10}$ sec in the arrival times of the two gamma rays. Variations of this amount would increase the total standard deviation to about 0.17×10^{-10} sec, in satisfactory agreement with the value obtained.

Additional possible errors of a more systematic nature

would include:

(i) Uncertainty of two per cent in the time calibration producing an uncertainty of $.05 \times 10^{-10}$ seconds in the result.

(ii) A possible systematic error in the positioning of the two types of sources, due to a difference in the distribution of the active material within the source itself. A difference here of 0.15 cm would produce an additional error of 0.1×10^{-10} second in the value for the mean lifetime, τ, but would not affect the experimental value of the rms lifetime, τ'.

(iii) The error involved in neglecting the random coincidence background was described on pg 102 as contributing about 2% ($.05 \times 10^{-10}$ sec) to the error in the estimate of the mean lifetime, τ, and about 5% (0.12×10^{-10} sec) to the error for the rms lifetime, τ'.

(iv) The finite lifetime of the Ne^{22} nuclear gamma ray decreases the observed lifetime of the positrons by $.05 \times 10^{-10}$ sec (Alkhazov et al, 1959). Since $\tau_\beta - \tau_\gamma$ = observed τ = 2.40×10^{-10} seconds, the true τ_β is therefore given by: 2.45×10^{-10} seconds.

Inclusion of the above estimates of possible systematic error yields a total standard error for the measurements, of:* $\left(s_m^2 + k_a^2 + k_b^2\right)^{\frac{1}{2}}$ where s_m^2 is the variance of the statistical distribution of results, and K_a and K_b are estimates of the systematic error.

* Smart, W. M., Combination of Observations, (Cambridge University Press, 1958), p. 53.

On substituting the appropriate values, we obtain for an estimate of the total error, $\left[(.04)^2+(.05)^2+(.1)^2\right]^{\frac{1}{2}}=$ 0.12×10^{-10} seconds.

On the basis of the preceding discussion, the final experimental values quoted for the lifetime of positrons in aluminum, are:
$(2.45 \pm 0.15) \times 10^{-10}$ seconds for the mean lifetime, τ , and
$(2.50 \pm 0.15) \times 10^{-10}$ seconds for the "rms lifetime, τ' ", i.e. the square root of the second moment about the mean.

A similar set of thirty eight measurements with a different absorber, tantalum, yielded the results:
$(2.30 \pm 0.15) \times 10^{-10}$ seconds for the mean lifetime, τ , and
$(2.30 \pm 0.15) \times 10^{-10}$ seconds for the "rms lifetime, τ' ", i.e. the square root of the second moment about the mean.

The indication of a slight difference in the absolute lifetime of positrons between aluminum and tantalum is further substantiated by the comparative measurements of Chapter VI where the lifetime in aluminum was found to be longer than that in tantalum by $(0.38 \pm 0.14) \times 10^{-10}$ seconds.

2. Comparison with a Prompt Source Consisting of Annihilation Gamma Rays.

A further measurement of the value of the positron lifetime in aluminum was obtained by employing a different prompt source. Since Co^{60} emits two gamma rays of high energy compared to the energy of the positron annihilation radiation, it was considered worthwhile to attempt to measure the lifetime of positrons in

aluminum by a method using lower energy prompt radiation, such as the annihilation radiation itself as the prompt source, and dependent on a new technique for comparing the resultant resolution curves. Since positron annihilation is described in terms of a second-order electronic transition, the expected mean delay between the two gamma rays would be of the order of $\frac{h}{\Delta E}$ from the uncertainty principle where ΔE is the energy involved in one of the transitions, 0.511 Mev. By this means, an estimate of 10^{-21} seconds is obtained for the mean lifetime of the transition from the intermediate to the final state, a value indicative of a most satisfactory "prompt" source. Using a prompt source of this type, however, requires that the side-channel analysers be so adjusted that both channels accept pulses corresponding to the top portion of the 0.511 Mev. Compton spectrum. Consequently, when the delayed resolution curves for positrons in aluminum were obtained, care was exercised to ensure that the two counters and the source were NOT co-linear, otherwise a high prompt coincidence counting rate (due to annihilation gamma rays) would have been recorded.

A. Experimental Procedure.

(a) Background Prompt Coincidence Contribution:

The possibility of detecting coincidences due to the 1.28 Mev gamma radiation being backscattered from one counter to the other would tend to be increased with this geometrical arrangement as compared to that discussed on page 96 . In order to reduce these background prompt coincidences to as small a value

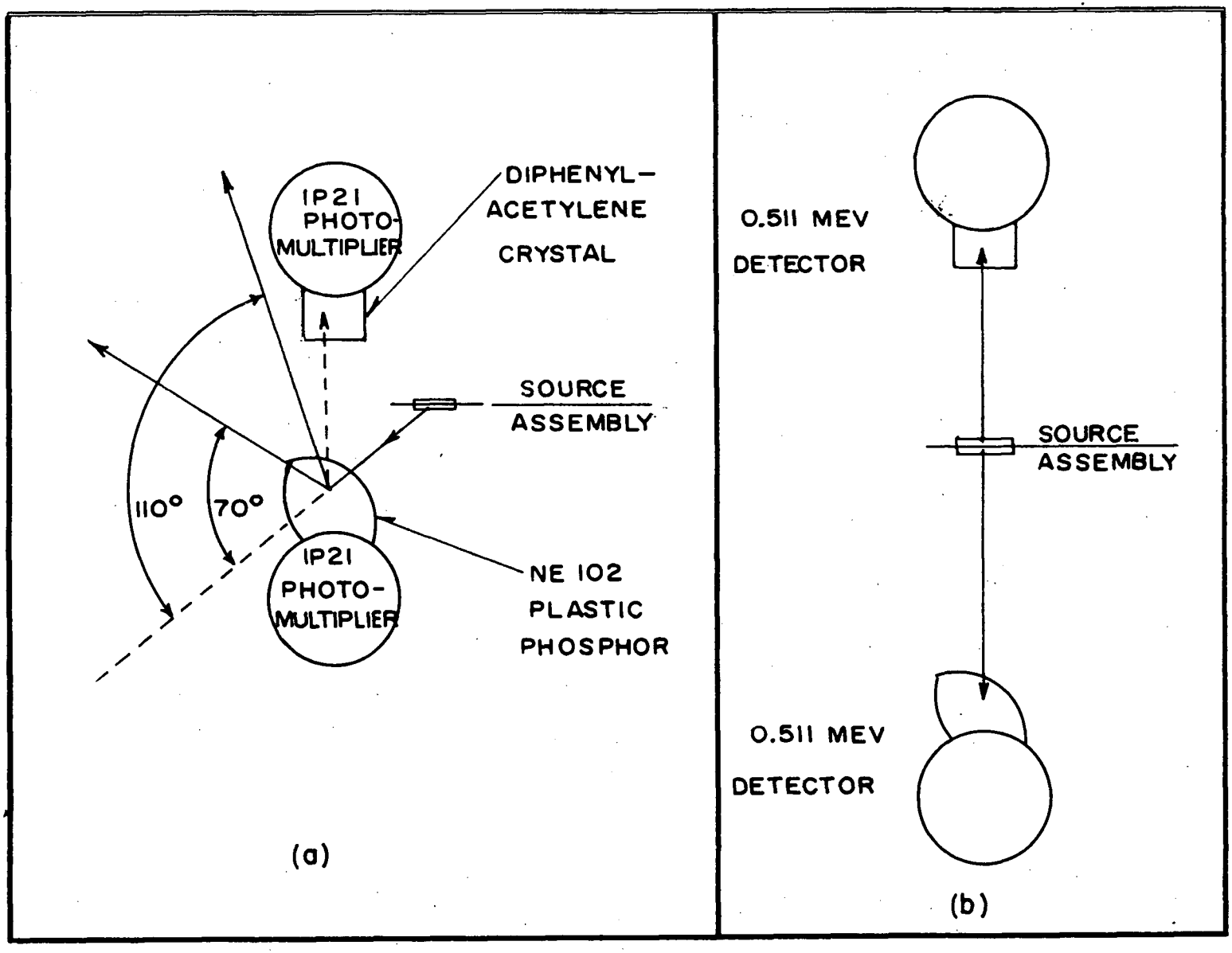

FIGURE 23. SOURCE AND COUNTER ARRANGEMENTS. (a) Geometry for: Na^{22} in Aluminum Delayed and Co^{60} Prompt Resolution Curves

(b) Geometry for: Annihilation Gamma Ray Prompt Resolution Curve

as possible the source was positioned as shown in fig23(a) to ensure that the scattering angle of the 1.28 Mev gamma rays required for detection of this gamma ray in both counters, would be greater than 110^{o}, thus restricting the recoil gamma ray to an energy of less than 300 Kev. Also, the fact that the scattering angle of the 1.28 Mev gamma ray had to be less than 70^{o} (and thus much less than the 110^{o} mentioned above) in order for the Compton interaction to produce a pulse in the 0.51 Mev portion of the 1.28 Mev spectrum in the first counter further assisted in restricting the number of coincidences resulting from this process.

As a result of these two conditions, the possibility of detecting coincidences due to back-scattered gamma rays was considered to be effectively eliminated. Experimental verification of this conclusion is discussed on page 113.

(b) Experimental Details Involved in the Measurements:

With this arrangement, either counter could detect the 0.51 Mev annihilation gamma ray or the equivalent portion of the Compton distribution of the associated 1.28 Mev gamma ray, thus forming a symmetric delayed resolution curve whose centroid position is the same as that for the prompt curve. The width or variance of the delayed resolution curve was, however, larger than that of the prompt curve and so an estimate of the positron lifetime could be obtained by a detailed comparison of these variances. The procedure for obtaining these measurements was as follows:

The counters were set close together to subtend a large solid

angle at the source, and a delayed resolution curve was obtained by placing the aluminum-covered Na^{22} source between them as shown in fig 23(a), offset somewhat from co-linearity. Side-channel window widths of four volts (in sixteen volts) were employed. Next a Co^{60} prompt curve was obtained by replacing the Na^{22} source by the approximately ten microcurie Co^{60} source. Lastly, the counters were separated to reduce the solid angle as illustrated in fig 23(b), and the sixty microcurie aluminum-covered Na^{22} source was inserted between them in a co-linear alignment, thus producing the desired prompt resolution curve by detecting the pairs of annihilation quanta. In this case, the source-counter distances were chosen so that the individual side-channel count rates were close to those obtained for the previous two runs. In this way, count-rate dependent effects were eliminated. A large separation of the counters was also useful in ensuring that only the pairs of annihilation gamma rays would be effective in producing coincidences as the ratio of coincidences due to annihilation gamma rays compared to those due to coincidences between annihilation gamma rays and the 1.28 Mev gamma rays is given by: $N\varepsilon^2\omega / N\varepsilon^1\omega^2 = 1/\omega$ where N is the disintegration rate of the source and the two counters are sssumed to have the same detection efficiency, ε , and solid angle, ω . Actually, the detection efficiency for the 1.28 Mev gamma ray will be significantly less than that for the 0.51 Mev gammas due to the different relative fractions of the two Compton spectra detected by the side channels. For the source counter distances used, of two to three inches, the ratio $1/\omega$ was at least 200/1. Examples of the experimental resolution

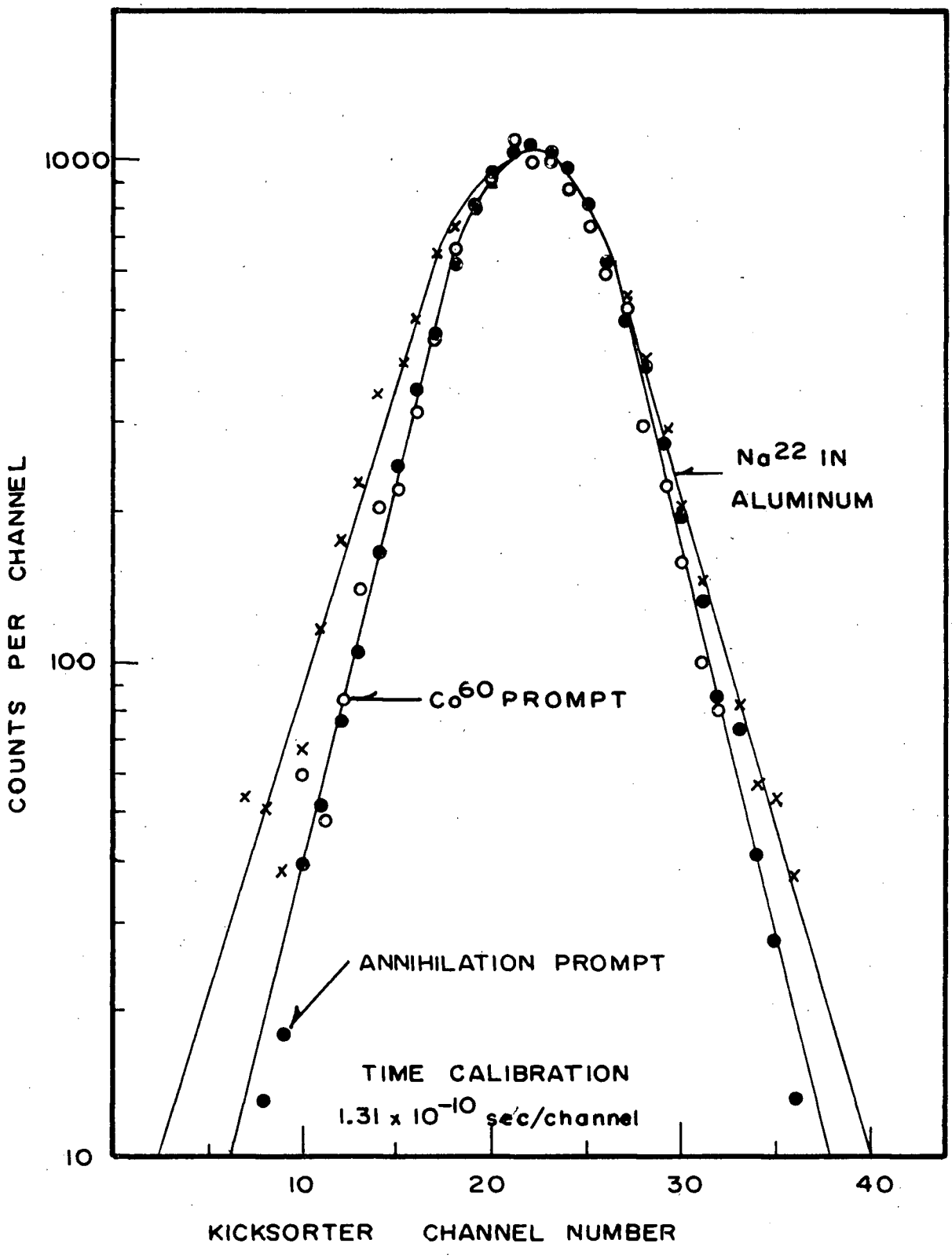

FIGURE 24. SYMMETRIC RESOLUTION CURVES

curves are given in fig 24.

Since only symmetric curves were obtained by this method, it was impossible to determine the value of τ, the first moment of the positron annihilation probability distribution function. Determinations of τ', the standard deviation of the distribution function, were obtained, however, by using the formula: $\tau' = \frac{1}{2}$ (variance of delayed curve - variance of prompt curve) $^{\frac{1}{2}}$, derived in Appendix C (ii).

Because the second moment calculations are so strongly dependent on the tails of the resolution curves as discussed in Appendix B, which analyses the effects of truncation loss, the 100-channel CDC kicksorter was employed for these measurements.

B. Results:

Two determinations of each type of resolution curve were obtained.

The variances of the Co^{60} prompt runs were both: 35.9×10^{-20} sec^2.

The variances of the annihilation radiation prompt curves were: 35.6×10^{-20} sec^2, and 35.9×10^{-20} sec^2.

The variances of the Na^{22} in aluminum runs were: 50.7×10^{-20} sec^2, and 49.2×10^{-20} sec^2.

The equality observed between the variances of the Co^{60} and annihilation radiation prompt resolution curves is further evidence for two previous observations, viz:

(i) The spectral shapes of the Compton distributions for

both the annihilation and Co^{60} gamma rays are sufficiently close over the range covered by the side-channel window widths employed, that effects resulting from energy-dependent instrumental time shifts are negligible in these measurements. These measurements, therefore, offer further experimental evidence for the conclusions outlined on page 103 regarding the lack of any dependence of the absolute lifetime results involving comparisons to Co^{60} prompt resolution curves on the window widths of the single-channel analyser employed in the annihilation channel (for the window widths employed in this work, at any rate).

(ii) Secondly, the observed agreement between these prompt variances also verifies the earlier assumption regarding the low intensity of the contribution of the back-scattered gamma rays to the recorded coincidences. The Co^{60} source would, of course, be more susceptible to the production of coincidences of this type than would the Na^{22} because two high-energy gamma rays are emitted per disintegration rather than one. Although these coincidences were described as "prompt" when compared to those resulting from positron decay (pg 110) they would in fact tend to broaden a truly prompt curve due to the flight time of the gamma ray between the two counters (a path length of the order of 10^{-10} seconds). The lack of any significant difference between the variances of the two types of prompt source can therefore be inter-

preted as evidence that the relative number of such back-scattered coincidences is less than a few per cent for the experimental arrangement employed.

The value of τ', the square root of the second moment about the mean of the positron annihilation distribution, calculated from the mean "prompt" variance of 35.8×10^{-20} sec^2 and the mean "delayed" variance of 50.0×10^{-20} sec^2 is: 2.65×10^{-10} seconds.

The standard deviation of the distribution of estimates of τ' is assumed to be approximately that of the distribution of τ' given in fig 22(b) obtained by the method in which a Co^{60} prompt source was employed; namely: 0.25×10^{-10} sec. Because of the small number of distinct experimental lifetime measurements performed by this method, very little reduction of this standard error is justified. The value offered, then, for the "rms lifetime" of positrons in aluminum, obtained by the method described in this section, is: $(2.65 \pm 0.25) \times 10^{-10}$ seconds.

C. Discussion of an Additional Source of Error.

As mentioned earlier, the mean values of all these symmetric resolution curves should be the same if the relative efficiencies of 0.51 Mev compared to 1.28 Mev gamma ray detection were the same for the two counter-analyser combinations. Since the two scintillation phosphors were of different shape and different material, this assumption is probably not warranted. The resulting lack of complete symmetry in the positron-in-aluminum resolution curves would result in a slight

shift at the centroid of these curves as compared to the symmetric prompt curves (the mathematical dependence of this shift is treated in Appendix C(ii)). Such a shift was observed, in fact, with the centroids of both the broadened resolution curves from Na^{22} in aluminum displaced by about 0.5×10^{-10} seconds with respect to the Co^{60} prompt curve. This error might certainly have been partly composed of a systematic positional error in the placement of the two sources, as discussed more fully on page 106. It is doubtful whether this could be the complete explanation, however, since such a deviation would correspond to a positional error of 0.75 cm, a value significantly larger than might be expected. Consequently, the degree of preferential counting necessary to produce a centroid shift of 0.5×10^{-10} sec was determined (thus yielding a measure of $(g_1 - g_2)$, Appendix C(iii)), and the corresponding effect on the variances of the resolution curves estimated. The effect of such a preferential detection on the final result was estimated to result in an error in the determination of the rms lifetime of about one per cent. That is, an interpretation of the observed centroid shift completely in terms of the asymmetry effect resulted in an error of but one per cent in the estimated value of τ'. If, on the other hand, a positional error in the placement of the two sources is considered to have contributed significantly to the observed centroid shift, then an even smaller asymmetry error would be expected.

3. Discussion and Conclusions:

Using Co^{60} to define the prompt coincidence resolution curve, a value of $(2.45 \pm 0.15) \times 10^{-10}$ seconds was deduced for the mean lifetime τ of positrons in aluminum. Variance analysis of the same curves also yielded an estimate of the root mean square deviation about the mean (τ') of the positron annihilation distribution function, viz: $(2.50 \pm 0.15) \times 10^{-10}$ sec.

An alternate method of obtaining a prompt resolution curve by using the annihilation gamma rays as a prompt source yielded a value for τ', of $(2.65 \pm 0.25) \times 10^{-10}$ sec, a value in agreement with that obtained by the former method.

The lifetime of positrons was also measured in a second absorber, tantalum, by comparison to the prompt source, Co^{60}, yielding the values $(2.30 \pm 0.15) \times 10^{-10}$ sec for τ, and,

$(2.30 \pm 0.15) \times 10^{-10}$ sec for τ'.

The equality between the mean and "rms" lifetime results for both absorbers can be considered as additional information about the nature of the decay of positrons in these metals. Some examples of this information are discussed in the following sections.

A. Nature of the Positron Annihilation Distribution.

Few distribution functions yield the same value for the mean as for the square root of the variance. The pure exponential function is one which does give the same value for each, however, and hence is a reasonable one to assume for the probability distribution function of the annihilation process. In contrast, both a linear and a gaussian decay curve would yield a value for

τ' of less than 80% of the value of τ (Appendix C(iv)). Such a possibility is well outside the errors quoted for the above results. These results, then, provide a partial check of the validity of the assumption of the pure exponential nature of positron annihilation in metals as suggested by Bell and Graham (1953).

B. Experimental Evidence Regarding Positron Thermalisation Times:

A finite slowing-down time of the positrons prior to a pure exponential decay would also give rise to a decrease in τ' relative to τ. If we assume:

(i) the positrons are thermalised in a mean time, t;

(ii) the variance of the probability distribution for thermalisation is, as for an exponential distribution, t^2. An assumed variance of less than t^2 as would result, for example, from a gaussian form of probability distribution would yield lifetime estimates (τ and τ') even more incompatible with the experimental results than for that assumed here.

(iii) the annihilation of the positrons from the thermalised state is given by the standard exponential probability distribution, of mean life, τ_β, and variance τ_β^2,

then, according to Appendix C(iv), these quantities are related to the experimental values of τ and τ' by:

$$\tau = \tau_\beta + t, \qquad (\tau')^2 = (\tau_\beta)^2 + t^2$$

If a value for t of 0.25×10^{-10} sec is assumed, for example, then since $\tau = 2.45$, $\tau_\beta = 2.20$ ($\times 10^{-10}$ sec).

Substituting back into the above formulae,

$\tau = 2.45 \times 10^{-10}$ sec, but

$\tau' = 2.21 \times 10^{-10}$ sec, almost two standard deviations removed from the experimental value. Thus, according to this example, a thermalisation time as large as 0.25×10^{-10} sec has a probability of less than ten per cent of characterising the annihilation process described in the assumptions. Smaller values of the assumed thermalisation time are obviously more compatible with the experimental results.

C. The Maximum Intensity of a Possible Long-lived Component of Positron Annihilation:

For a long-lived component with a lifetime less than one nanosecond and within the resolution time of the apparatus, an investigation of the maximum intensity allowed such a component again involves a comparison of the expected lifetimes (for τ and τ') with the experimentally-observed ones. Let us assume for this case:

(i) the thermalisation time of the positrons is negligible compared to the lifetime of the positrons;

(ii) the annihilation of the positrons is characterised by two components, a short-lived one (τ_1) of about that indicated by the measured value of τ, and a long-lived one (τ_2) of about 5×10^{-10} sec, say.

If we assign, for the sake of a numerical value, an intensity for the long-lived component of five per cent, then, by the formulae given in Appendix C(iv), the observed mean

life $\tau = \frac{\tau_1 + f\tau_2}{1+f}$, which on solving for τ_1 , gives 2.32 x 10^{-10} sec, while $\frac{\tau'}{\tau} = 1 + \frac{2f(\tau_1-\tau_2)^2}{(\tau_1+f\tau_2)^2}$, which on substituting for τ_1, τ_2, f gives 1.11, indicating an experimental τ of 2.45 x 10^{-10} sec and an experimental τ' of 2.70 x 10^{-10} sec. Since the difference in these values exceeds the standard error involved in the measured values by more than 1½ times, the intensity of any long-lived component of the positron lifetime of about ½ nsec mean life is probably (to a 90% confidence level) less than 5%.

A check of the existence of a long-life component of a value of 10 x 10^{-10} sec or more can, on the other hand, be obtained more readily from an investigation of the "delayed" side of the resolution curve shown in fig 21. Such a component of the decay would manifest itself by an increased number of counts at kicksorter channel numbers of about 70. The fact that there are less than about 9 true coincidence counts in channel 71 (the accuracy of this estimate being limited by the statistics and random coincidence background) would indicate an upper limit for the intensity of such a component of about 1% rather than the 6% value obtained by Gerholm (1956). In conclusion, then, no indication of a long-lifetime component is observed, the experimental uncertainties allowing a maximum intensity for such a component of

less than 1% for lifetimes of the order of 10 x 10^{-10} sec, and

less than 5% for a lifetime of about 5 x 10^{-10} sec.

CHAPTER V

POSITRON LIFETIMES IN AMORPHOUS SUBSTANCES

As a further check of the time calibration of the equipment measurements were made of the resolution curves of positrons annihilating in teflon and quartz. By using the 100-channel kicksorter, the long-lived components of the lifetime (of one to three nanoseconds mean life, Bell and Graham, 1953) could be detected while still retaining the same gain and time-constant settings as used on the previous measurements. The time calibration used for these measurements was given in fig 11. Although these lifetime measurements encompassed a larger time interval (about eight nanoseconds) than that covered by the time calibration curve of fig 11, the calibration was assumed to apply equally well over the extended time interval.

1. Experimental Procedure.

Day-long runs were performed with absorbers consisting of 5/8 inch square samples of 1/8 inch thick teflon and quartz, mounted on the spring clip holders described on page 99 . The quartz was of a pure, vitreosil type. The positioning of the source and counter and the use of a four-volt window on the annihilation gamma-ray side-channel analyser were the same as for the measurements described in Chapter IV, Section 1. A Co^{60} prompt curve was also obtained to indicate the zero of time.

2. Results.

The results of these measurements are illustrated in fig 25

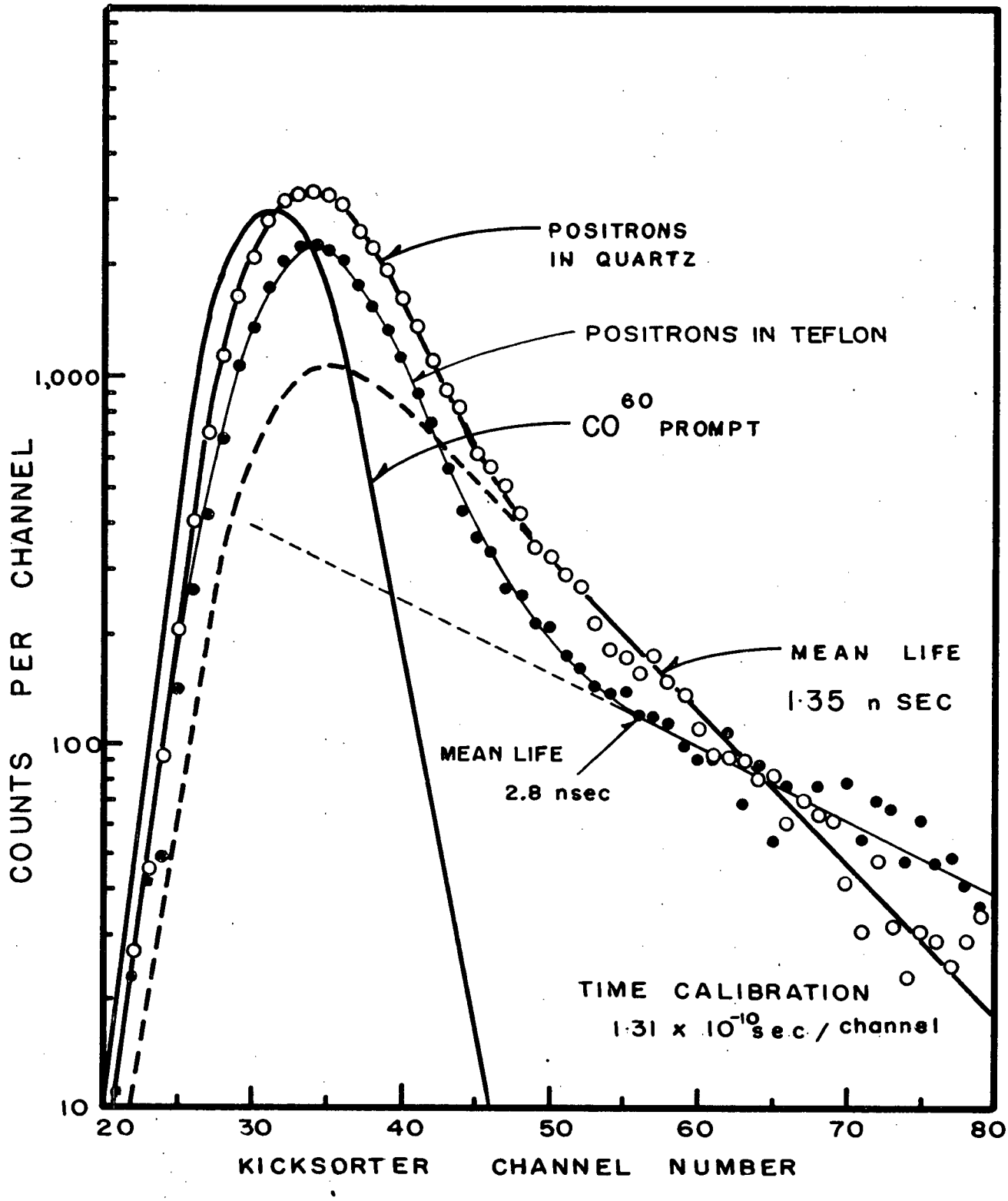

FIGURE 25. COMPLEX POSITRON ANNIHILATION IN TEFLON AND QUARTZ.

where the straight line drawn through the long-lived tails are least squares fits. The least-squares analyses yielded the following results:

Teflon: mean life, τ_2: (2.8 ± 0.25) nsec; intensity of τ_2: (28 ± 3) %

Quartz: mean life, τ_2: $(1.34 \pm .05)$ nsec; intensity of τ_2: (47 ± 3) %.

The errors quoted for these values are only statistical in nature and do not include possible systematic errors such as the uncertainty in the time calibration of two per cent. The satisfactory fit of the tails of the resolution curves by an exponential curve indicates the lack of any gross non-linearity in the time calibration curve.

The measured intensities of the τ_2 components are expected to be a little low in both cases due to positron absorption in the source. Such absorption was estimated in Chapter IV, Section 1, to be about 3% for the collodion-backed Na^{22} source. Thus, for Teflon, the corrected intensity is (29 ± 3) %, and for Quartz, is (49 ± 3) %.

Another possible source of error is that resulting from a contribution to the counts in the tails of fig 25 from highly-delayed positron annihilations which produce time sorter output pulses on the "wrong" half of the triangular time calibration curve (given in fig 6). As a result, a small background of exponential shape decreasing towards the left of fig 25 should be considered. The right-hand limit of the abscissa in fig 24 is, however, about five nanoseconds from the equivalent point on the other half of the time calibration

curve. Thus, the exponential background mentioned above is decreased by an additional five nanoseconds of delay, which for the right-hand limit of the teflon resolution curve amounts to an error of 14%, decreasing rapidly for lower channel number. The corresponding error at the right-hand limit of the quartz resolution curve is only 5% due to the shorter lifetime of the τ_2 component in quartz. Since the statistical errors ascribed to the points of this portion of the resolution curves are larger than these values, this background effect is unobservable. The effect of this background would be to increase slightly the measured value of τ_2 for teflon over the true value, but should have negligible effect in the value of τ_2 for quartz.

The final errors are also increased slightly by the addition of the uncertainty of 2% in the slope of the time calibration curve. The final results, then, are:

Teflon: $\tau_2 = (2.7 \pm 0.3)$ nsec, of intensity: (29 ± 4) %.

Quartz: $\tau_2 = (1.35 \pm 0.1)$ nsec, of intensity: (49 ± 4) %.

In addition, differences between the total resolution curve for quartz, and the extrapolated shape of the τ_2 component (indicated in fig 25) were taken, the resulting curve then representing the expected resolution curve for the τ_1 component alone. A moments analysis of this curve as compared to the Co^{60} prompt curve yielded a value for the short lifetime, τ_1, of: $(3.6 \pm 1) \times 10^{-10}$ sec.

3. Discussion and Conclusions.

The final results are in satisfactory agreement with the

published results:

Teflon: $\tau_1 =$ (2.1 ± 0.3) nsec (Gerholm, 1956)

$\tau_1 =$ (3.5 ± 0.4) nsec (Bell and Graham, 1953)

with an intensity of about 30%.

Vitreosil Quartz: $\tau_1 =$ (1.53 ± .05) nsec (Green and Bell, 1957).

with an intensity of : (53 ± 8) %

In conclusion, the satisfactory agreement between the results obtained from these measurements and the published results for these amorphous materials constitutes a further check of the value of the slope and the degree of linearity of the time calibration curve for this instrumenet.

CHAPTER VI

COMPARATIVE LIFETIMES OF POSITRONS IN VARIOUS METALS

The comparison measurements of the lifetimes of positrons in various metals was described in Chapter II, Section 5B(c), as being free of most of the sources of systematic error that plague absolute determinations of positron lifetimes in metals. In summary, the following reasons were presented for the improved accuracies obtainable by comparative lifetime measurements:

(i) Since the same Na^{22} source is employed in both absorbers, the unknown and the comparative, it need not be moved, and so errors due to variations in the positioning of the source are eliminated.

(ii) As the energy spectra of the radiations are the same for both absorbers, there need be no concern about the energy-dependent instrumental time shifts occurring in the time sorter thus enabling the use of wider windows in the side-channel analysers and hence higher coincidence counting efficiencies.

(iii) The use of the one source and constant counter-source distances assures equal count-rates in the two limiters, and hence elimination of difficulties due to count-rate effects.

The last statement applies of course only when the gamma-ray attenuation is the same in both samples. The "sandwiched" absorber method used by DeBenedetti and Richings (1952) ensures

that such absorptions are the same, by equalizing the total gamma-ray absorptive material in both samples. If the source is termed S, the sample A, and the reference material B, then one source-absorber unit is arranged in the form BASAB, and the other in the form ABSBA. This procedure was also followed in our set of measurements. The reference absorber used for these measurements was aluminum, for which the absolute lifetime of positrons had been determined (as discussed in Chapter IV). Because of the reduced errors characteristic of this method, the comparative measurements of positron lifetimes in metals could be obtained to an accuracy of about 0.1×10^{-10} sec or 4% of the absolute lifetime in aluminum.

1. Experimental Procedure.

The experimental procedure involved was very similar to that described in Chapter IV, Section 1, for absolute lifetime determinations. The same source-counter geometries were employed, the same Na^{22} source was used, and the same method of affixing the absorber samples to the source was followed. The annihilation gamma-ray window width was increased to six volts for these measurements, however, to increase the coincidence counting efficiency. The thickness of the metal absorbers required to stop 0.56 Mev positrons were obtained for a limited number of metals from the measurements of Seliger (1955), and estimated for the rest from the calculations of Nelms (1956). For most metals, these values corresponded to thicknesses between .010 and .020 in. A series of measurements of about $1\frac{1}{2}$ hours duration were then obtained for the two absorbers employed in

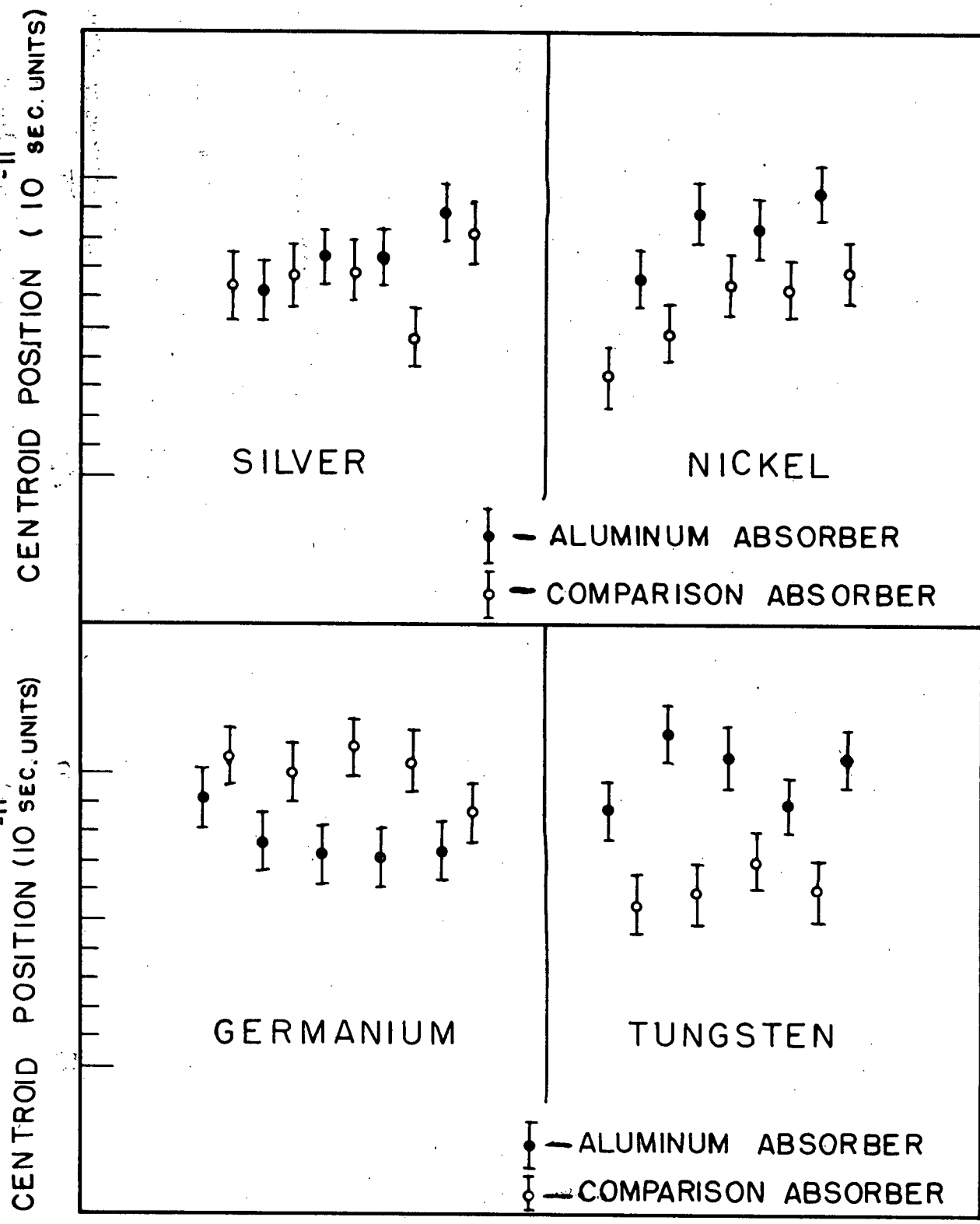

FIGURE 26. COMPARATIVE LIFETIME MEASUREMENTS

alternate fashion. The metal samples, if not available in this laboratory, were obtained either from the UBC Metallurgy Dept. or purchased from a commercial supplier. Since the resolution curves obtained were so very similar to each other, the thirty-channel Marconi kicksorter was employed. There was no necessity of correcting the results for truncation loss since these had very little effect on the lifetime differences measured.

2. Results.

The moments program of Appendix H was again used in conjunction with the Alwac computer for these calculations. As before, the gain of the equipment was adjusted for a kicksorter channel width of about 1×10^{-10} second. The results for silver, nickel, germanium and tungsten are shown in fig 26, with the centroids plotted in sequential order. The scatter in these results indicates a standard deviation of about 0.2×10^{-10} sec. The results were obtained either by determining the difference between the mean values of the centroids for the two absorbers, or by applying the least squares analysis of the type indicated in Appendix G. The former was normally employed when the centroid distributions (like most of those of fig 26) were reasonably horizontal, and the latter calculation used when a significant slope existed in the experimental results (as in the nickel curve of fig 26) implying the existence of a slow electronic drift of the apparatus. The results for a variety of metals are tabulated in fig 27, where the values are given in the form $\overline{\Delta\tau} \pm t_f \sigma_{\bar{\tau}}$; $\overline{\Delta\tau}$ is the calculated estimate of the

METAL	ATOMIC NUMBER	LIFETIME DIFFERENCE $\tau_{Al}-\tau_X$ (10^{-10} sec)	METAL	ATOMIC NUMBER	LIFETIME DIFFERENCE $\tau_{Al}-\tau_X$ (10^{-10} sec)
TITANIUM	22	$\cdot 04 \pm \cdot 08$	SILVER	47	$\cdot 10 \pm \cdot 10$
VANADIUM	23	$\cdot 24 \pm \cdot 05$	CADMIUM	48	$\cdot 04 \pm \cdot 06$
IRON	26	$\cdot 33 \pm \cdot 07$	INDIUM	49	$\cdot 08 \pm \cdot 10$
COBALT	27	$\cdot 31 \pm \cdot 06$	TIN	50	$-\cdot 10 \pm \cdot 08$
NICKEL	28	$\cdot 29 \pm \cdot 05$	GADOLINIUM	64	$-\cdot 33 \pm \cdot 10$
COPPER	29	$\cdot 07 \pm \cdot 13$	TANTALUM	73	$\cdot 38 \pm \cdot 14$
ZINC	30	$\cdot 30 \pm \cdot 20$	TUNGSTEN	74	$\cdot 39 \pm \cdot 10$
GERMANIUM	32	$-\cdot 31 \pm \cdot 05$	GOLD	79	$-\cdot 08 \pm \cdot 05$
ZIRCONIUM	40	$\cdot 25 \pm \cdot 22$	LEAD	82	$0 \pm \cdot 13$
MOLYBDENUM	42	$\cdot 44 \pm \cdot 08$	BISMUTH	83	$-\cdot 08 \pm \cdot 10$
PALLADIUM	46	$\cdot 07 \pm \cdot 10$			

FIGURE 27. TABLE OF COMPARATIVE LIFETIME RESULTS

increase in the mean lifetime of positrons in aluminum over that in the sample material,

t_f is obtained from Student's t distribution, with n-1 degrees of freedom (where n is described below), and enlarges the error because of the uncertainty introduced by the small number of measurements, and $\sigma_{\bar{\tau}}$ is the expected standard deviation of the mean, $\overline{\Delta\tau}$, calculated from $\left(\frac{\sigma_1^2}{n_1} + \frac{\sigma_2^2}{n_2}\right)^{\frac{1}{2}}$ where σ_i and n_i are the standard deviation and number of measurements obtained for the particular absorbers. If the number of measured resolution curves, n, is the same for both absorbers, then $\sigma_{\bar{\tau}}^2 = \frac{\sigma_1^2 + \sigma_2^2}{n} = \frac{\sigma^2}{n}$ where σ is the expected standard deviation of the distribution of estimates of $\Delta\tau$. The variances themselves were calculated from: $\sigma^2 = \frac{\Sigma(\tau_i - \bar{\tau})^2}{n-1}$.

Most of the metal samples were obtained from the UBC Van de Graaff group, which had employed such metals as target backings at various times. Their purities were estimated to be greater than 99%. The purities of several of the metals obtained commercially are given below:

.026 inch thick Vanadium,	99.5%.
.030 inch Palladium,	99.9%.
.050 inch Gadolinium,	99.9%.
.070 inch Bismuth,	99.999%.

The germanium was a .043 inch slice of intrinsic germanium cut from a single crystal grown by the UBC Solid-State group.

3. Errors.

The errors quoted for these lifetime differences are all statistical in nature, being derived from the variations about

the mean which characterised a given set of measured values. Other possible errors, of a more systematic nature, were also considered.

(i) Time Calibration: An error of $\pm$ 2% in the time calibration would introduce an error of $\pm$ .01 x 10^{-10} sec in a measurement of a time of 0.5 x 10^{-10} sec. Since this error is less than one-fifth the statistical errors, it was neglected as a significant source of error for the comparative lifetimes.

(ii) Positron Flight Time to the Absorber: Since not all the absorber surfaces were completely plane, slight variations in the flight time of the positrons between the source and the absorber due to small variations in the distance travelled, were considered as a possible source of error. To determine the magnitude of this effect, a series of runs were performed using two aluminum absorbers identical in physical characteristics, except that one possessed a .016 inch spacer around its edges to maintain it at a distance from the source. The other absorber was clamped around the source in the usual fashion. The results of this set of measurements indicated an increased lifetime in the "distant" aluminum absorber of (.05 $\pm$ .06) x 10^{-10} sec. Since this value is no greater than the errors quoted, and since the variations in the source-absorber distance due to surface irregularities was expected to be much less than .016 inches, this error was also considered insignificant compared to the statistical error.

4. Miscellaneous Measurements:

As a check of the consistency of these short time measurements with those of other investigators, a comparison measurement between the lifetimes of positrons in aluminum and mica was performed. Following the experimental procedure for the comparative lifetime determinations in metals, a series of measurements employing a mica absorber of thickness 175 mg/cm^2 were performed, yielding the value: $(0.85 \pm 0.1) \times 10^{-10}$ sec for the increased positron lifetime in mica as compared to aluminum. This result is in good agreement with the value of $(0.7 \pm 0.5) \times 10^{-10}$ sec obtained by Bell and Graham, (1953).

Several additional comparative measurements involving the metal samples were performed as checks of internal consistency. (a) Since both the iron and nickel samples yielded lower lifetimes for the absorbed positrons than did aluminum, a comparison measurement between these two metals was performed. The result indicated that the positron lifetime in iron is greater than that in nickel by $(.08 \pm .08) \times 10^{-10}$ sec, in confirmation of the earlier comparison measurements indicating that the lifetime of positrons is the same in both metals, viz. $(0.30 \pm 0.10) \times 10^{-10}$ sec less than in aluminum.

(b) Since both the iron and cobalt samples were formed from sintered powders, rolled to the appropriate thickness, the question concerning the effect of the sample structure on the positron lifetimes might be raised. Thus, a set of measurements to compare the lifetime of positrons in the sintered iron absorber to that in a sample of welding-steel were performed. These

results indicated a shorter positron lifetime in steel by $(0.12 \pm .08) \times 10^{-10}$ sec, indicating that, within the statistical error, there is little dependence of the positron lifetime in iron on the gross structure or method of formation of the iron sample.

CHAPTER VII

DISCUSSION AND CONCLUSIONS

1. Summary of Results.

These measurements show that the absolute lifetime of positrons in aluminum is $(2.45 \pm 0.15) \times 10^{-10}$ seconds, with the results strongly indicative of a pure, exponential decay (see Chapter IV for details). Furthermore, measurements of the relative lifetimes of positrons in a variety of metals (about 21 in number) compared to aluminum indicated the existence of statistically-significant variations of the lifetimes in these metals, the values ranging from 2.0 to 2.75 ($\times 10^{-10}$ sec), a total variation of about 30% of the lifetime in aluminum. Our value of the absolute lifetime of positrons in aluminum is in good agreement with the measurements of:

Minton (1959) who obtained $(2.4 \pm 0.6) \times 10^{-10}$ sec, and

Gerholm (1956), of $(2.5 \pm 0.3) \times 10^{-10}$ sec,

but disagrees with those of:

Ferguson and Lewis (1953), of $(1.6 \pm 0.6) \times 10^{-10}$ sec, and

Bell and Graham (1953), of $(1.5 \pm 0.3) \times 10^{-10}$ sec.

The last value given above (Bell and Graham, 1953) was obtained by a quite different technique, described more fully on pg 53 , whereby the positrons themselves were used to define the prompt resolution curve. This method lacks the symmetry inherent in the method of the other workers, (including the method described in this thesis) where gamma-ray detection is employed throughout, in that one form of "radiation" (namely

positrons) was employed in determining the prompt resolution curve and another form, the annihilation gamma rays, for the delayed resolution curve.

Gerholm (1953) pointed out a number of possible sources of systematic errors inherent in the method of Bell and Graham (as described in more detail in Chapter II , Section 5C).

The results for the comparative lifetimes are also in general agreement with those of previous workers (with details given in Chapter VI), except that the present results, with their reduced errors indicate the existence of significant lifetime differences which were masked by the large probable errors of the earlier measurements. In addition, whereas the comparative measurements of Bell and Graham (1953) appeared to indicate a lifetime dependence on the atomic number of the absorber, with decreased lifetime resulting from the use of an absorber of higher atomic number, the results of Chapter VI failed to indicate any such dependence (as may be observed by referring to fig 26). The physical parameters of the absorber on which these results do depend, and the conclusion that can be drawn from them are described in the following sections.

2. Interpretation of Results.

A. Annihilation During Collisions with Conduction Electrons:

The details of this mechanism are discussed in Chapter II, Section 2 (A and B), with the positron lifetimes being estimated on the basis of the following theories:

(i) Annihilation of stationary (in reality, thermalised) positrons with plane wave electrons of a momentum dis-

tribution given by the simple Sommerfeld free-electron theory of a metal. In this case, the annihilation rate of the positrons is expected to be proportional to the conduction electron density, and is expected to be of the order of (0.5 to 2.0) x 10^9 sec^{-1}.

(ii) A collisional annihilation process essentially identical to that of (i), above, except that coulomb interactions between the positron and electron are taken into account, thereby modifying the electronic wave-functions so that they can no longer be regarded as plane waves. In this case, positron annihilation rates of about (5 to 10) x 10^9 sec^{-1} are obtained, with a dependence on the conduction electron density (N) of something between $N^{2/3}$ and N^1.

The compatibility of these expectations with the observed annihilation rates (R) was tested by examining a plot of R vs N. In this case, only those metals for which the angular correlation results are in <u>good</u> agreement with the interpretation in terms of annihilation with conduction electrons were considered (Groups A and B, below). The Lang and DeBenedetti (1957) separation of metals into three groups on the basis of measured angular correlation functions was used to determine the "good" metals. The groups are:

<u>Group A</u>: (Li, Na, Be, Mg, Al, Ge, Sn, Bi). These metals yield angular correlation functions composed of central inverted parabolas with small tails at large angles.

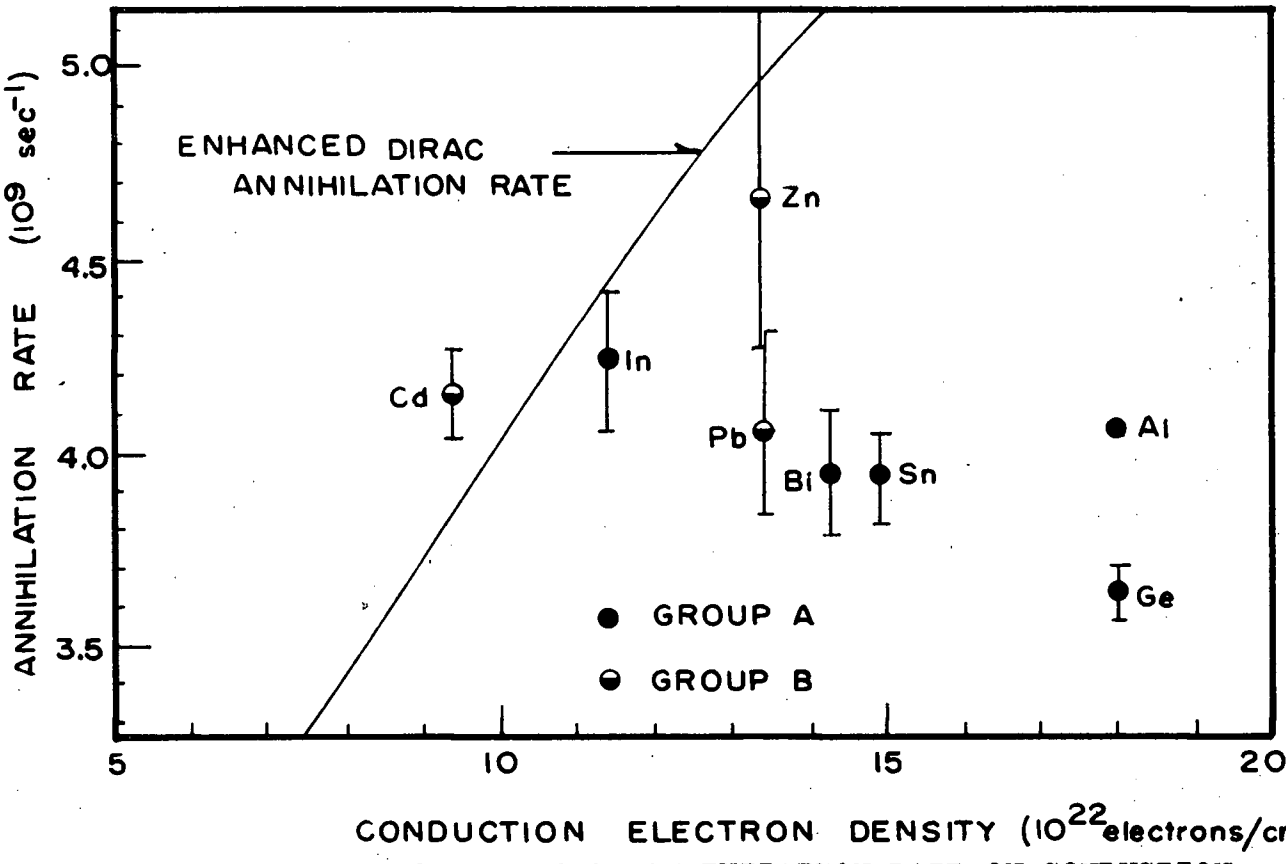

FIGURE 28. DEPENDENCE OF ANNIHILATION RATE ON CONDUCTION ELECTRON DENSITY FOR GROUP A AND B METALS

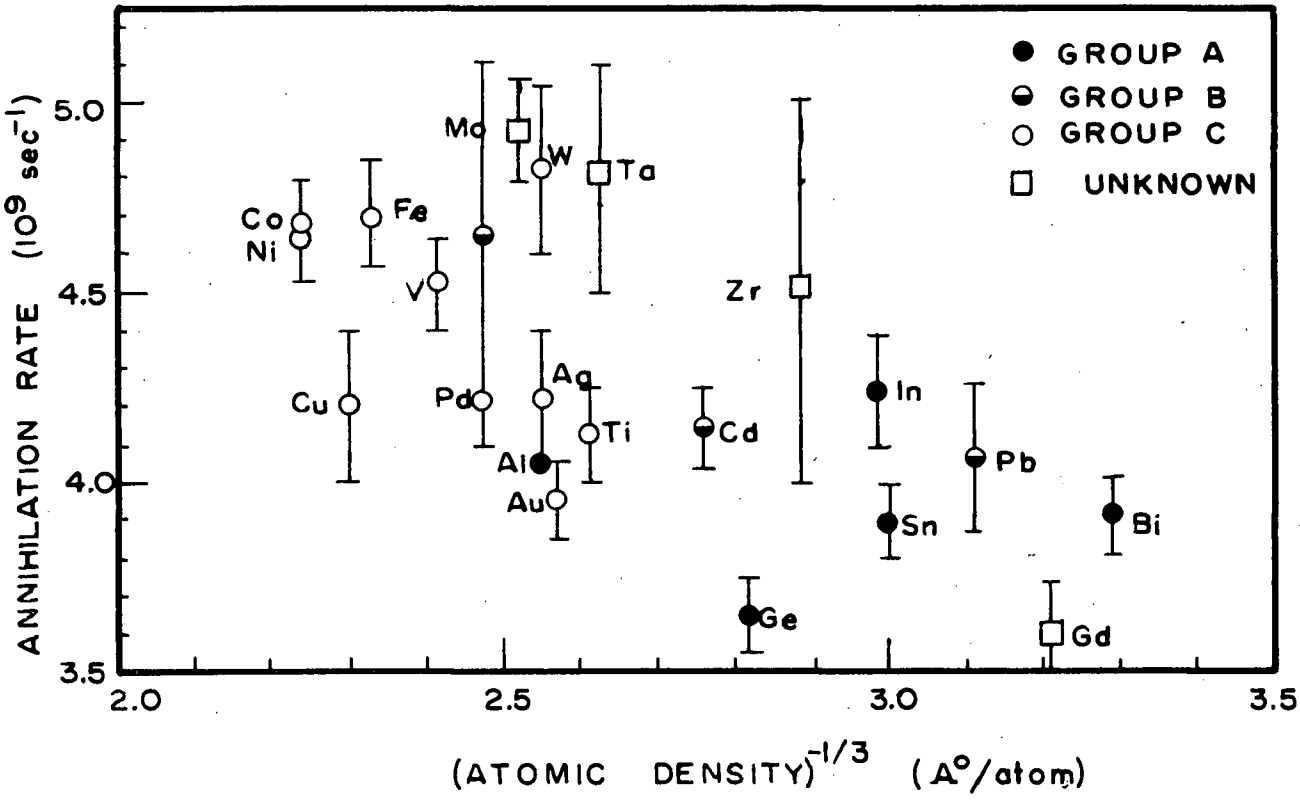

FIGURE 29. ANNIHILATION RATE DEPENDENCE ON MEAN ATOMIC SPACING

Group B: (Ca, Ba, Zn, Cd.). These metals again are characterized by central parabolas, but have larger tails. Their distinction between Groups A and B is rather arbitrary.

Group C: (Cu, Ag, Au, Fe, Co, Ni, Rh, Pd, Pt, W). These metals exhibit bell-shaped angular distributions.

The observed annihilation rates as a function of the conduction electron density for the metals of Groups A and B are given in fig 28.

The solid line in fig 28 is the expected dependence of the coulomb-enhanced annihilation rate on the conduction electron density as described by Ferrell (1956), and discussed in more detail in Chapter II, Section 2 B. From the data presented in this figure, it may be concluded that the annihilation rate of positrons is independent of the conduction electron density, at least for those metals (Groups A and B) for which this interpretation would appear to be valid. The failure of this theoretical approach in explaining the observed positron annihilation rates in the Groups A and B metals suggests an examination of the compatibility of the alternative mechanism, that of annihilation from bound positron-electron systems.

B. Positronium and Positronium Ion Formation:

On the basis of the assumption of formation of bound positron-electron systems, the results of fig 28 are adequately explained. In fact, positronium ion formation would seem to be most consistent with the results, since the repulsion of the conduction electrons by the excess negative charge of the ion

(in other words, the production of a "charge hole" around the ion) would reduce the rate of annihilation of the bound positrons with nearby conduction electrons, thereby strengthening the independence of the annihilation rate on the conduction electron density. On the other hand, positronium atoms, being neutral in charge, would not produce such a "charge hole" with the result that some dependence of the annihilation rate on the density of the conduction electrons in the vicinity of the positronium atoms might be expected.

C. Annihilation with Core Electrons:

A comparison of the annihilation rates of the various metals in fig 27 indicated that the Group C metals generally yield a faster annihilation rate than the Group A and B metals. Group C metals are also characterized by an increased proportion of high-momentum positron annihilation (Stewart, 1957, and Lang and DeBenedetti, 1957), an effect generally attributed to one or both of the following mechanisms (Lang and DeBenedetti, 1957):

(i) The positrons, although thermalised, have a significant zero-point motion because of their confinement in the periodic potential of the lattice (excluded-volume effect, favoured by Lang and DeBenedetti, 1957).

(ii) The positrons annihilate with higher momentum core electrons as well as with valence electrons (favoured by Berko and Plaskett, 1958).

Although these effects were originally applied to collisional annihilations between the positrons and electrons, it would appear that they are just as applicable for the case of

positronium ion formation. In this case, effect (i) would be attributed to a zero-point motion of the positronium ion itself. This explanation, however, suffers from the difficulty of attempting to interpret the very high momentum portions of the tails of the angular correlation curves (corresponding to kinetic energies of the ions of ten to twenty electron volts) in terms of motion of the ion as a whole. Such an explanation is considered implausable because of the relatively low binding energy of the positron-electron system (6.78 ev). If the lower momentum portions of the tails are attributed to this effect, however, the relative number of these higher momentum annihilations would be expected to be larger for closer packing of the metal atoms. One would not expect, however, (at least to first order) a dependence of the lifetime of the ion on the atomic packing, since the annihilation rate of the ion is independent of its velocity, and hence of the nature of its physical environment, except, of course, for the slight increase in electron density at the positron resulting from the increased confinement of the positronium ion in a lattice of smaller dimensions.

On the other hand, effect (ii) would predict a definite dependence of the annihilation rate on the size of the crystal lattice because the probability for annihilation of the positron in the positronium ion is proportional to the overlap of the positron wave-function with the wave-functions of both its associated electron, and the high-momentum core electrons of the metal ions. Thus, on the basis of this interpretation, an increased annihilation rate should result for those metals

characterized by more closely-packed atoms and thus greater penetrations of the core electrons into the region occupied by the positronium ion.

Fig 29, a plot of the measured positron annihilation rate vs the mean inter-atomic spacing for the various metals suggests the existence of such an effect. The measure of the "mean interatomic spacing" used here is merely the cube root of the reciprocal of the atomic density. As a result, however, of the many different forms of crystal structure (face-centred cubic, body-centred cubic, hexagonal close-packed, etc.), the "space" available for the positronium system in a metal may vary considerably even amongst metals of the same atomic density. As an example, the diameter of the largest solid sphere that will fit in both the face-centred cubic, and body-centred cubic, structures is one of diameter equal to the lattice constant minus the metal ion diameter, whereas the density of metal atoms per unit cell is twice as large for the face-centred cubic as for the body-centred cubic structure. Therefore, for metals of the same atomic density, those with face-centred cubic lattices have slightly larger unit cells (and therefore more "room" for a positronium ion) than do those with a body-centred cubic structure. If this interpretation of the mechanism of positron annihilation is at all meaningful one should expect a more significant dependence of the various annihilation rates on some measure of the unit cell size, such as the lattice constant. The next figure (fig 30) illustrates a plot of the annihilation rate vs lattice constant for the

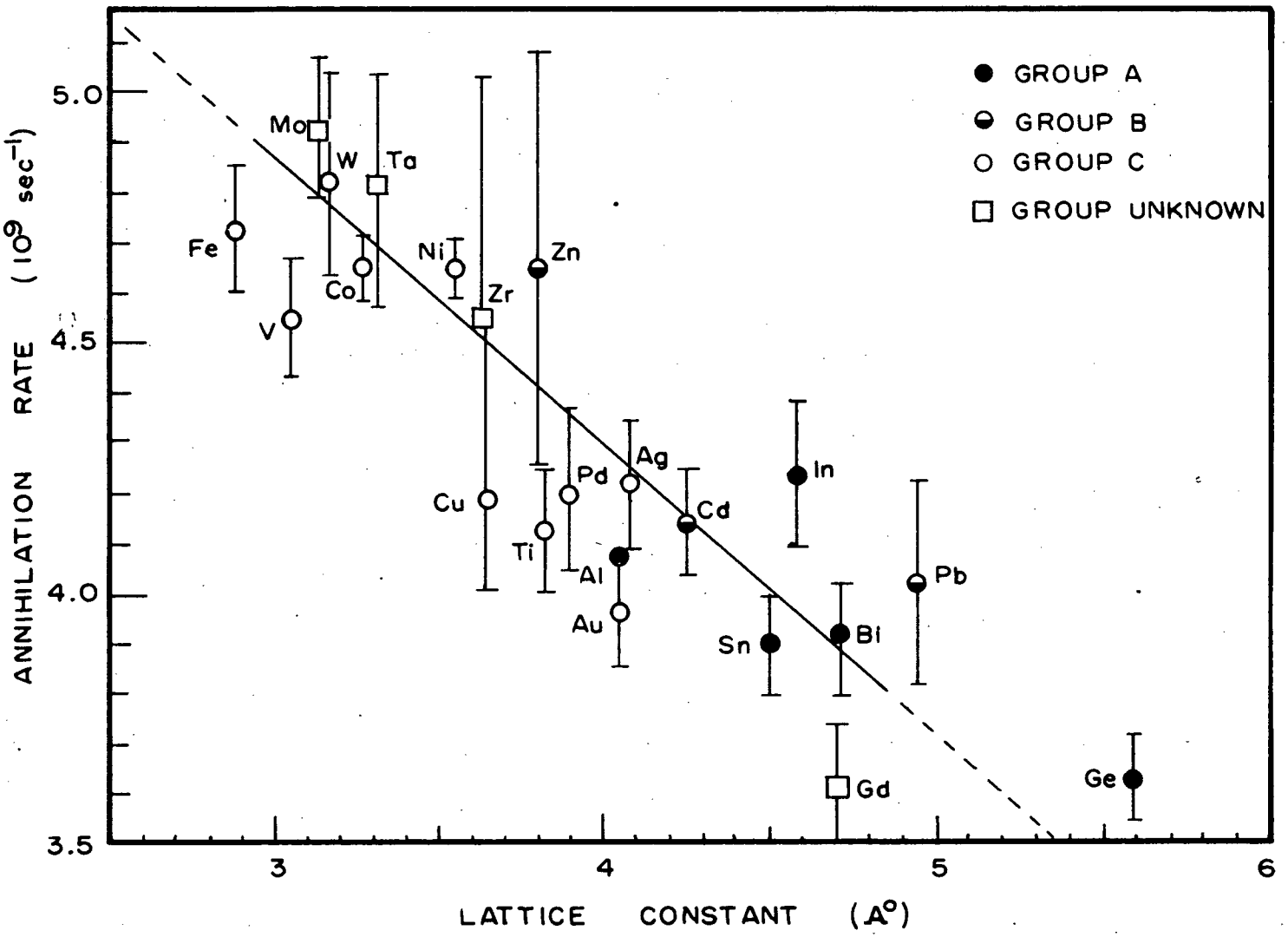

FIGURE 30. POSITRON ANNIHILATION RATE AS A FUNCTION OF LATTICE CONSTANT

metals investigated. The standard errors shown on all the figures in this section indicate the uncertainty in the annihilation rates in the metals concerned as compared to the annihilation rate in aluminum. The total error for any individual point should include, therefore, the 0.25×10^9 sec^{-1} standard error of the estimate of the annihilation rate in aluminum. The fact that the scatter of the measured values is much smaller for this figure than for the previous one serves to indicate that the positron annihilation rate is more dependent on the lattice size than the mean interatomic spacing. Both these plots (figures 29 and 30) serve also to indicate that DeBenedetti's Group A and B metals are, in fact, those with relatively large interstitial volumes, whereas the Group C metals are those characterized by smaller interstitial regions, an observation consistent with the interpretation of the high-momentum tail in terms of a "pick-off" annihilation between the positron in the positronium ion and the core electrons, as described above. In fact, on the basis of the relative positions of the metals in fig 30 with respect to the DeBenedetti groupings, gadolinium would be expected to yield an angular correlation function descriptive of the metals of Groups A and B.

The values for the lattice constants used for fig 30 were obtained from Seitz, "The Modern Theory of Solids", (McGraw-Hill Book Co., 1940), First Edition, pg 4. For metals with body-centred cubic and face-centred cubic lattices, the lattice constants were obtained directly from the table in Seitz. For the case of hexagonal-close-packed structures which are

characterized by two different lattice constants, a and c, however, a rather rough approximation was used. Since the largest solid sphere that can fit in this lattice is one of diameter somewhere between a and c for the values characterizing most of the metals, a simple arithmetic mean of a and c was used as a measure of the "effective" lattice constant for fig 30.

A possible dependence of the observed positron annihilation rate on physical characteristics of the metal other than those of density and lattice constant (as illustrated in figs 28-30) was also examined. Neither the fractional ionic volume (defined by the ratio of the total ionic volume in a unit cell to the volume of the unit cell) nor the average density of outer core electrons of the metal ions, for example, yielded as strong a dependence as that of fig 30. For the body-centred cubic and face-centred cubic metals on the other hand, somewhat less scatter than that indicated in fig 30 resulted when a correction to the abscissa of fig 30 for the finite ion diameters was included by plotting the positron annihilation rate against the lattice constant minus the metal ion diameter. The scatter in the experimental points was reduced for all the metals of the lattice structure defined above, except for the three metals, copper, silver, and gold. A possible explanation for the deviations observed for these three metals is given on pg 147 of this chapter.

D. Experimental Estimate of the Lifetime of the Positronium Ion:

Assuming the existence of the positronium negative ion in these metals, the lifetime of such a bound system can be esti-

mated from the seven measured positron lifetimes in the Group A and B metals on the assumption that the fraction of core electron (pick-off) annihilations to positronium ion annihilations is given by the ratio of the intensities of the gaussian angular correlation component and the parabolic component (obtained from the data of Lang and DeBenedetti, 1957). That is, assuming that the total probability for annihilation, P_t, is given by:

$$P_t = P_{ion} + P_{p-o} ,$$

where P_{ion} is the characteristic annihilation rate for the negative positronium ion, and P_{p-o} is the annihilation rate for the pick-off process involving annihilation of the positron with the core electrons, and further, that $P_{p-o}/P_{ion} = A_g/A_p$, the ratio of the gaussian component to the parabolic component in the angular correlation work, then $P_{ion} = P_t - P_{p-o} = P_t(1 + A_g/A_p)^{-1}$. The results of this calculation for the seven metals (Zn, Al, Cd, Sn, Bi, Pb, Ge) yielded a mean value for the annihilation rate of the positronium ion of: $(3.16 \pm 0.10) \times 10^9$ sec^{-1}, where the error quoted is the statistical standard deviation of the mean. Inclusion of the standard error of the annihilation rate for the reference metal, aluminum, yields: $(3.16 \pm 0.27) \times 10^9$ sec^{-1}, corresponding to a lifetime of $(3.16 \pm 0.3) \times 10^{-10}$ sec. This is in good agreement with the theoretical mean lifetime of the positronium ion of $(3.26 \pm 0.35) \times 10^{-10}$ sec (Ferrell, 1956).

If, instead of the ionic state, annihilation from a positronium atom (with rapid electron exchange) is assumed, a large discrepancy exists between the measured lifetime and the theoretical value of 5×10^{-10} seconds (Garwin, 1953). A

modification of the order of 35% would be required in the theoretical estimate of the annihilation rate for the singlet positronium state before consistency with the experimental results could be obtained.

E. Effect of a Magnetic Field on the Angular Correlation Results.

In some ferromagnetic metals, Hanna and Preston (1958) observed a small enhancement of the two-photon annihilation rate when an external magnetic field was applied in a direction tending to align the electrons of the metal in a direction anti-parallel to the polarization of the positron. This enhancement was only observed, however, for those positron-electron pairs of relatively high momenta, the low momenta pairs being characterized by a slight decrease in the number of two-photon annihilations.

In terms of the model of positron annihilation presented above, this effect is attributed to an enhancement of the pick-off annihilation rate of the positrons with aligned core electrons of the metal. This interpretation does require the assumption that the initial direction of positron polarization characteristic of the incident positrons is retained by many of them even after being captured into bound positronium ion systems, thus resulting in the formation of positronium ions with the positrons predominantly aligned in one direction. The application of a magnetic field would not be expected to affect the annihilation rate of the ion itself, because the two electrons form a closed shell, thus preventing the occurrence of any

net alignment of the spin directions of these electrons with that of the positron. If a pick-off annihilation process is assumed to exist then, the two-photon annihilation rate would certainly be expected to increase when the spin directions of the core electrons were aligned antiparallel to those of the positrons because of the increased singlet nature of the wave-function of the annihilating pair. An enhanced annihilation rate with the core electrons would also result in a decreased number of annihilations from the ionic state, i.e. P_{p-o}/P_{ion} and thus Ag/Ap would increase, an effect in agreement with the observed decrease in the number of two-photon annihilations of low positron-electron momenta. Furthermore, the results of fig 30 indicate a much reduced "pick-off" annihilation rate for gadolinium than for iron suggesting a relatively small wave-function overlap with the core electrons. Thus, the two-photon enhancement effect at high positron-electron momenta would be expected to be correspondingly smaller for gadolinium as compared to iron. This expectation is also in complete agreement with the results of Hanna and Preston for gadolinium cooled to -100°C. At this temperature gadolinium is strongly ferromagnetic, yet the results failed to indicate any significant enhancement effect at all, either in the wings or in the central peak of the angular correlation function.

3. Suggestions for Further Measurements.

In reviewing the metals that have been employed in this investigation, it can be seen that those metals characterized by compact crystal lattices are well represented, whereas those

of larger lattice spacings are somewhat few in number. It would therefore be of interest to measure positron lifetimes in the metals: strontium, calcium, silicon, and barium, all (except silicon) having been investigated in angular correlation measurements according to which they have been classified as Group A or B metals. These metals are also distinguished in having lattice constants in excess of five angstrom units and thus should be characterized by mean lifetimes between 2.50 and 3.00 ($\times 10^{-10}$ seconds). Calcium and silicon, in particular, (from a comparison with fig 30) should lead to positron lifetimes of 2.7 to 3.0 ($\times 10^{-10}$ seconds). The fact that these metals have been classified as belonging to Groups A or B, indicative of a low intensity of core electron annihilations, is further evidence in support of this prediction.

Since many of the rare-earth metals are also characterised by large crystal lattices, they should also be investigated in detail, both with regards to lifetime and angular correlation measurements. Although most of them have lattice structures very similar to that of the rare-earth metal studied in this work, gadolinium (with a hexagonal, close-packed structure; $a \simeq 3.5$ A°, and $c \simeq 5.6$ A°), there are two or three of them with quite different lattice structures. Samarium, for example, has a rhombohedral lattice with the lattice constants, $a = 3.6$ A°, and $c = 26.3$ A°. Europium, on the other hand, has a body-centred cubic lattice of lattice constant 4.6 A°, and ytterbium is characterized by a face-centred cubic lattice of lattice constant 5.5 A°. Thus, on the basis of the model presented here, one should expect very similar results for

ytterbium as for calcium, since calcium also has a face-centred cubic lattice of 5.5 A^{o} lattice constant, and in addition an ionic radius almost identical to that of ytterbium, viz. 1.00 A^{o}.

More accurate measurements of the absolute positron lifetime measurements in the metals with large crystal lattices should also yield a better experimental estimate of the mean lifetime of the negative positronium ion. Gray tin in particular, the crystalline phase acquired by normal white tin after prolonged exposure to temperatures of the order of $-40^{o}C$, has probably the largest lattice constant of any metal, viz. 6.46 A^{o}, and should therefore lead to a positron lifetime of about 3.0×10^{-10} seconds. It would, in fact, be interesting to attempt to detect a difference in the mean lifetimes between white and gray tin, in order to test the dependence of the positron lifetime on the nature of the crystalline state.

Two other metals of interest are lithium and potassium. These metals have extremely low conduction electron densities (1.3×10^{22} electrons/cm^{3} for potassium, a value 1/13 of that for aluminum), whereas their lattice constants are effectively the same as those of most other metals; lithium, for example, has a smaller lattice constant than aluminum, viz. 3.50 A^{o}, while that for potassium is almost as large as germanium, viz. 5.33 A^{o}. A check of the annihilation rates of positrons in these metals compared to the expected rates from fig 30 in terms of the lattice constants only (independent of the conduction electron density) should offer a quite exacting test of the present interpretation of the annihilation process. A test of the dependence of the annihilation rate on the crystalline

structure should also be detectable using some selected alloys, those, for instance, which change their crystal structure when a particular concentration of the solute metal is reached. An investigation of the details of positron decay (both the development of a parabolic angular correlation function and the development of the single short positron lifetime) as a metal is allowed to change its state from a high-pressure gas to the liquid and solid states should also be very useful in shedding more light on the mechanism of positron annihilation in metals.

4. Conclusions.

The results for the positron lifetimes in metals indicate a simple, exponential form of decay of mean lifetime varying between 2.0 and 2.7 ($\times 10^{-10}$ sec), depending on the crystalline structure of the metal absorber. The value of the lifetime is attributable to the formation of a positronium ion (a bound state of a positron and two electrons) in a time small compared to the positron lifetime, which then decays with its own characteristic lifetime. A decrease in the measured lifetimes in metals of more compact lattices is attributed to a form of "pick-off" annihilation with the core electrons of the neighbouring metal ions. The relative number of core electron annihilations to the annihilations from the bound state itself, is indicated by the degree of enhancement of the annihilation rate as mentioned earlier, and by the relative intensity of the high-momentum component in the annihilation gamma ray angular correlation curves. The angular correlation results for many of the transition metals of Group C are difficult to interpret in

detail, because the relatively large overlap in the wave-functions of the 3d electrons between the various atoms in the crystal results in the addition of a significant number of these electrons to the valence band, thus complicating the analysis of the measured momentum distributions in terms of the simple Sommerfeld free-electron model. The angular correlation results for the Group A and B metals indicates a momentum distribution of the positron-electron pair essentially identical to that of the conduction electrons. This can be interpreted in terms of the existence of a rapid electron exchange mechanism between the electrons of the positronium ion and the conduction electrons, probably resulting to a large extent from the significant overlap that must exist between the electronic wave-functions of the positronium ion electrons and the valence electrons of the surrounding metal atoms. This picture of the annihilation mechanism receives further support from the agreement between the observed and theoretical values for the mean lifetimes of the negative positronium ion. It is considered that the model described here is appropriate for nearly all the metals investigated in this work, because the ratio of the metal ion to unit cell volumes are characteristically less than 20%, indicating a relatively small dependence of the space available for the positronium system in the lattice on the volume of the metal ions. For the three noble metals, copper, silver, and gold, however, this ratio lies between 30% and 65%. In fact, Mott and Jones (1936, pg 174) describe the noble metals as "consisting of ions for which the closed d shells must be regarded as

touching". For these metals then, an interpretation of positron annihilation not in terms of the formation of positronium, but rather by direct collisional annihilations with the conduction electrons and some of the 3d electrons as suggested by Berko and Plaskett (1958) may be the more correct approach.

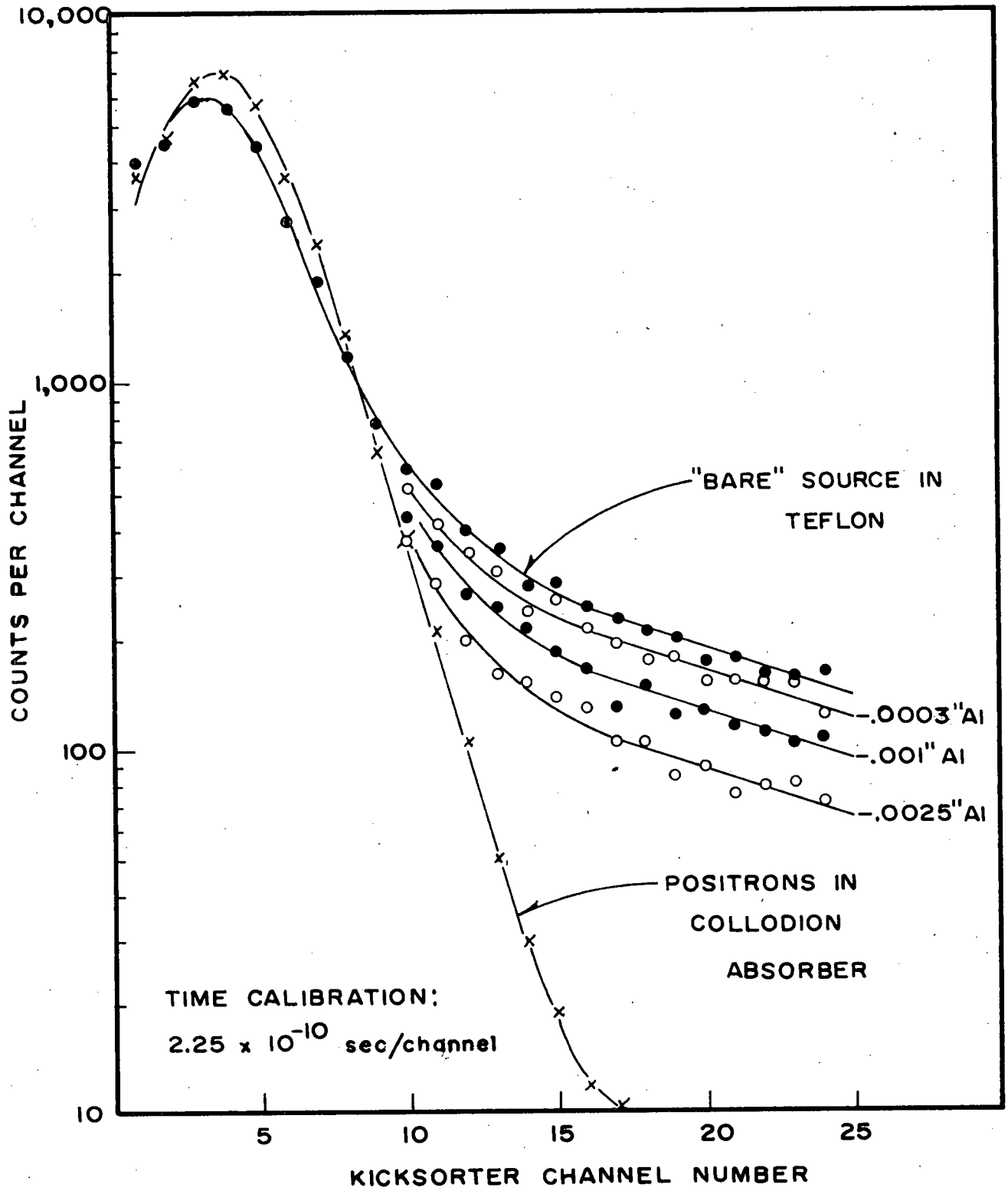

FIGURE 31. DELAYED RESOLUTION CURVES FOR VARIOUS ALUMINUM ABSORBER THICKNESSES

APPENDIX A.

POSITRON ABSORPTION IN THIN ALUMINIM FOILS.

An estimate of the Na^{22} positron loss in thin aluminum foils was obtained by the method of Hatcher, Millett and Brown (1958), whereby the source of positrons was covered with thin sheets of aluminum of the appropriate thicknesses, and the whole arrangement covered with a teflon absorber. The decrease in the intensity of the long-lived component of positron annihilation in the teflon produced by increasing the thickness of the aluminum is a measure of the absorption of the positrons in the aluminum. The fraction r of positrons annihilating in the foils is given by: $1 - r = \frac{F_t(x)}{f_t(x)}$ (Hatcher et al, 1958), where $f_t(x)$ is the intensity of the long-lived component of the positrons in teflon, and $F_t(x)$ is the intensity after the source has been covered by the extra aluminum. These ratios were calculated by summing the same fifteen channels on the tails of the delayed resolution curves for the various thickness absorbers (after first subtracting the random coincidence backgrounds).

Because of the very significant dependence of the fraction of back-scattered positrons on the atomic number of the absorber, these values are expected to be only very approximate for heavy elements, but should be fairly close for light elements of atomic number about that of the mean for teflon.

The Na^{22} source used for these measurements was the 0.5 mg/cm^2 collodion-backed source. The delayed resolution curves for several thicknesses of absorber are shown in fig 31.

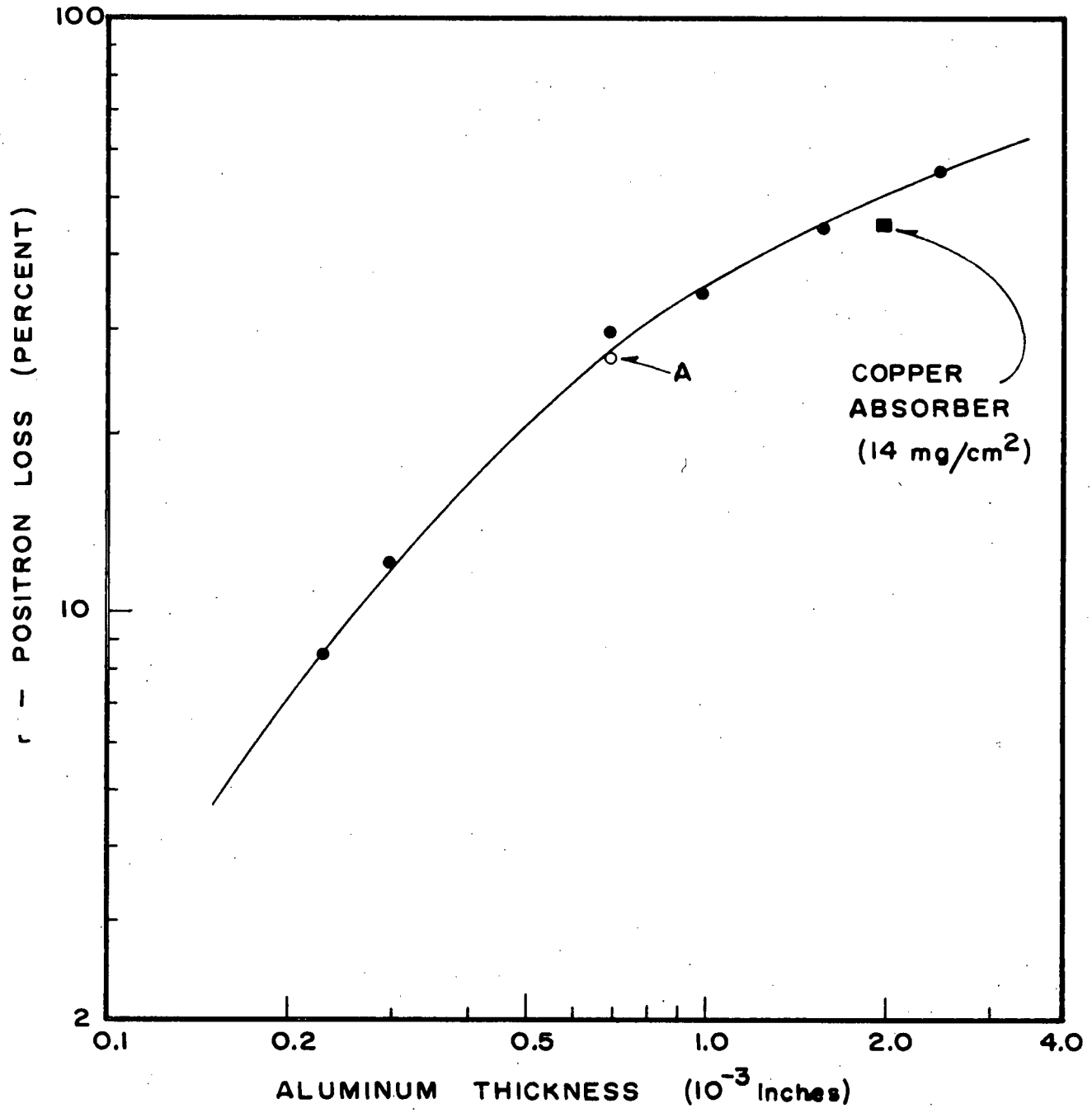

FIGURE 32. SODIUM-22 POSITRON LOSS IN THIN ALUMINUM ABSORBERS

The experimental values of r as a function of the absorber thickness are illustrated in fig 32. The point indicated by the letter 'A' is a check of the value for .0007 inches of aluminum obtained by repeating the whole procedure eight months later, with modified circuitry in the equipment.

The results for small absorber thicknesses indicate a positron absorption of about 10% for a .0002 inch aluminum absorber, a value significantly smaller than that measured by Hatcher et al (1958) of (18 $\pm$ 5)%. Possible reasons for this discrepancy are described in Chapter IV, Section 1C(a).

APPENDIX B.

TRUNCATION LOSS.

A Discussion of the Errors Introduced into the Estimated Moments of Decay Distribution Curves when an Insufficiently Large Range of the Abscissa of the Resolution Curves is Considered, i.e. When the Resolution Curve is Truncated at Some Point.

Considering the coincidence resolution curves illustrated in fig 19, the error introduced into a calculation of the first two moments of the positron decay distribution due to a neglect of the portion of the curves to the right of the dashed line, T, is treated in this appendix.

The correction term necessary to correct the calculated moments (using truncated resolution curves) was determined from a detailed analysis of the delayed and prompt resolution curves obtained using the 100 channel kicksorter. Use of this kicksorter enabled measurements with a sufficiently extensive range of channels that no truncation corrections were necessary in the resulting moment calculations. However, truncation errors were introduced, and their effects determined, by computing the moments of the curves as a function of the channel number describing the point T (fig 19). The fractional number of counts contained in the truncated tail of the resolution curve compared to the number of counts under the whole curve was also obtained

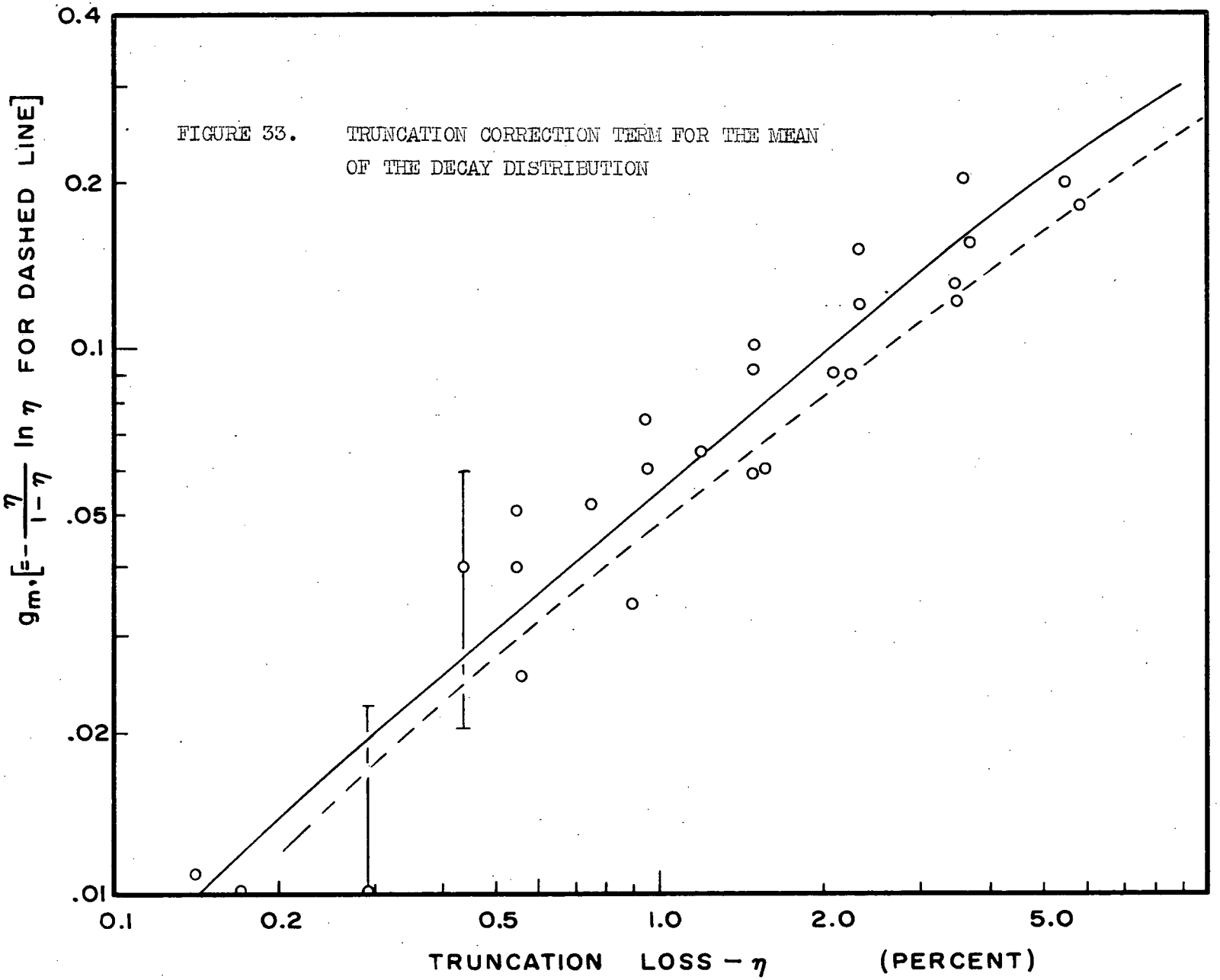

FIGURE 33. TRUNCATION CORRECTION TERM FOR THE MEAN OF THE DECAY DISTRIBUTION

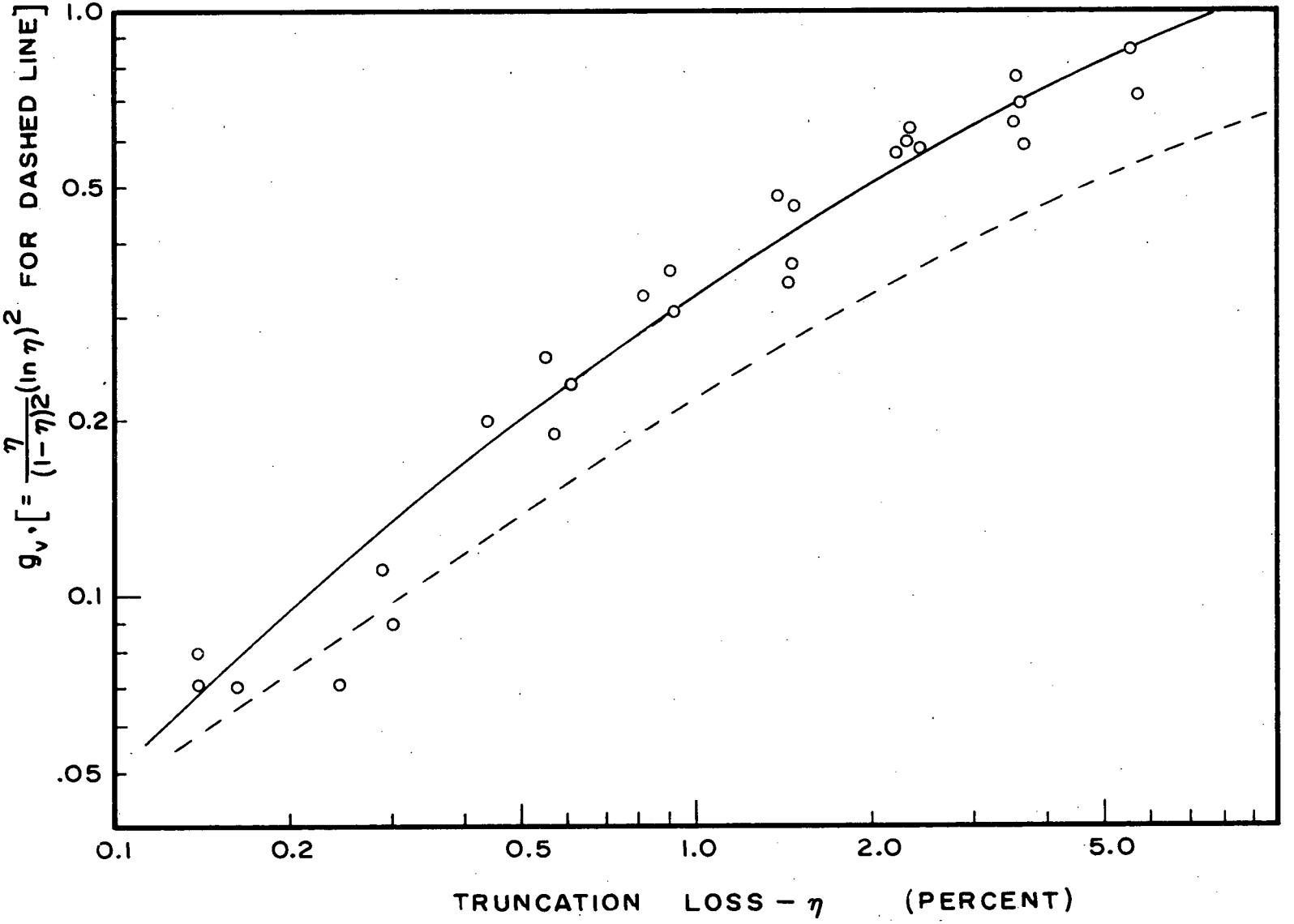

FIGURE 34. TRUNCATION CORRECTION TERM FOR THE VARIANCES OF THE DECAY DISTRIBUTION

as a function of the value of T. With this information, then, a truncation correction for the experimental moments (obtained using the 30 channel kicksorter, for example) was plotted as a function of the "truncation loss" in the number of counts recorded (figs 33 and 34). "Truncation loss" was used as the dependent variable because it could be determined directly from measurements involving the 30 channel kicksorter by determining the ratio of counts contained in the thirtieth, "overflow" channel, to the sum of the counts in all the channels. The 'true' moments could then be obtained from the 'observed' moments by applying the correction corresponding to the measured truncation loss.

The resulting curves for:

(i) Truncation correction for the measured means, and

(ii) Truncation correction for the measured variances,

of the positron decay distribution are indicated in figs 33 and 34.

The 'true' moments are obtained by using the following relationships:

'True' mean $= (1 - g_m)^{-1}$ x ('Observed' mean)

'True variance = $(1 - g_v)^{-1}$ x ('Observed variance)

The dashed lines shown in figs 33 and 34 are rough theoretical estimates of the corrections g_m, and g_v, and are given primarily to indicate that the experimentally-determined corrections are quite reasonable in their absolute values and in their dependence on the truncation loss.

The theoretical value was obtained assuming that:

(i) the delayed resolution curve was a pure exponential, $\lambda e^{-\lambda t}$, and

(ii) the prompt resolution curves were effectively zero over the range considered.

-A- Thus, the "truncation loss" in the recorded counts due to a truncation of the curve at a time τ_o is:

$$\eta = \lambda \int_{\tau_o}^{\infty} \lambda e^{-\lambda t} dt = e^{-\lambda \tau_o}$$

-B- Ratio of the 'true' mean to the 'observed' mean, where the true mean = $1/\lambda$.

The 'observed' mean $= \langle t \rangle = \dfrac{\lambda \int_o^{\tau_o} t\, e^{-\lambda t} dt}{\lambda \int_o^{\tau_o} e^{-\lambda t} dt} = \dfrac{1}{\lambda} + \dfrac{-\tau_o e^{-\lambda \tau_o}}{1 - e^{-\lambda \tau_o}}$

and the $\dfrac{\text{'true' mean}}{\text{'observed' mean}} = \dfrac{1}{1 - g_m} = \left(1 - \dfrac{\lambda \tau_o e^{-\lambda \tau_o}}{1 - e^{-\lambda \tau_o}}\right)^{-1}$.

The dashed line of fig 32 is a plot of $g_m = -\dfrac{\eta}{1-\eta} \ln \eta$ vs η.

-B- Ratio of 'true' variance to 'observed' variance, where the true variance = $1/\lambda^2$

The 'observed' second moment $= \langle t^2 \rangle = \dfrac{\lambda \int_o^{\tau_o} t^2 e^{-\lambda t} dt}{\lambda \int_o^{\tau_o} e^{-\lambda t} dt} = \dfrac{2}{\lambda^2} - \dfrac{2\tau_o e^{-\lambda \tau_o}}{\lambda(1 - e^{-\lambda \tau_o})} - \dfrac{\tau_o^2 e^{-\lambda \tau_o}}{1 - e^{-\lambda \tau_o}}$

So the 'observed' variance = second moment - (first moment)^2 =

$$= \frac{1}{\lambda^2} - e^{-\lambda \tau_o} \left(\frac{\tau_o}{1 - e^{-\lambda \tau_o}}\right)^2$$

Thus, the $\dfrac{\text{'true' variance}}{\text{'observed' variance}} = \dfrac{1}{1 - g_v} = \left(1 - (\lambda \tau_o)^2 \dfrac{e^{-\lambda \tau_o}}{(1 - e^{-\lambda \tau_o})^2}\right)^{-1}$

where $g_v = \eta \left(\dfrac{\ln \eta}{1 - \eta}\right)^2$.

APPENDIX C.

RESOLUTION CURVE ANALYSIS.

Newton (1950) analysed the effect of a finite instrumental resolution time on the measurement of short time delays. In particular, the detection of pairs of radiations emitted with a relative time delay described by a probability distribution, f(t), yields an experimental "delayed-coincidence" resolution curve: F(t) related to P(t) by a "convolution" integral: $F(T) = \int_{-\infty}^{\infty} f(t)P(T-t)dt$, where P(t) is a "prompt" resolution curve produced by the instrument when the detected radiations were emitted simultaneously.

(I) Bay's General Analysis

Bay (1950 and 1955) showed generally that the m^{th} moment of F(T), $M^m[F(T)]$, where F(T) is defined by:

$$F(T) = \int_{-\infty}^{\infty} f(t)P(T-t)dt, \text{ is:}$$

$$M^m[F(T)] = \sum_{n=0}^{\infty} \binom{m}{n} M^{(m-n)}[P(T)]\, M^{(n)}[f(t)] .$$

The various moments of f(t) can therefore be determined from the measured moments of F and P by the following relations:

(1) $M^1[F] = M^1[P]M^0[f] + M^0[P]M^1[f]$.

Noting that $M^0[Q] = \int_{-\infty}^{\infty} x^0 Q(x)dx = 1$,

we have: $\underline{M^1[f] = M^1[F] - M^1[P]}$, in agreement with the results of Newton (1950)

(2) $M^2[F] = M^2[P] + 2M^1[P]M^1[f] + M^2[f]$.

If we now consider, in particular, moments about the mean, writing $\mathfrak{M}^m[F]$ as the m^{th} moment of F about the mean, $M^1[F]$,

then $\mathfrak{M}^1[Q] \equiv 0$,

and $\mathfrak{M}^2[F] = \mathfrak{M}^2[P] + \mathfrak{M}^2[F]$

or: $\underline{\mathfrak{M}^2[f] = \mathfrak{M}^2[F] - \mathfrak{M}^2[P].}$

(3) Similarly: $\underline{\mathfrak{M}^3[f] = \mathfrak{M}^3[F] - \mathfrak{M}^3[P]}$.

The corresponding relationships for the higher moments are obtained in a similar way, but contain additional cross terms, eg.

$$\mathfrak{M}^4[F] = \mathfrak{M}^4[P] + 6\mathfrak{M}^2[P]\mathfrak{M}^2[f] + \mathfrak{M}^4[f].$$

(II) Symmetric Curve Analysis:

A radioactive source is assumed to emit pairs of gamma rays, γ_i , and γ_i , where γ_i is emitted a short time, t, after γ_i , with a probability distribution of f(t)dt, for $t \geq 0$,

and 0, for $t < 0$.

The detector biases are assumed to be adjusted so that the relative number of detected coincidences of the type:

(a) γ_i detected by counter (1), and γ_i by counter (2) is = g_1 and

(b) γ_i detected by counter (1), and γ_i by counter (2) is = g_2,

where $g_1 + g_2 = 1$.

For the discussion of part (I), g_1 was assumed to be 1, and $g_2 = 0$.

For the present case the apparent decay distribution of the source is of the form:

$$f^x(t) = g_1 f(t) + g_2 f(-t),$$

so that: $$M^1[f^x] = \int_{-\infty}^{\infty} t f^x(t)dt = g_1 \int_{0}^{\infty} tf(t)dt + g_2 \int_{-\infty}^{0} tf(-t)dt$$
$$= g_1 \int_{0}^{\infty} t\, f(t)dt - g_2 \int_{0}^{\infty} tf(t)dt = (g_1 - g_2)M^1[f].$$

Similarly: $$\mathfrak{m}^2[f^x] = \int_{-\infty}^{\infty} (t - \bar{t})^2 f^x dt$$
$$= \mathfrak{m}^2[f] + \left\{1 - (g_1 - g_2)^2\right\}\left\{M^1[f]\right\}^2.$$

For the special case of an exponential decay, ie $f(t) = \lambda e^{-\lambda t}$.

$M^1[f] = 1/\lambda = \tau$, and $\mathcal{M}^2[f] = (1/\lambda)^2 = \tau^2$.

So: $\mathcal{M}^2[f^x] = \tau^2 + \left\{1 - (g_1-g_2)^2\right\}^2$

and: $\tau = \left\{\frac{\mathcal{M}^2[f(x)]}{2-(g_1-g_2)^2}\right\}^{1/2}$

If we consider the two special cases, (a) $g_1 = 1$; $g_2 = 0$,

(b) $g_1 = g_2 = \frac{1}{2}$,

then, for the first moments, (using the results of (I)), we obtain: (a) $\tau = M^1[f^x] = M^1[F] - M^1[P]$

(b) $M^1[f^x] = M^1[F] - M^1[P] = 0$.

and for the second moments:

(a) $\tau = \left\{\mathcal{M}^2[f^x]\right\}^{1/2} = \left\{\mathcal{M}^2[F] - \mathcal{M}^2[P]\right\}^{1/2}$

(b) $\tau = \left\{\frac{1}{2}\mathcal{M}^2[f^x]\right\}^{1/2} = \left\{\frac{1}{2}\left(\mathcal{M}^2[F] - \mathcal{M}^2[P]\right)\right\}^{1/2}$

(III) Determining the Mean Lifetimes of Radioactive Sources Without Using a 'Prompt' Source.

Two radioactive sources, both described by an exponential decay, one of mean life: τ_1 , and the other τ_2 , are assumed to be measured by a fast coincidence circuit, yielding the experimental delayed resolution curves: $F_1(T)$ and $F_2(T)$, respectively:

Now, from (I), $M^1[f_1] = \tau_1 = M^1[F_1] - M^1[P]$

and $M^1[f_2] = \tau_2 = M^1[F_2] - M^1[P]$,

So: $\tau_2 - \tau_1 = M^1[F_2] - M^1[F_1]$ = a measured value, G_1. (1)

Similarly, from $\mathcal{M}^2[f_j] = \tau_j^2 = \mathcal{M}^2[F_j] - \mathcal{M}^2[P]$, $j = 1,2$

we obtain: $\tau_2^2 - \tau_1^2 = (\tau_1 + \tau_2)(\tau_2 - \tau_1) = \mathcal{M}^2[F_2] - \mathcal{M}^2[F_1]$ (2)

and dividing (2) by (1):

$$(\tau_2 + \tau_1) = \frac{\mathcal{M}^2[F_2] - \mathcal{M}^2[F_1]}{M^1[F_2] - M^1[F_1]} = \text{another measured value, } G_2.$$

So: $\tau_1 = \frac{1}{2} (G_2 - G_1)$

and: $\tau_2 = \frac{1}{2} (G_2 + G_1)$

(IV) Calculations of the Moments for Various Forms of f(t)

In the preceding examples, various characteristics of the experimental resolution functions were examined on the assumption of either an exponential or a general decay distribution characterizing the source. In this section are listed the results of determinations of several moments for an assortment of types of decay distributions, f(t).

f(t)	MEAN $M'[f]$	VARIANCE $m^2[f]$	$m^3[f]$	$\frac{\{m^2[f]\}^{1/2}}{M'[f]}$	$\frac{\{m^3[f]\}^{1/3}}{M'[f]}$
EXPONENTIAL $\lambda e^{-\lambda t}$; $\tau = \frac{1}{\lambda}$	τ	τ^2	$2\tau^3$	1.0	1.260
LINEAR $b\left(1-\frac{bt}{2}\right)$; $\tau = \frac{1}{b}$	$\frac{2}{3}\tau$	$\frac{2}{9}\tau^2$	$\frac{3}{50}\tau^3$	0.707	0.588
GAUSSIAN $\sqrt{\frac{2}{\pi}}\frac{1}{\sigma}e^{-\frac{1}{2}\left(\frac{t}{\sigma}\right)^2}$; $\tau=\sigma$	$\sqrt{\frac{2}{\pi}}\tau$	$\left(1-\frac{2}{\pi}\right)\tau^2$	$\left(\frac{4}{\pi}-1\right)\sqrt{\frac{2}{\pi}}\tau^3$	0.756	0.755
MIXED DECAY; DOUBLE EXPONENTIAL $\frac{\lambda_1 e^{-\lambda_1 t} + f\lambda_2 e^{-\lambda_2 t}}{1+f}$ $\tau_1=\frac{1}{\lambda_1}$ $\tau_2=\frac{1}{\lambda_2}$	$\frac{\tau_1 + f\tau_2}{1+f}$	$\frac{(\tau_1+f\tau_2)^2+2f(\tau_1-\tau_2)}{(1+f)^2}$		$\left\{1+\frac{2f(\tau_1-\tau_2)}{(\tau_1+f\tau_2)^2}\right\}^{1/2}$	

$f(t)$	MEAN $M'[f]$	VARIANCE $m^2[f]$	$m^3[f]$	$\frac{\{m^2[f]\}^{1/2}}{M'[f]}$	$\frac{\{m^3[f]\}^{1/3}}{M'[f]}$
DELAYED EXPONENTIAL $f = 0, \quad 0 \leq t < T$ $= \lambda e^{-\lambda t}, \quad t \geq T$	$T + \tau$	τ^2	τ^3	$\frac{\tau}{T+\tau}$	$\frac{1.26\tau}{T+\tau}$
SIGNIFICANT THERMALISATION TIME $\lambda e^{-\lambda t} \int_0^t p_f(\tau) e^{\lambda\tau} d\tau$ (see App. E)	$M'[p_f] + \tau$	$m^2[p_f] + \tau^2$		$\frac{\{m^2[p_f] + \tau^2\}^{\frac{1}{2}}}{M'[p_f] + \tau}$	
SIGNIFICANT 1.28 MEV LEVEL LIFETIME $\frac{\lambda_\gamma \lambda_\beta}{\lambda_\gamma + \lambda_\beta} e^{-\lambda_\beta t}; \quad t \geq 0$ $\frac{\lambda_\gamma \lambda_\beta}{\lambda_\gamma + \lambda_\beta} e^{\lambda_\gamma t}; \quad t \leq 0$ (see App F); $\tau_\beta = 1/\lambda_\beta$, $\tau_\gamma = 1/\lambda_\gamma$	$\tau_\beta - \tau_\gamma$	$\tau_\beta^2 + \tau_\gamma^2$		$\left\{1 + \frac{2\tau_\beta \tau_\gamma}{(\tau_\beta - \tau_\gamma)^2}\right\}^{\frac{1}{2}}$	

APPENDIX D.

SPINOR FUNCTION OF NEGATIVE POSITRONIUM ION

Problem: To determine the ratio of two-photon to three-photon emission from the positronium ion.

Since the annihilation of a positron creates a number of gamma rays in a quantum state with integral angular momentum, a representation of the spinor function of the positronium ion as a linear combination of such eigenfunctions would facilitate calculation of the relative numbers of photons emitted per annihilation. Let the spinor functions defining the individual positron and electrons be:

(α_p, β_p) for the positron, and

(α_1, β_1), (α_2, β_2) } for the two electrons.

These three spinors may be combined in the following way to produce spinors which are eigenfunctions of the angular momentum operator.[1]

$$
\begin{aligned}
{}^{3/2}\chi_{3/2} &= \alpha_p \alpha_1 \alpha_2 \\
{}^{1/2}\chi_{3/2} &= \frac{1}{\sqrt{3}} \left[\alpha_p \alpha_1 \beta_2 + \alpha_p \beta_1 \alpha_2 + \beta_p \alpha_1 \alpha_2 \right] \\
{}^{-1/2}\chi_{3/2} &= \frac{1}{\sqrt{3}} \left[\beta_p \beta_1 \alpha_2 + \beta_p \alpha_1 \beta_2 + \alpha_p \beta_1 \beta_2 \right] \\
{}^{-3/2}\chi_{3/2} &= \beta_p \beta_1 \beta_2
\end{aligned}
$$

Symmetric spinor configurations.

$$
\begin{aligned}
{}^{1/2}\chi_{1/2} &= \frac{1}{\sqrt{6}} \left[\alpha_p \alpha_1 \beta_2 + \alpha_p \beta_1 \alpha_2 - 2 \beta_p \alpha_1 \alpha_2 \right] \\
{}^{-1/2}\chi_{1/2} &= \frac{1}{\sqrt{6}} \left[\beta_p \beta_1 \alpha_2 + \beta_p \alpha_1 \beta_2 - 2 \alpha_p \beta_1 \beta_2 \right]
\end{aligned}
$$

1 Schiff, L. I., Quantum Mechanics, (McGraw-Hill Book Co., Inc., Toronto, 1949) First Edition, pg. 229.

$$^{1}/_{2}\psi_{1/2} = \frac{1}{\sqrt{2}}\left[\alpha_p \alpha_1 \beta_2 - \alpha_p \beta_1 \alpha_2\right]$$

$$^{-1}/_{2}\psi_{1/2} = -\frac{1}{\sqrt{2}}\left[\beta_p \alpha_1 \beta_2 - \beta_p \beta_1 \alpha_2\right]$$

Antisymmetric spinor configurations.

However, since the total wave-function of the system must be antisymmetric with respect to interchange of the two electrons (1 and 2), and since the spatial part of the wave function, a 1s ground state, is symmetric (this wave-function is given on pg 34), the spinor portion then, must be antisymmetric, viz. the final pair of functions given above,

$$^{1}/_{2}\psi_{1/2} = \frac{1}{\sqrt{2}}\left[\alpha_p \alpha_1 \beta_2 - \alpha_p \beta_1 \alpha_2\right] \qquad \text{and}$$

$$^{-1}/_{2}\psi_{1/2} = \frac{1}{\sqrt{2}}\left[\beta_p \beta_1 \alpha_2 - \beta_p \alpha_1 \beta_2\right]$$

corresponding to a total angular momentum of $\frac{1}{2}\hbar$

Following annihilation, the final state is represented by a product of two spinor functions, one a spinor corresponding to a total angular momentum of quantum number 1 or 0 (representing the emitted gamma rays), and one of angular momentum of $\frac{1}{2}\hbar$ (representing the recoil electron). As a result, an expansion of the initial state in terms of a linear combination of the spinor functions of the final state is desired.

If the recoil electron is defined to be the second electron (the two electrons are indistinguishable), then $^{\pm 1/2}\psi_{1/2}$ can be expanded in terms of $\alpha_2, \beta_2, {}^{\pm 1,0}\varphi_1, {}^{0}\varphi_0$

where $^{1}\varphi_1 = \alpha_p \alpha_1$

$$^{0}\varphi_1 = \frac{1}{\sqrt{2}}\left(\alpha_p \beta_1 - \beta_p \alpha_1\right)$$

$$^{-1}\varphi_1 = \beta_p \beta_1$$

$$^{0}\varphi_0 = \frac{1}{\sqrt{2}}\left(\alpha_p \beta_1 - \beta_p \alpha_1\right)$$

Thus we obtain:

$$\tfrac{1}{2}\psi_{\frac{1}{2}} = \frac{1}{2}\left[\sqrt{2}\,\beta_2{}^{1}\varphi_1 - \alpha_2{}^{0}\varphi_1 - \alpha_2{}^{0}\varphi_0\right]$$

$$-\tfrac{1}{2}\psi_{\frac{1}{2}} = \frac{1}{2}\left[\sqrt{2}\,\alpha_2{}^{-1}\varphi_1 - \beta_2{}^{0}\varphi_1 - \beta_2{}^{0}\varphi_0\right]$$

The total spinor function of the ion is now composed of an admixture of triplet and singlet spinor functions occurring with the same relative weights as those characterising free positron-electron collisions of random relative orientations:

(i) a triplet state of J = 1, and m value of $\pm$ 1 occurring with a weight of $\frac{1}{2}$,

(ii) a triplet state of J = 1, and m = 0, with a weight of $\frac{1}{4}$, and

(iii) a singlet state of J = 0, with a weight of $\frac{1}{4}$.

APPENDIX E.

EFFECTS OF (a) SIGNIFICANT POSITRON SLOWING DOWN TIME, or (b) SIGNIFICANT BOUND STATE FORMATION TIME, ON THE RESOLUTION CURVES.

Problem: It is desired to determine the nature of the apparent decay distribution, f(t), for the situation described by:

(a) annihilation of the positrons from some state S with a probability distribution: $\lambda e^{-\lambda t}$, with the condition that,

(b) the annihilating state, S, is formed at a time t to t + dt with a probability $p_f(t)\,dt$.

Thus, this description can be applied to:

(i) Thermalised positron annihilation with free electrons with an annihilation probability given by the Dirac cross-section, thus leading to an exponential decay as indicated in (a) above. The effect of a significant thermalisation time is included in the $p_f(t)$ of part (b).

(ii) Positron annihilation from a positronium ion state, S, is described by (a), above. The effect of a significant formation time for the positronium ion (the formation time including both positron thermalisation time and electron capture times) is contained in the function $p_f(t)$.

Now, the total probability for annihilation of the positron in a time t to t + dt after the instant of emission of the positron is:

$$f(t)\,dt = \left[\int_0^t p_f(\tau)\,\lambda\, e^{-\lambda(t-\tau)}\,d\tau\right]dt = \lambda\, e^{-\lambda t}\,dt \int_0^t p_f(\tau)\, e^{\lambda\tau}\,d\tau$$

The first moment of f(t) is:

$$M'[f] = \int_0^\infty t\lambda e^{-\lambda t}\left[\int_0^t p_f(\tau)\, e^{\lambda\tau}\, d\tau\right] dt$$ which, on integrating by parts,

$$= \int_0^\infty (t + 1/\lambda)\, p_f(t)\, dt = \underline{1/\lambda + M'[p_f(t)]}.$$

Similarly, the second moment of f(t) is:

$$M^2[f] = \int_0^\infty t^2 \lambda e^{-\lambda t}\left[\int_0^t p_f(\tau)\, e^{\lambda\tau}\, d\tau\right] dt$$ Again, integrating by parts,

$$M^2[f] = \int_0^\infty \left(t^2 + \frac{2t}{\lambda} + \frac{2}{\lambda^2}\right) p_f(t)\, dt = M^2[p_f(t)] + \frac{2}{\lambda} M'[p_f(t)] + 2/\lambda^2$$

The second moment about the mean is therefore,

$$m^2[f(t)] = M^2[f(t)] - \{M'[f(t)]\}^2$$

Thus, $$\underline{m^2[f(t)] = m^2[p_f(t)] + 1/\lambda^2}.$$

Alternatively, these results could have been obtained directly from the equations of Appendix C by noting the equivalence between

$$f(t) = \int_0^t p_f(\tau)\, \lambda e^{-\lambda(t-\tau)}\, d\tau = \int_{-\infty}^{\infty} p_f(\tau)\, g(t-\tau)\, d\tau$$

where $p_f(\tau) = 0$ for $\tau < 0$

and $g(t-\tau) = \lambda e^{-\lambda(t-\tau)}$, $\tau \le t$

$= 0$, for $\tau > t$

and the function $F(T) = \int_{-\infty}^{\infty} f(t)\, P(\tau - t)\, dt$

given at the beginning of Appendix C(I):

APPENDIX F.

THE EFFECT ON THE POSITRON DECAY FUNCTION, f(t), OF A SIGNIFICANT LIFETIME OF THE 1.28 Mev STATE OF Ne^{22}.

The decay scheme for Na^{22} is indicated in fig 16.

Let the actual positron decay function be: $\lambda_\beta e^{-\lambda_\beta t}$

and the gamma-ray function be: $\lambda_\gamma e^{-\lambda_\gamma t}$

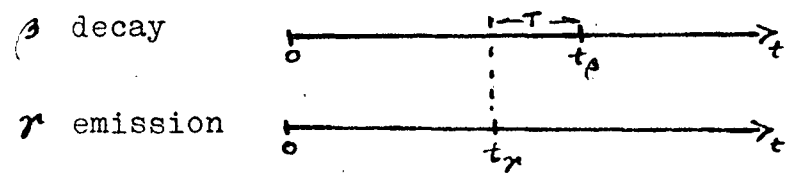

If the case of a β decay in the time t_β to $t_\beta + dt$, and a gamma emission in the time t_γ to $t_\gamma + dt$ is considered, the measured time delay between them is $T = t_\beta - t_\gamma$. The probability that these two events will occur as described is:

$$f' dt_\gamma = \lambda_\beta \lambda_\gamma e^{-\lambda_\beta t_\beta} e^{-\lambda_\gamma t_\gamma} dt_\gamma dt_\beta$$

where: $|dt_\beta| = |dt_\gamma| = |dt| = |dT|$

On substituting for t_β: $f'(\tau) dt_\gamma = \lambda_\beta \lambda_\gamma e^{-\lambda_\beta T} e^{-(\lambda_\beta + \lambda_\gamma) t_\gamma} dt_\beta dt_\gamma$

and the total probability of a positron decaying T sec <u>after</u> the emission of the gamma ray is:

$$f(T_+) dT = \int_0^\infty f'(\tau) dt_\gamma = \frac{\lambda_\beta \lambda_\gamma}{\lambda_\beta + \lambda_\gamma} e^{-\lambda_\beta T} dT$$

But the positron may also annihilate <u>before</u> the emission of the gamma ray, i.e. T may be < 0.

For this case, however, since t_β cannot be < 0, then only that time interval for t_γ from $+|T|$ to ∞ may be considered. In other words, since $t_\gamma = t_\beta - T$ and so equals $-T$ when $t_\beta = 0$, then t_γ must be $> -T$.

Thus $f(T_-)dT = \int_{-T}^\infty f'(\tau) dt_\gamma = \frac{\lambda_\beta \lambda_\gamma}{\lambda_\beta + \lambda_\gamma} e^{\lambda_\gamma T} dT$

That is: $f(t) = \frac{\lambda_\beta \lambda_r}{\lambda_\beta + \lambda_r} e^{-\lambda_\beta t}, \quad t \geq 0$

$\frac{\lambda_\beta \lambda_r}{\lambda_\beta + \lambda_r} e^{-\lambda_r t}, \quad t \leq 0$

In the limit of $\lambda_r \to \infty$ (that is, a negligible 1.28 Mev lifetime compared to $1/\lambda_\beta$) then $f(t) = \lambda_\beta e^{-\lambda_\beta t}, \quad t \geq 0$

$= 0, \quad t < 0$, as expected.

APPENDIX G.

"COMPOSITE" LEAST SQUARES ANALYSIS OF DATA.

In the comparative lifetime measurements illustrated in fig 26, it is desired to obtain the best estimate of the differences of the lifetimes of the positrons in the two metals.

Let the data of fig 26 be represented in the form shown in the accompanying diagram:

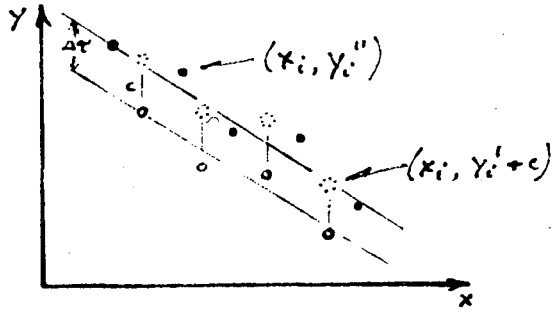

The constant difference, $\Delta\tau$, between the lifetimes is defined to be c.

The problem is to determine the best straight-line through the composite points (y_i'' and $y_i' + c$)(since the same instrumental drift should apply to both sets of points) in the customary least-squares fashion, and also to obtain an explicit estimate of the unknown constant, c.

If the number of points of (x_i, y_i') is n', and the number of points (x_i, y_i'') is n", where $n = n' + n''$ and the best linear fit is $y = mx + b$, then the total squared error is:

$$\varepsilon^2 = \sum_{\text{all points}} (y_i - mx_i - b)^2 + 2c \sum_{y_i'}' (y_i' - mx_i - b + c/2)$$

where: $$\sum y_i = \sum' y_i' + \sum'' y_i''.$$

Now, setting $\frac{\partial \varepsilon^2}{\partial m} = \frac{\partial \varepsilon^2}{\partial b} = \frac{\partial \varepsilon^2}{\partial c} = 0$, the following three equations are obtained:

(1) $m \Sigma x_i^2 + b \Sigma x_i - c \Sigma' x_i = \Sigma x_i y_i$

(2) $m \Sigma x_i + b n - c n' = \Sigma y_i$

(3) $m\Sigma' x_i + bn' - cn' = \Sigma' y_i'$

By solving this set of simultaneous equations, the line $y = mx + b$ and also the constant, c, can be determined.

Special Case

For the special case of very little experimental drift, $m \simeq 0$.

$$c = \frac{n'\Sigma y_i - n\Sigma' y_i'}{n'(n-n')} = \frac{n'\Sigma y_i - n'\Sigma' y_i'}{n'(n-n')} - \frac{n\Sigma' y_i' - n'\Sigma' y_i'}{n'(n-n')}$$

$$= \frac{\Sigma y_i - \Sigma' y_i'}{n-n'} - \frac{\Sigma' y_i'}{n'} = \frac{\Sigma'' y_i''}{n''} - \frac{\Sigma' y_i'}{n'}$$

which is merely the difference in the mean values of the ordinates of the two groups of points.

APPENDIX H

COMPUTER PROGRAM FOR CALCULATION OF MOMENTS.

The program used for the calculations of the moment of the coincidence resolution curves is given below.

With the program in the working channels, the computer is ready to receive a series of four digit numbers (positive, decimal integers), such as a series of ordinates of a resolution curve (in proper sequential order). These four digit numbers must be separated by one character, either a 'space' or a 'carriage return'. At the termination of the sequence of numbers, indicated by altering the form described above (e.g. by inserting a 'period' or other character, other than a 'space' or 'carriage return', after a four-digit number), the computer types out the following symbols and numbers:

m3 (third moment about the mean)

Σ (total number of counts, i.e. the sum of all numbers in the sequence)

m (the first moment of the sequence)

ss (variance, or second moment about the mean).

The program is called into the working channels preparatory to an analysis by the call letters: "al20 carriage return"

```
a004
00000000 00000000 00000000 00000000
00000000 00000000 00000000 00000000
79041160 791af785 5b444180 00000000
790ff785 5b1e7907 0311060c 5b491400
5b137900 1160791d 5b444000 05000094
11607912 f7851120 02070209 00000003
f7855b16 00000000 5b465900 0000005b
79051160 5a05a05a 030e0491 00000001

a104
81a02800 c5043800 e702eb00 a311eb00
f1443132 611f4901 c506e702 c5044103
61004900 2800f301 eb00a301 e702eb00
e7013200 19311124 c50b4103 e717bf0b
61024902 651b19b5 2800a311 29326504
e5003200 11244102 eb00c503 4904790a
61034903 2800a311 bf06c507 f785871f
e500bd04 eb00c505 41042800 5b0e1108
```

BIBLIOGRAPHY

Alkhazov, D.K., Grinberg, A.P., Lemburg, I.Kh., Rozhdestvenskii, V.V., (1959) Soviet Physics, JETP 36, 222.

Basson, J.K., (1954) Phys Rev 96, 691

Bay, Z., (1950) Phys Rev 77, 419.

(1955) Phys Rev 100, 1197.

Bay, Z., Henri, V.P., McLernon, F., (1955) Phys Rev 97, 561.

Bég, M.A.B., and Stehle, P.M., (1959) Phys Rev 113, 1545.

Bell, R.E., Graham, R.L., and Petch, H.E., (1952) Can J. Phys 30, 35.

Bell, R.E., and Graham, R.L., (1953) Phys Rev 90, 644.

Bell, R.E., (1954) Annual Reviews of Nuclear Science, Vol 4, 93.

Bell, R.E., and Malmfors, K.G., (1955) (in) Beta- and Gamma-Ray Spectroscopy, (edited by) K. Siegbahn (North-Holland Pub. Co., Amsterdam).

Berko, S., and Zuchelli, A.J., (1956) Phys Rev 102, 724.

Berko, S., and Plaskett, J.S., (1958) Phys Rev 112, 1877.

Bohm, D., and Pines, D., (1952) Phys Rev 85, 338.

(1953) Phys Rev 92, 609.

Coleman, C.F., (1955) Nature 175, 1027. (reported by Allen and Egelstaff)

Daniel, E., (1957) Jour de Phys et le Rad 18, 691.

DeBenedetti, S., Cowan, C.E., Konneker, W.R., and Primakoff, H., (1950) Phys Rev 77, 205.

DeBenedetti, S., and Richings, H.J., (1952) Phys Rev 85, 377.

Deutsch, M., (1951A) Phys Rev 82, 455.

(1951B) Phys Rev 83, 866.

(1953) Prog in Nucl Phys 3, 131.

Dirac, P.A.M., (1930) Proc Camb Phil Soc 26, 361.

Dixon, W.R., and Trainor, L.E.H., (1955) Phys Rev 97, 733.

DuMond, J.W.M., Lind., D.A., and Watson, B.B., (1949) Phys Rev 75, 1226.

Ferguson, A.T.G., and Lewis, G.M., (1953) Phil Mag 44, 1339.

Ferrell, R.A., (1956) Rev Mod Phys 28, 308.

Garwin, R.L., (1953) Phys Rev 91, 1571.

Gell-Mann, M., (1959) Rev Mod Phys 31, 834.

Gerholm, T.R., (1956) Arkiv Fysik 10, 523.

Green, R.E., and Bell, R.E., (1957) Can J. Phys 35, 398.

(1958) Radiation Lab Report, University of McGill, Montreal, P.Q.

Hanna, S.S., and Preston, R.S., (1958) Phys Rev 109, 716.

Hatcher, C.R., Millett, W.E., and Brown, L., (1958) Phys Rev 111, 12.

Heinberg, M., and Page, L.A., (1956) Bull Am Phys Soc II, 1, 168.

Hylleraas, E.A., (1947) Phys Rev 71, 491.

Jones, G., and Warren, J.B., (1956) J. Sci Inst 33, 429.

Jones, G., (1955) MSc Thesis, University of B.C., Vancouver, B.C.

Karpman, V.I., and Fisher, I.Z., (1956) Doklady Akad Nauk SSSR 111, 1212. (in English) Soviet Physics (Doklady), 1, 765.

Landsberg, P.T., (1949) Proc Phys Soc (London) A62, 806.

Lang, G., DeBenedetti, S., and Smoluchowski, R., (1955) Phys Rev 99, 596.

Lang, G., and DeBenedetti, S., (1957) Phys Rev 108, 914.

Lee-Whiting, G.E., (1955) Phys Rev 97, 1557.

Mackenzie, I.K., (1953) PhD Thesis, University of B.C., Vancouver, B.C.

Massey, H.S.W., and Mohr, C.B.O., (1954) Proc Phys Soc 67A, 695.

Metzger, F.R., (1956) Phys Rev 103, 983.

Millman, J., and Taub, H., (1956) "Pulse and Digital Circuits", McGraw-Hill Book Co., Inc., Toronto.

Minton, G.H., (1954) Phys Rev 94, 758.

(1959) Private Communication.

Mott, N.F., and Jones, H., (1936) "The Theory of the Properties of Metals and Alloys", Dover Publications, Inc., N. York, 1958.

Neilson, G.C., (1955) PhD Thesis, University of B.C., Vancouver, B.C.

Neilson, G.C., and James, D.B., (1955) Rev Sci Inst 26, 1018.

Nelms, A.T., (1956) Nat Bur of Standards, Circular 577.

Newton, T.D. (1950) Phys Rev 78, 490.

Ore, A., (1948) Phys Rev 73, 1313.

Ore, A., and Powell, J.L., (1949) Phys Rev 75, 1696.

Page, L.A., Heinberg, M., Wallace, J., and Trout, T., (1955) Phys Rev 98, 206.

Page, L.A. (1957) Phys Rev 106, 394.

Page, L.A., and Heinberg, M., (1957) Phys Rev 106, 1220.

Parratt, L.G., (1959) Rev Mod Phys 31, 616.

Pond, T.A., and Dicke, R.H., (1952) Phys Rev 85, 489.

Post, R.F., and Schiff, L.I., (1950) Phys Rev 80, 1113.

Prescott, J.R., (1959) Private Communication.

Riley, P.J., (1958) MSc Thesis, University of B.C., Vancouver, B.C.

Rupaal, A.S., (1959) Private Communication.

Seliger, H.H., (1955) Phys Rev 100, 1029.

Sommerfeld, A., Houston, W.V., and Eckart, C., (1928) Zeit f Phys 47, 1.

Stelson, P.H., and McGowan, F.K., (1955) Phys Rev 99, 112.

Stewart, A.T., (1955) Phys Rev 99, 594.

(1957) Can J. Phys 35, 168.

Stewart, A.T., (1959) Phys in Canada 15, 20.

Strominger, D., Hollander, J.M., and Seaborg, G.T., (1958) Rev Mod Phys 30, 585.

Sunyar, A.W., (1957) Bull Am Phys Soc II, 2, 37.

Ticho, H.K., and Gauger, J., (1956) Rev Sci Inst 27, 354.

Wallace, P.R., (1955) Phys Rev 100, 738.

Warren, J.B., and Griffiths, G.M., (1951) Can J. Phys 29, 325

Warren, J.B., and Jones, G., (1958) Bull Am Phys Soc II, 3,327

Widmaier, W., (1958) IRE Trans Nucl Sci, NS-5, 114.